LEIDSE GEOLOGISCHE MEDEDELINGEN, Deel 46, Aflevering 1, pp. 57—155, 17-12-1970

PETROLOGY OF A PART OF THE WESTERN GALICIAN BASEMENT BETWEEN THE RIO JALLAS AND THE RIA DE AROSA (NW SPAIN) WITH EMPHASIS ON ZIRCON INVESTIGATIONS

BY

C. E. S. ARPS

ABSTRACT

The present area covers a part of the axial zone of the Hesperian Massif. Rocks of metamorphic and intrusive origin occur in three structural units: the central zone (which in fact forms part of what is called the "blastomylonitic graben"), the migmatic complex and the rocks in the S and SW. During the Hercynian orogeny these units were placed in juxtaposition. With respect to their age and composition the rocks can be subdivided into pre-Hercynian metasediments, metabasic rocks and orthogneisses, and Hercynian migmatites, palingenic granites and intrusive granodiorites, granites, pegmatites, aplites, quartz veins, granite porphyries, lamprophyres and olivine dolerites.

Based on petrological evidence, the geological history can be reconstructed as follows:

Pre-Hercynian metasediments, bearing traces of a probably Precambrian deformation and metamorphism (resorbed staurolites and garnets enclosed in Hercynian metamorphic minerals) have intruded along fundamental N-S trending faults in the Upper Ordovician (460–430 $\times$ 10^6 years ago) by means of megacrystal-bearing two-mica granites, biotite granites and peralkaline granites. The intrusion of a basic dyke-swarm took place between the emplacements of the latter two types of granite series. During the Hercynian orogeny the pre-Hercynian rocks were at first penetratively deformed; the metasediments were (re)-folded and the granites were phyllonitized into coarse-grained augengneisses or mylonitized into granite mylonites (central zone). This Hercynian main phase deformation was followed by a period of Abukuma-type plutonometamorphism. A widespread metablastic recrystallization of the non-migmatic rocks of the central zone is characteristic. The metamorphic mineral assemblages in the non-migmatic rocks of the central zone are indicative of the cordierite-amphibolite facies and the mineral assemblages of the metasedimentary rocks in the SW and W indicate greenschist facies conditions, while the inclusions in the palingenic two-mica granite suffered superimposed hornblende-hornfels facies conditions. At deeper levels the Hercynian metamorphism culminated in anatexis. During a short period of tension and normal faulting the non-migmatic rocks of the central zone were brought into juxtaposition with the migmatites. More or less synchronously the active fundamental faults, separating the central zone from the western migmatites facilitated the rise of large amounts of granodioritic magma; immediately afterwards the ultimate products of anatexis, in as much as they were capable of intrusion, penetrated the migmatic complex and the granodiorites in the form of successive phases of two-mica granites. This period of plutonic activity was interrupted by the second and third Hercynian deformations that were only locally of a penetrative nature. The majority of the Hercynian granites and granodiorites were weakly foliated during the second deformation while the third deformation locally phyllonitized and mylonitized the rocks in the N, SW and W.

The Hercynian orogenic cycle was concluded with the intrusion of a post-kinematic two-mica granite, two biotite granites ($280 \pm 11 \times 10^6$ years ago), some granite porphyries and lamprophyres. The few olivine dolerite dykes are probably younger.

Accessory zircon occurring in metasediments, orthogneisses, migmatites and granites has been investigated for crystal habit, growth phenomena, inclusions, resorption, fluorescence and other properties.

The various rock-types contain zircon populations with a more or less typical habit: i.e. a combination of the forms {101}, {100} and /or {110} and sometimes {301} and {201} for the zircons of the blastomylonitic orthogneisses, the post-kinematic granites and granite porphyries, while a combination of {101}, {211} and {100} and/or {110} is characteristic for the pre-Hercynian coarse-grained augengneisses and the Hercynian megacrystal-bearing granodiorites and two-mica granites. The zircons in the rocks belonging to the megacrystal-bearing granodiorite series clearly show differences in evolution. The zircons in the migmatic rocks indicate that conditions for anatexis favoured the regeneration of zircon. The fluorescence colours of the zircon crystals are yellow, orange and brown; some zircon populations also contain emerald green fluorescent crystals. A zonal variation in fluorescence colours is also present.

CONTENTS

INTRODUCTION

THE INVESTIGATIONS

This paper presents the results of petrological, mineralogical and structural investigations of an area in western Galicia (NW Spain) situated around Noya, between the Río Jallas in the NNW and the Ría de Arosa in the SSE.

The investigations are part of a regional program, covering large parts of western Galicia and being carried out by students and graduates of the Department of Petrology, Mineralogy and Crystallography of the Geological Institute (Leiden University) under the supervision of Prof. Dr. E. den Tex and his staff.

The area was mapped using the 1 : 25,000 maps edited by the Cartografía Militar de España. The following maps were used: Sheet 93 (Sierra de Outes), quadrants I (Mazaricos), II (Sierra de Outes), III (El Pindo) and IV (Cée); Sheet 119 (Noya), quadrants I (Noya) and II (Villa y Puerto del Son); Sheet 120 (Padrón), quadrants III (Ourolo) and IV (Lousame); Sheet 151 (Puebla del Caramiñal), quadrant I (Puebla del Caramiñal) and Sheet 152 (Villagarcía), quadrant IV (Villagarcía).

The scope of the investigations was to describe the basement rocks of the area and to investigate their mutual relationships. The results are presented in Chapter I; a geological map and a chronological table are included in the backflap.

The results of a detailed study of accessory zircon crystals from the majority of the rocks in the area are presented in Chapter II. Crystal morphology and other mineralogical properties are discussed with respect to the possible modes of origin of the rocks concerned.

GEOLOGICAL SETTING

The crystalline basement of western Galicia forms part of the axial zone of the Hesperian massif (Galician-Castilian zone, according to Lotze, 1945). The relatively deeper parts of this predominantly Hercynian orogen consist mainly of metamorphic rocks and granites. The rocks vary widely in composition and age; they can be subdivided into pre-Hercynian and Hercynian rocks (den Tex, 1966); part of the pre-Hercynian rocks are of Precambrian age. An important fault-zone divides the Galician sector of the Galician-Castilian zone into an eastern part ("domaine externe", Capdevila, 1965) and a western part. In the latter four geotectonic units were distinguished (Parga-Pondal, 1956; den Tex, 1966): 1) the Ordenes "basin", 2) the Hercynian migmatic front, 3) the "blastomylonitic graben" and 4) the late-Hercynian and epi-Hercynian plutonic massifs (Fig. I-1). Evidence of two orogenic cycles has been reported from several terrains in western Galicia e.g. by Floor (1966) from SW Galicia ("blastomylonitic graben"), by Vogel (1967) from the Cabo Ortegal Complex in northern Galicia, by Warnaars (1967) and van Zuuren (1969) from the western and southern rims of the Ordenes "basin" respectively and by Hilgen (in press) from the Lalin Complex, south of the Ordenes "basin". The area under consideration in this paper covers a part of the "blastomylonitic graben" and the surrounding migmatic complex. Many Hercynian granites and granodiorites are also present.

PREVIOUS WORK

Publications dealing with geological investigations in northwestern Spain have recently been summarized by Parga-Pondal (1966). Ph. D. theses by Leiden graduates containing detailed studies of various areas have been presented by Floor (1966), Vogel (1967), Warnaars (1967) and van Zuuren (1969). Other contributions were made at the first and third reunions on the geology of Galicia and Northern Portugal (1965 and 1969); these have been published in volume 36 of the Leidse Geologische Mededelingen (1966) and in volume 81 of the Boletín Geológico y Minero, respectively.

The greater part of the present area (Fig. I-1) was preliminarily mapped in the summers of 1961 and 1962 by Avé Lallemant (1964), ten Bosch (1964), von Metzsch (1964) and the present author (1965) as part of an undergraduate training program. The fieldwork for this thesis was completed in the years 1964, 1965 and 1966. The regions NW and N of the present area were mapped by de Graaff (1962), Koster van Groos (1962) and Rubbens (1963).

The results of structural and petrological work on the Barbanza Peninsula were published by von Raumer (1963). Avé Lallemant (1965) reported briefly on the petrology, petrofabrics and structural geology of the area directly N of the Ría de Noya y Muros. Van Zuuren (1965) described the tin and tungsten ore deposits at San Finx, 12 km ESE of Noya.

As a part of a combined geological, oceanological and biological survey of the Ría de Arosa (Brongersma & Pannekoek, 1966), the geomorphology of the surroundings of the Ría has been described by Pannekoek (1966), while Floor (1968) discussed briefly the basement rocks in the drainage area of the Ría. The sedimentology of the northern shores of the Ría de Arosa in relation to the hinterland were discussed by Arps & Kluyver (1969); the Quaternary fluviomarine terrace deposits, located in distinct levels along the coasts of the Ría de Arosa and the Ría de Noya (see appendix I: geological map), were investigated by the present author (Arps, 1965 and Arps & Kluyver, 1969).

EXPLANATION OF SYMBOLS AND TERMS

Sample numbers and storage. – The location of the selected hand specimens mentioned in the text and in tables

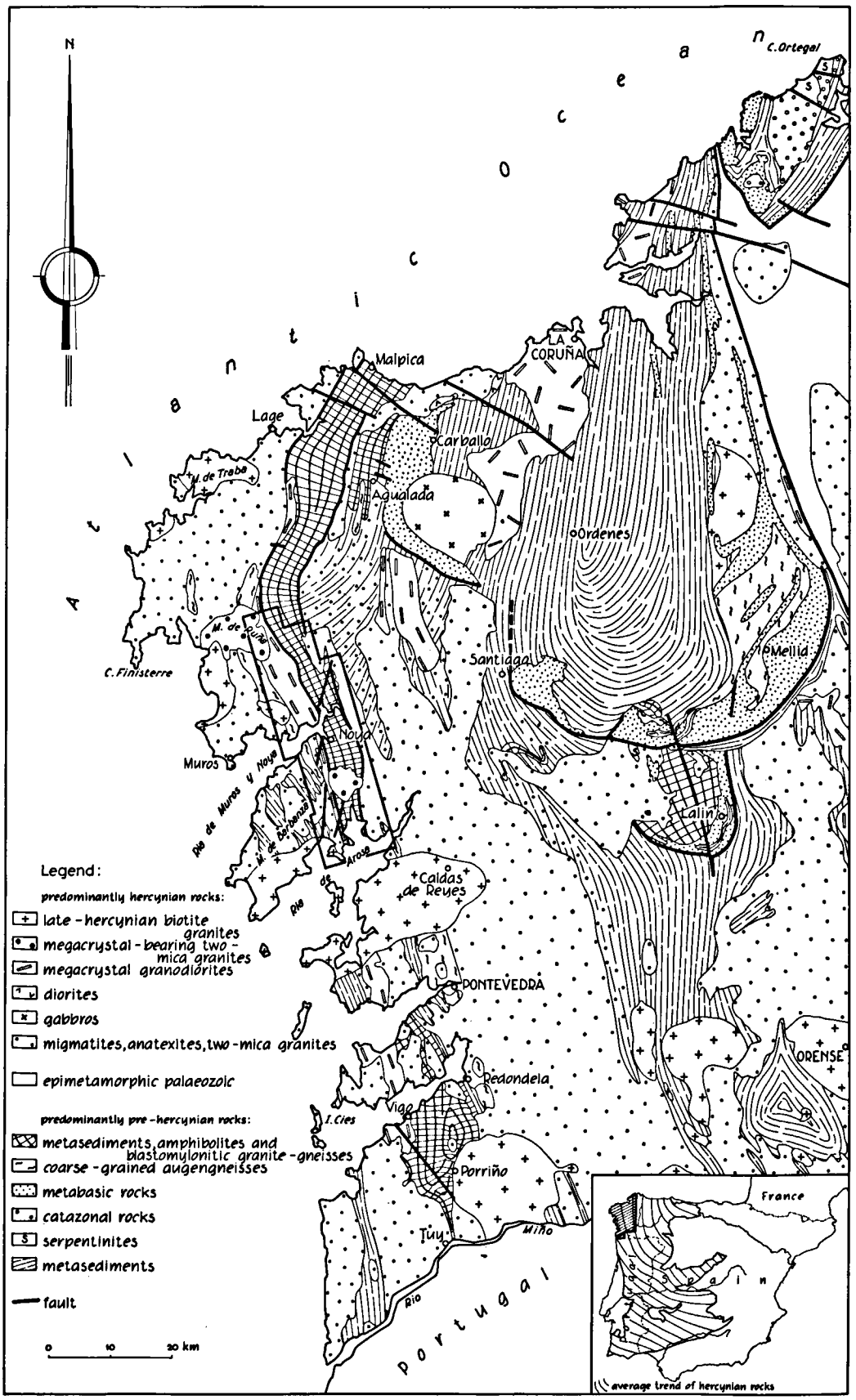
N
C. Ortegal
Malpica
LA CORUÑA
Lage
Carballo
M. de Traba
Aqualada
Ordenes
C. Finisterre
Santiago
Mellid
Noya
Muros
Ria de Muros y Noya
Lalin
Caldas de Reyes
PONTEVEDRA
ORENSE
Redondela
Vigo
I. Cies
Porriño
Tuy
Miño
Rio
Portugal
Legend:
predominantly hercynian rocks:
late-hercynian biotite granites
megacrystal-bearing two-mica granites
megacrystal granodiorites
diorites
gabbros
migmatites, anatexites, two-mica granites
epimetamorphic palaeozoic
predominantly pre-hercynian rocks:
metasediments, amphibolites and blastomylonitic granite-gneisses
coarse-grained augengneisses
metabasic rocks
catazonal rocks
serpentinites
metasediments
fault
0 10 20 km
France
average trend of hercynian rocks

I-1 to I-6 is indicated on the sample map (Appendix IV). These samples of the author's collection are deposited at the Rijksmuseum van Geologie en Mineralogie in Leiden. The samples are numbered from RGM-St. 141678 to St. 141864; in the tables as well as on the sample map, however, the prefix RGM-St. 141 is omitted and only the last three numbers are used. A few samples of other collections are also mentioned in the text (de Graaff, 1962; Koster van Groos, 1962; Rubbens, 1963).

Terms and abbreviations. – The following subdivisions were used in describing the grain sizes of the rocks:

< 3 cm	very coarse-grained	
3 cm – 5 mm	coarse-grained	
5 – 1 mm	medium-grained	
1 – 0.33 mm	fine-grained	
0.33 – 0.01 mm	microcrystalline	aphanitic
< 0.01 mm	cryptocrystalline	aphanitic

For crystallographic properties the following abbreviations were used: n(Na) for the refractive index of garnet in Na-light; α, β and γ for the refractive indices of biaxial minerals. Anorthite percentages were determined according to the methods of Fouqué and Rittmann (Tröger, 1959).

The terms foliation and schistosity have been used in the sense of Harker (1956). F_1, F_2 etc. indicate the phases of folding in chronological order; s_1, s_2 etc. are s-surfaces including foliations, schistosities, cleavages and axial planes in chronological order.

ACKNOWLEDGEMENTS

The author feels greatly indebted to Professor E. den Tex for his interest and valuable suggestions during the laboratory investigations as well as the preparation of this manuscript.

Sincere thanks are due to Dr. P. Floor for his continuous and unselfish interest in the field and during the preparation of this thesis. The author owes his thanks to Dr. P. Hartman for his valuable advice on crystallographical problems. Furthermore I am indebted to Professor H. J. Zwart for reading and commenting the manuscript.

I am grateful to Dr. P. van Gijzel for his kind cooperation in carrying out the fluorescence-microscopical investigations and for the fruitful discussions with respect to this subject.

Thanks are due to Dr. P. Maaskant for carrying out some electron microprobe analyses and to Mr. K. J. Roberti for preparing the computer program.

The pleasant cooperation and many fruitful discussions with my colleagues and friends Dr. P. C. Zwaan, Dr. H. G. Avé Lallemant, Dr. A. van Zuuren, Mr. J. P. Engels, Mr. H. Koning, Mr. C. F. Woensdregt, Mr. J. D. Hilgen, Mr. J. J. M. W. Hubregtse, Mr. H. J. W. G. Schalke and Mr. L. O'Herne were greatly appreciated.

I wish to extend my thanks to Dr. I Parga-Pondal of the Laboratorio Geológico de Lage for his valuable advice during the fieldwork in Galicia.

Thanks are due to Mrs. G. P. Bieger-Smith for correcting the English manuscript and to Dr. B. van Hoorn for translating the abstract into Spanish.

The advice and support of many members of the technical and administrative staff of the Geological Institute, Leiden, made the publication of this paper possible. The illustrations and maps were prepared by Mr. J. Bult, Miss C. P. J. Roest and Mr. B. G. Henning, the photographic illustrations by Mr. W. C. Laurijssen and Mr. W. A. M. Devilé and the X-ray photographs by Mr. A. Verhoorn. Thin sections were made by Mr. M. Deyn, Mr. J. Verhoeven, Mr. C. J. van Leeuwen and Mr. J. Schipper; the constituent parts of the mineral separation system were made by Mr. J. D. van Royen and Mr. C. J. van Klink (Kamerlingh Onnes Laboratory, Leiden). The manuscript was typed by Miss T. W. Terpstra, Miss C. C. Zuiderduin, Miss C. M. Boer and Mrs. N. K. I. Arps-Hill.

Financial support for the fieldwork was received from the Molengraaff-Fonds (1965 and 1966) and the Van Oosterom Onderwijs-Fonds.

CHAPTER I

PETROLOGY AND STRUCTURAL HISTORY OF THE AREA AROUND NOYA

THE ROCKS OF THE INVESTIGATED AREA

The rocks in the investigated area can be divided into pre-Hercynian and Hercynian crystalline rocks and Quaternary sediments. The latter were mentioned in the introduction, but we are now interested in the rocks of the crystalline basement.

Three major rock groups can be distinguished:
1. The non-migmatic rocks of pre-Hercynian age
2. The rocks of the migmatic complex
3. The intrusive rocks

The rocks of the *first* group occur as two separate units. The first unit is called the central zone; this zone includes non-migmatic mesozonal metasediments, granite gneisses and amphibolites. The second unit is located in the south-southwestern part of the

Fig. I-1. Simplified geological map of western Galicia according to Parga–Pondal (1963) as well as unpublished reports of the Dept. of Petrology, Mineralogy and Crystallography, Leiden University. The area under consideration is indicated.

area and consists of epi-mesozonal metasediments and amphibolites. Granitic rocks found in the western part of the area enclose large xenoliths, rafts and roof pendants that originally belonged to the second unit.

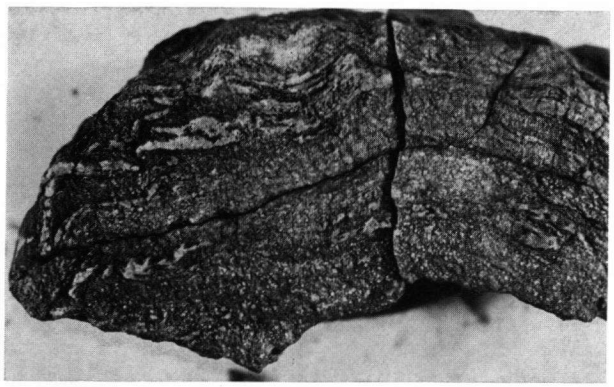

Fig. I-2. Recumbent F_1-folds in the plagioclaseblast-bearing paragneiss 3 km NNW of Val. F_2 resulted in an open folding and a weak s_2 (St. 141693, × 4/5).

The rocks of the *second* group are characterized by the fact that the constituent rocks are all more or less migmatized ("mobilized"), causing many types of migmatic structures.

The rocks of the *third* group embrace all the Hercynian parautochthonous and allochthonous intrusives. They can be subdivided into syn-kinematic and post-kinematic intrusives.

THE NON-MIGMATIC ROCKS (PRE-HERCYNIAN)

The rocks of the central zone

The central zone of the present area is part of a long and relatively narrow belt extending from Malpica on the NW Galician coast to Tuy at the Portuguese border (Fig. I-1). The zone is limited on both sides by faults; the one forming the western border can generally be recognized more easily in the field. On both sides the different rocks directly adjacent to the fault are predominantly cataclastic. In general the eastern fault-zone separates two rock-series with similar origins but different Hercynian histories; to the east the sequence is migmatic.

The central zone consists of rocks of sedimentary and igneous origin. The metasediments are mainly paragneisses (metagreywackes) and mica schists (metapelites) intercalated with para-amphibolites, metaquartzites, graphite schists and very fine-grained, tough calc-silicate lenses.

The rocks of igneous origin are granitic gneisses which vary in age of emplacement, composition and structural habit. There are also many ortho-amphibolites. The orthogneisses occur as oblong bodies in the paragneisses; the rocks are easily recognizable in the field by their generally leucocratic character and their pronounced texture, which is linear, planolinear and sometimes augen-bearing. In composition the rocks vary from biotite orthogneisses to amphibole-bearing and per-alkaline orthogneisses. The amphibole-bearing orthogneisses are partly melanocratic.

The intrusion of basic dykes, now present as numerous amphibolite lenses, took place before the emplacement of the amphibole-bearing orthogneisses but after the biotite orthogneisses. The amphibolite lenses were found to lie concordant with the regional schistosity; their location in the field is schematically indicated on the geological map.

The central zone was called "Complejo Antiguo" by Parga-Pondal (1956); this term was more accurately redefined at the first Geological Congress of Santiago de Compostela in 1965 as "The complex of pre-Hercynian, mainly acid, igneous rocks" (Floor, 1966, p. 187). In fact this new term now refers to the orthogneisses of the present area. More recently the zone has been characterized as a structural unit by den Tex & Floor (1967), who considered it to be a "blastomylonitic and polymetamorphic graben".

Evidence of deformation and metamorphism

The rocks of the central zone were greatly deformed during the Hercynian orogeny; with a few exceptions most of the pre-Hercynian structures in the paragneisses and schists seem to have been obliterated (Fig. I-4).

At least three more or less penetrative Hercynian deformation phases can be distinguished: F_1, F_2 and F_3 respectively. The first phase was the strongest; the metasediments were sharply folded, while the pre-Hercynian granites and basic intrusions became mylonitic gneisses and amphibolites respectively. The second and third deformations were weaker and only partly penetrative.

It is supposed that the three deformations were the

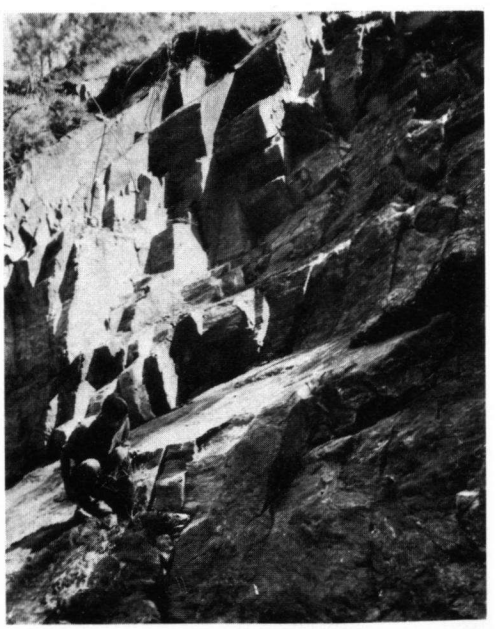

Fig. I-3. A banded paragneiss (s_1) along the road from Sierra to Val. A second schistosity (s_2) was superimposed, resulting in a megascopical rod-structure.

Fig. I-4. A sub-vertically banded hornfelsic paragneiss 200 m N of Val. The photomicrograph (negative print) shows an isoclinal fold (F_1) enclosed in a mica-rich band. There is probably the crest of an older fold in one of the limbs of the F_1-fold (St. 141695, × 4).

result of similarly directed compressive stresses, although the original position of s_1 is difficult to determine. There are indications that in places at least s_1 was a sub-horizontal foliation plane with a sub-horizontal (N)NW-(S)SE directed B_1-axis (Fig. I-2 and I-3). After F_1 but not later than F_2, s_1 may have changed to a more sub-vertical position; possibly the combination of the important fault movements, including the subsidence of the central zone, and the ensuing F_2 deformation were responsible for the steepening and folding of s_1 just before s_2 developed. In any case there is no reason to believe that the present regional schistosity of the metasedimentary rocks and orthogneisses was principally induced by F_2.

The second deformation resulted in a (N)NW-(S)SE striking sub-vertical crenulation cleavage with a sub-horizontal B_2-axis, while F_3 produced only very locally a N-S striking cleavage with a sub-vertical B_3-axis (Avé Lallemant, 1965, p. 166).

In most of the pre-Hercynian rocks of the central zone, especially in the central and southern parts, s_2 developed more or less parallel to s_1 and cannot be distinguished from it. F_2 penetrated the schistose paragneisses and schists more than the massive para- and orthogneisses. The effects of F_3, as a cleavage in the rocks of the central zone, are only locally visible in the orthogneisses.

Thus at present most of the metasediments have (N)NW-(S)SE striking sub-vertical schistosity planes, which dip very regularly to the SW in the central and southern parts of the central zone, while N of the Ría de Noya y Muros they dip variably to the SW and the NE.

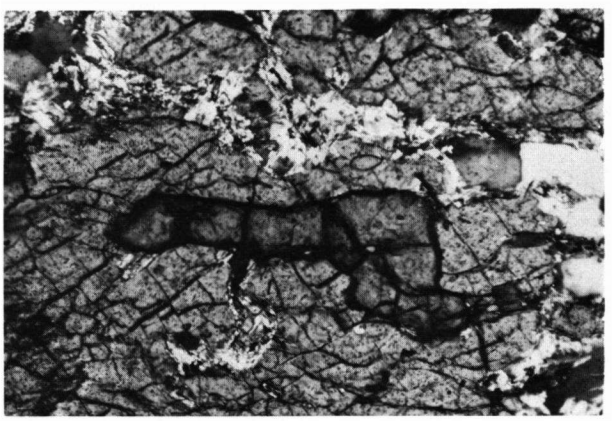

Fig. I-5. a. A resorbed staurolite inclusion in andalusite from a staurolite-andalusite-sillimanite-bearing two-mica schist 3 km ENE of Noya (St. 141684, × 100).

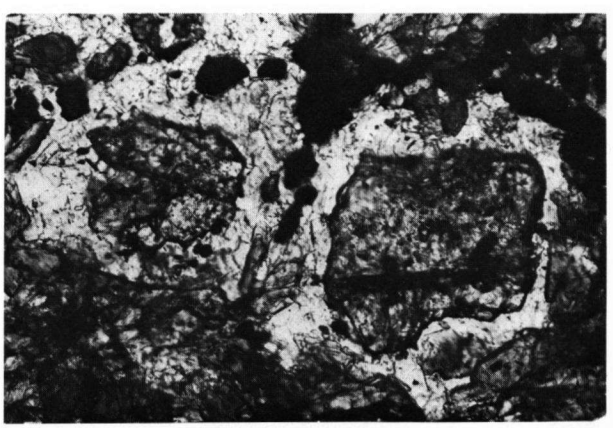

b. A resorbed garnet inclusion in plagioclase from an amphibolite 3 km SE of Noya (× 200).

The variable dip of the schistosity planes depends on the rate of penetration of F_2 and the attitudes of s_1 and s_2.

Near Val, 8 km NNW of Sierra de Outes, the "hornfelsic" paragneisses are banded locally. Within the relatively narrow mica-rich bands isoclinal folds are sometimes visible. These folds are F_1-folds and probably bear traces of older folds (Fig. I-4).

The orthogneisses are linear to planolinear and the lineation plunges slightly to the NW or SE. When it can be measured, the dip of the foliation is generally rather steep, especially near the western fault. Although subordinate, a sub-horizontal foliation is present, e.g. NW of Val. The influence of F_2 on the orthogneisses is difficult to discern. Probably only in those outcrops where s_1 was in a sub-horizontal position during F_2 can the results of a slight folding be seen (Plate III-b). The planolinear and linear structures are believed to have been present before F_2 occurred. This assumption may be backed by the fact that the orthogneisses, present in the "blastomylonitic graben" SE and E of Vigo, have similar structures but show no evidence of F_2 (Floor, 1966).

The third deformation resulted in a dextral slip along N-S striking planes (Fig. I-17b) and a subsequent period of wrench faulting. In the orthogneisses, in the neighbourhood of Noya, many small-scale conjugate sets of N-S or NNE-SSW dextral and E-W or WNW-ESE sinistral wrench faults are found.

The Hercynian regional metamorphism started after F_1 and lasted until shortly before F_3. At certain levels, metamorphism ultimately culminated in anatexis; evidence of this anatexis was found in the rocks of the migmatic complex (see p. 79). The rocks of the central zone were not affected by anatexis, although some pegmaplitic and granitic veins and bodies may be regarded as ultimate palingenic products of anatexis at lower levels in the central zone. A later subsidence along the fundamental fault brought the non-migmatic rocks into their present juxtaposition with the migmatites and granites outside the central zone.

During metamorphism the mylonitic orthogneisses recrystallized into blastomylonitic orthogneisses (Plates III and IV-a and b); a metablastic growth (plagioclase and hornblende) occurred in the paragneisses and basic rocks respectively (Plate II-a and b).

Ignoring most of the minor constituents and later retrogressive alterations, the Hercynian metamorphic

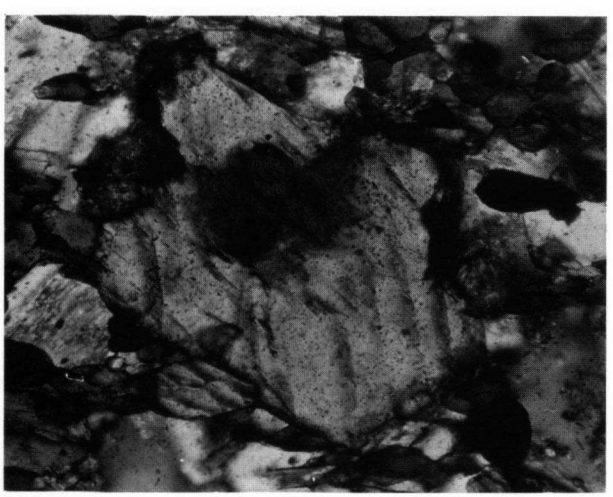

Fig. I-6. a. A cummingtonite crystal with a core of blue-green hornblende (St. 141740, × 130).

b. A relatively young cummingtonite crystal cutting through blue-green hornblendes with parallel orientation (St. 141738, × 150).

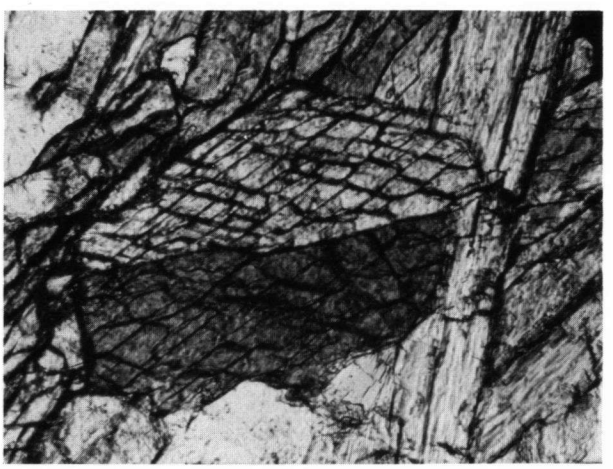

c. Sharp boundary in basal section dividing hornblende from cummingtonite. Amphibolite inclusion in migmatites 3.4 km ENE of Val (× 150).

mineral assemblages diagnostic for grade and facies series of the central zone are:

metapelites: muscovite + biotite + quartz ± andalusite ± sillimanite ± garnet

metagreywackes: biotite + muscovite + plagioclase (15–30 % An) + quartz ± andalusite ± sillimanite ± garnet

metabasites: blue-green hornblende + plagioclase (25–50 % An) ± quartz ± biotite ± garnet ± cummingtonite ± clinopyroxene

When cummingtonite is present, the anorthite percentages of plagioclase are generally higher than 35 %; it may reach a bytownitic composition.

calc-silicate rocks: plagioclase (An 55 %) + quartz ± clinopyroxene ± blue-green hornblende ± garnet ± biotite

The minerals that characterize the Hercynian metamorphic sub-facies have grown post-kinematically

with respect to F_1. Indications of a progressive metamorphism of the present facies series are observed in the following relations.

paragneisses and schists: muscovite → andalusite → sillimanite; muscovite → sillimanite; biotite → sillimanite

Because potash-feldspar has never been found to grow together with sillimanite, the reactions must have taken place under pressures, $P(H_2O)$, greater than 2500 bar according to Winkler (1967, Fig. 40) or even higher than 3500 bar when compared with Fig. 1 of Hietanen (1967); the temperatures were at least 640° or 570 °C respectively.

The plagioclases of the metablastic paragneisses carry (resorbed) inclusions of biotite, muscovite and garnet (Figs. I-10 and I-12a), while resorbed biotite, garnet and staurolite are present as inclusions in andalusite poikiloblasts.

amphibolites: blue-green hornblende → cummingtonite (Fig. I-6).

Cummingtonite occurs together with blue-green hornblende in quartz-bearing amphibolites. The transition of common hornblende into cummingtonite is a strong indication of a decrease in pressure during later stages of metamorphism.

The reversible reaction Tschermak's molecule + quartz ⇆ cummingtonite + anorthite + water is sensitive to pressure changes and moves to the right with a decrease in pressure as long as quartz is present in excess (Shidô, 1958). In some garnet-bearing amphibolites the resorbed garnets were always found enclosed in plagioclase and not in direct contact with hornblende (Fig. I-5b).

The resorbed staurolites and the turbid and resorbed garnets in some paragneisses and schists, as well as the garnet relics in a few amphibolites, may probably be regarded as remnants of an older pre-Hercynian metamorphism (Floor, 1966, p. 171). It is not quite clear whether the s_1 of the plagioclase metablasts represent the same pre-Hercynian metamorphism, since the process of metablastic recrystallization is a Hercynian mechanism that started after F_1. Investigations on the character of Hercynian metamorphism of the rocks in the "blastomylonitic graben" between Malpica and Tuy have revealed that with a few local exceptions the overall picture is quite comparable. Staurolite, andalusite and sillimanite have been encountered in many samples, while the amphibolites contain blue-green hornblende, epidote and garnet with local growths of cummingtonite. Cordierite has only been reported in the S (Floor, 1966, p. 25). The reason that this mineral has been found neither in the present area nor further N may be the retrogressive influence of F_2 and F_3. With the exception of a weak N-S compression after F_1, neither deformation acted in the area E and SE of Vigo.

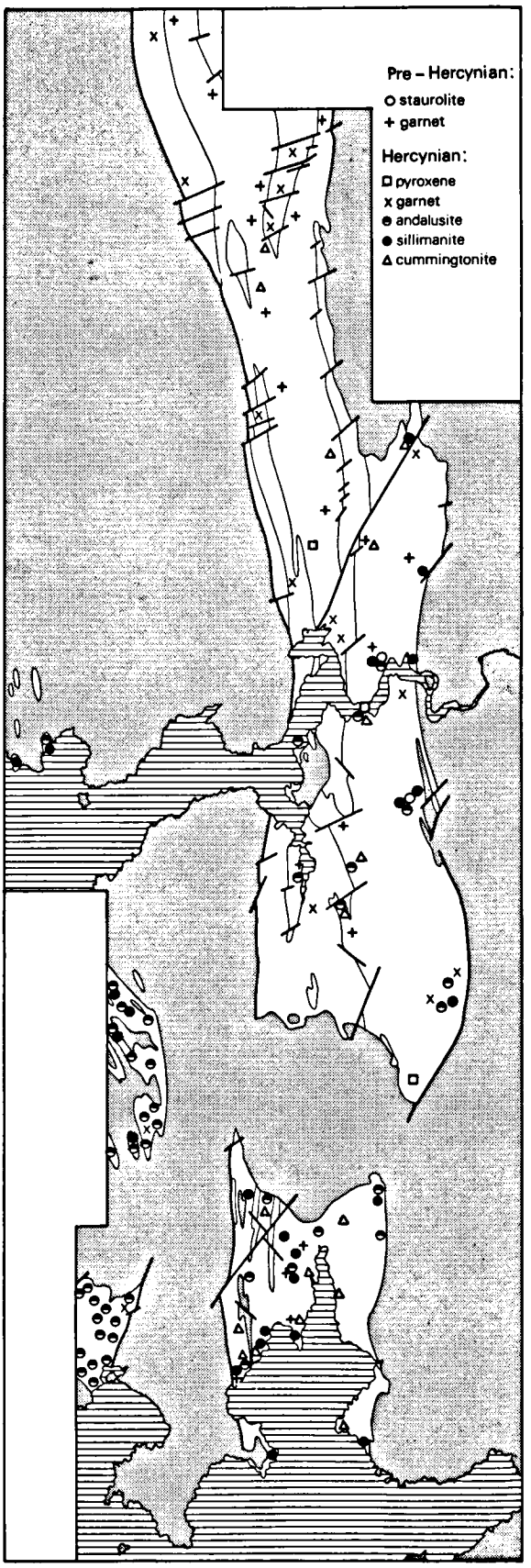

Fig. I-7. The distribution of the diagnostic metamorphic minerals in the non-migmatic rocks of the area.

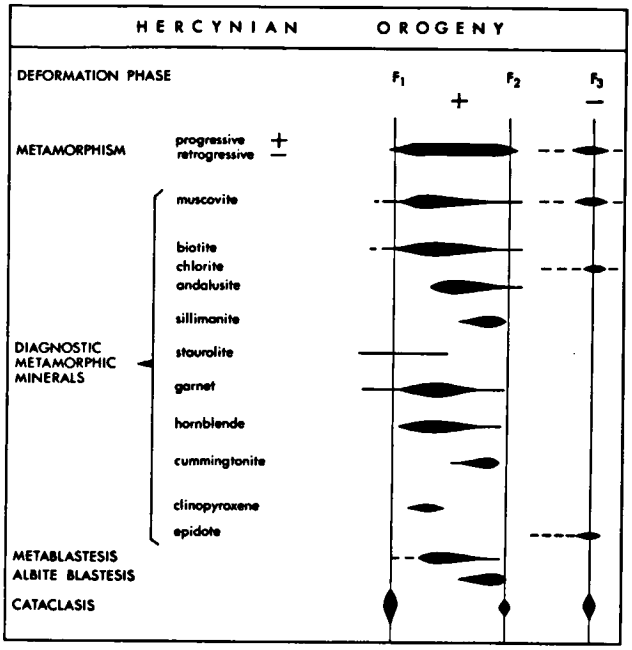

Fig. I-8. Paragenetic table showing the relations between deformation, metamorphism and crystal growth in the non-migmatic rocks of the central zone.

From the observations in the present area it can be deduced that the association biotite + muscovite + quartz ± oligoclase ± garnet was initially stable in the paragneisses and schists and blue-green hornblende + oligoclase/andesine ± quartz ± garnet ± pyroxene in the amphibolites; the metamorphism however continued under slightly different conditions, i.e. a relative increase of T over P (especially in the S and E), resulting in a more abundant growth of andalusite and sillimanite as well as the introduction of cummingtonite. It finally culminated at appropriate levels in large-scale anatexis. All occurrences of diagnostic metamorphic minerals have been indicated on the map of Fig. I-7. The metamorphic mineral assemblages of the rocks of the central zone are indicative of a low pressure-high temperature lineage of orogenic plutonism (den Tex, 1965), located in the andalusite-staurolite-cordierite sub-facies and probably just reaching the cordierite-sillimanite sub-facies of the amphibolite facies. In the nomenclature of Winkler (1967), the paragenesis of the minerals is comparable to the Abukuma-type low pressure facies series (with $P(H_2O)$ ca. 3000–3500 bar) located in the cordierite-amphibolite facies, or more specifically in the andalusite-cordierite-muscovite and probably locally even the sillimanite-cordierite-muscovite-almandine sub-facies. In Fig. I-8, the time and rate of growth of the diagnostic metamorphic minerals have schematically been indicated in relation to the general phases of Hercynian metamorphism and deformation.

Retrogradation becomes important where F_3 was active, i.e. along shear planes, mylonitic zones and faults. Sericitization, chloritization and epidotization are frequently encountered. Secondary veins filled with adularia ± chlorite ± titanite and epidote veins are common features near important faults (Fig. I-12b).

Paragneisses, schists and para-amphibolites (Precambrian)

The largest group of metasedimentary rocks in the central zone are the dark grey schistose biotite-muscovite paragneisses. Some varieties are fine-grained (aphanitic); others are massive with a hornfelsic appearance or clearly metablastic with oval plagioclase metablasts up to about 2.5 mm.

To the E of the central zone, especially E and SE of Noya, the paragneisses grade into highly fissile, light grey or brown two-mica schists. Relatively narrow, concordant intercalations of graphite schists and mica-bearing metaquartzites occur; E of Noya the latter rock-type has exceptionally large dimensions.

The texture of the paragneisses is generally planar, linear or massive, depending on composition, grain size and structural history. Locally faint traces of a probably tectonic banding are present (Fig. I-4 and Plate I-a and b). Quartz lenses, veinlets and bands are frequently encountered concordant or accordant with the banding or schistosity. Some of the small and narrow quartz lenses may have originated by metamorphic differentiation but the larger are often accordant veins, some of which have been folded or boudinaged (Fig. I-9).

Swarms of amphibolite lenses are present in the paragneisses and some of the orthogneisses of the central zone. Hardly any have been found in the mica schists. It is supposed that some of the amphibolites have a sedimentary origin.

Biotite-muscovite paragneisses and muscovite-biotite schists. – The ordinary paragneisses always include biotite, plagioclase and quartz. The minerals may occur in varying amounts and grain sizes. The content of muscovite increases towards the E, combined with a decrease in plagioclase and an increase in quartz.

General mineralogy of the paragneisses and schists (Table I-1).* – *Quartz* occurs as relatively small inclusions in the plagioclase metablasts of the paragneisses; the shape of the inclusions varies from droplets or irregular grains to flat plates in parallel orientation (Plate II-a and b). Most of the paragneisses contain in addition individual grains of quartz and numerous small, thin concordant quartz bands, while the two-mica schists are generally free of plagioclase but contain instead quartz, which is often entirely concentrated in bands and lenses.

Unstrained equidimensional quartz with polygonal outlines (Spry, 1968) occurs in some places but highly undulose grains with irregular outlines and mortar zones are more frequent.

With a few exceptions *plagioclase* is the only feldspar found in the paragneisses. A metablastic growth of plagioclase on a

* For Tables I-1 to I-6 see appendix III in backflap.

regional scale is characteristic (Plate II). The individual grains and metablasts are rarely twinned; {001} twins are more frequent than {010} twins. Plagioclase is often normally zoned; anorthite values vary between 10 % and 35 % with an average of about 25 % (Fig. I-14). A widespread albitization of oligoclase took place along certain zones near the amphibole-bearing orthogneisses (Fig. I-11).

Occasionally *potash feldspar* may be present or even abundant, as in sample St. 141678 which is taken from a paragneiss adjacent to granitic and pegmaplitic dykes. A metasomatic origin of the fresh potash feldspar in the paragneiss seems evident; the possibility that the grains represent relics of a higher grade of metamorphism is excluded.

Secondary *adularia* may have filled up cracks in heavily deformed paragneisses near important faults, such as those found 2.5 km SE of Pte. Olveira (St. 109750, Fig. I-12b), 5.5 km SE of Val (St. 141681) or near Pte. Beluso. In the paragneisses near the fault SE of Pte. Beluso (St. 141680), a secondary adularization of plagioclase took place without the simultaneous chloritization of biotite.

Small and early flakes of *biotite* and *muscovite* occur as inclusions, often in parallel orientation, in plagioclase (Fig. I-12a) and andalusite. But the main portion of the micas is dispersed throughout the rock as in the fine-grained paragneisses with a hornfelsic appearance (see p. 69), or is concentrated in bands. A new generation of micas may have grown in the newly formed s_2 cleavage. The colour of biotite varies from dark to reddish brown; green biotite is subordinate.

Chlorite, with blue or yellowish brown polarization colours, is commonly present and is usually secondary to biotite and occasionally garnet. There is however also a new generation arranged perpendicularly or obliquely to the schistosity or in spherulitic aggregates. *Sericite* is secondary to andalusite or sillimanite.

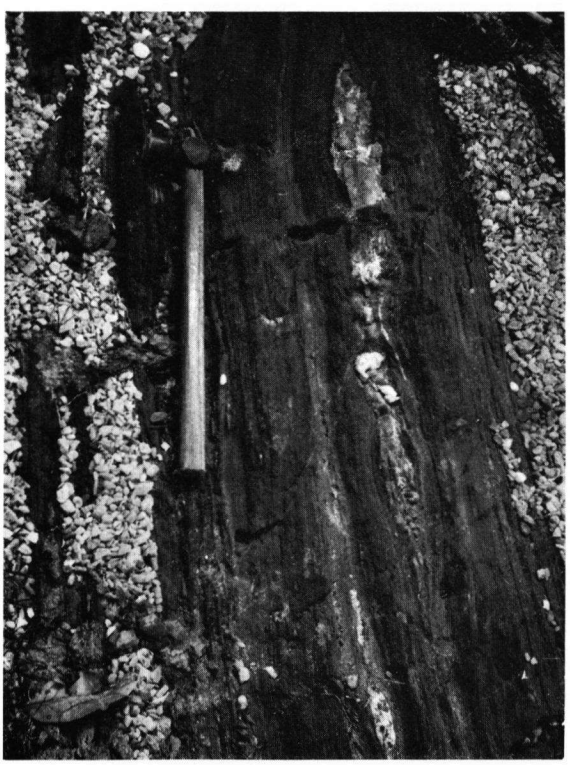

Fig. I-9. a. Narrow concordant quartz lenses in the paragneiss 2 km N of Abanqueiro.

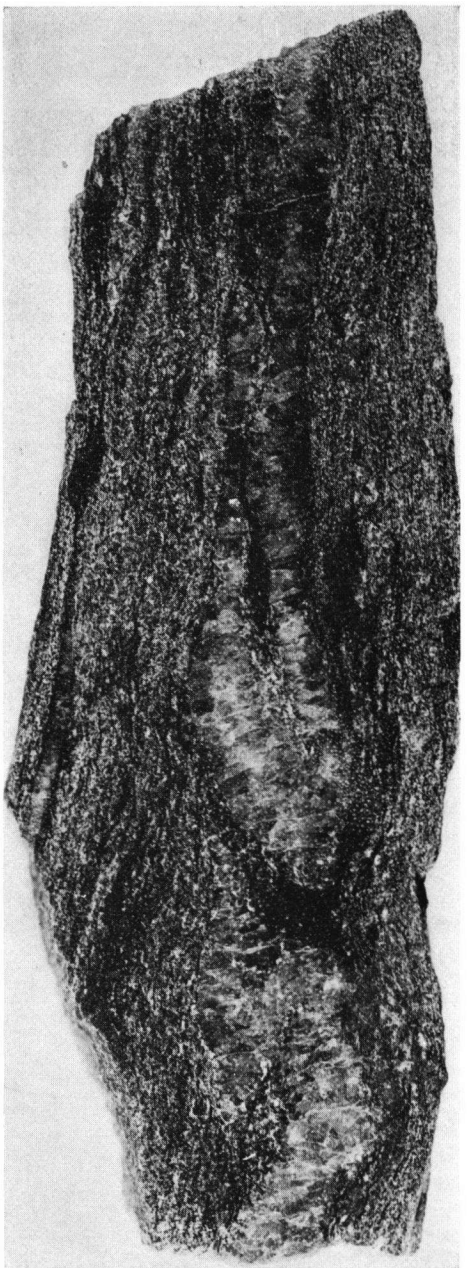

b. A folded (F_1) quartz band lying concordant in a paragneiss; the dark spots are andalusites in which relics of staurolite may occur (St. 141689, × 5/4).

Generally *andalusite* has grown post-kinematically with respect to F_1. When F_2 has affected the rocks, the andalusites are pre-F_2 and the micas then bend around them slightly (St. 141688). Most andalusites contain inclusions of quartz, biotite, opaque minerals and sometimes resorbed garnet and staurolite (Fig. I-5a and samples St. 141684, St. 141689). A progressive transition from andalusite to sillimanite is present; most of the andalusites were later partly or completely sericitized.

Sillimanite, variety fibrolite, grew from andalusite, but more often from muscovite and biotite. The tiny needles may extend into the adjacent quartz.

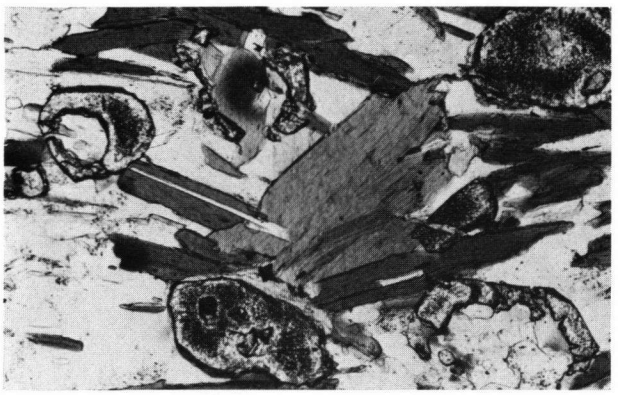

Fig. I-10. An oligoclase metablast enclosing resorbed, relictic and turbid garnets and biotite (s_1) (Paragneiss St. 141688, × 100).

Garnet is either represented by relatively small, strongly resorbed and turbid individual grains, which generally occur within the plagioclase metablasts where they were more effectively guarded against later metamorphic influences (Fig. I-10 and I-12a), or by larger sub-idiomorphic grains scattered throughout the rock. With respect to the origin and the relative age of similar enclosed and resorbed garnets, Floor (1966, p. 171) concluded that they can be connected with a pre-Hercynian metamorphism. He based his conclusion on the fact that the garnets were found ". . . . enclosed within plagioclase and cordierite metablasts and also within quartz, tourmaline and apatite that is in its turn surrounded by andalusite, generally without alteration products". For the present area, it can be assumed that the garnet relics (sometimes atoll garnets) found in plagioclase metablasts without alteration products are probably of pre-Hercynian origin, and probably have the same age as staurolite. In sample St. 141694, the relatively large grains (1.8 mm) are only partly enclosed in the albite metablasts.

Fig. I-25 is a graphic representation of a_0 and n(Na) for garnet samples from several rock-types of the area, according to the methods of Frietsch (1957) and Sastri (1958). Plots for the garnets belonging to the paragneisses and schists are located in a more or less restricted part of the diagram. Plot numbers 1 and 2 are "enclosed and resorbed" garnet samples.

Graphite is a main constituent in the graphite schists; trains of small graphite particles however may be present in the metasediments including some of the para-amphibolites (St. 141690 and St. 141735).

Tourmaline crystals, very often zoned with a bluish-green core and a brown rim, are always present in accessory amounts. In sample St. 141691, a relatively old tourmaline vein was folded by F_2 (Plate I-c), while some larger unstrained crystals are post-F_2. Along the contacts of quartz bands with the paragneisses and schists, a rather widespread tourmalinization frequently occurs.

Zircons in variable amounts and dimensions (Chapter II) are generally well-rounded and have a frosted appearance. The smallest grains were encountered in the metapelites and metagreywackes (ca. 0.005 mm) and the larger grains in the metaquartzites. In thin section it is generally extremely difficult to distinguish between sedimentary zircon and monazite or xenotime.

Investigations of heavy mineral concentrations have indicated that strongly resorbed *monazite* and *xenotime* are often present in greater amounts than zircon.

Often the metasedimentary rocks contain significant quantities of *apatite;* the crystals are euhedral or subhedral. Other accessories are *rutile*, as euhedral and often twinned crystals in albite metablasts; *titanite*; *anatase*; *magnetite; ilmenite* and other *opaque minerals.*

Plagioclaseblast-bearing paragneisses. – Broadly two groups of metablastic paragneisses can be distinguished; the metablasts of both types are highly poikilitic but the assemblages of the mineral inclusions, as well as the composition of the hosts, are different.

The first and larger group of paragneisses contains xenoblastic oligoclases, which contain numerous small inclusions of quartz droplets (∅ : 5–20 μ) or irregularly shaped grains (Plate II-a and b) and in addition relatively small micas, sometimes in parallel orientation, resorbed opaque minerals and incidentally resorbed, zoned and turbid garnets. Generally the poikiloblasts are neither twinned nor zoned.

The second group contains ovoid albite or albitized oligoclase metablasts (∅ : 2–5 mm) which are clearly visible to the naked eye.

These paragneisses crop out in the northern part of the area, in the neighbourhood of the amphibole-bearing orthogneisses.

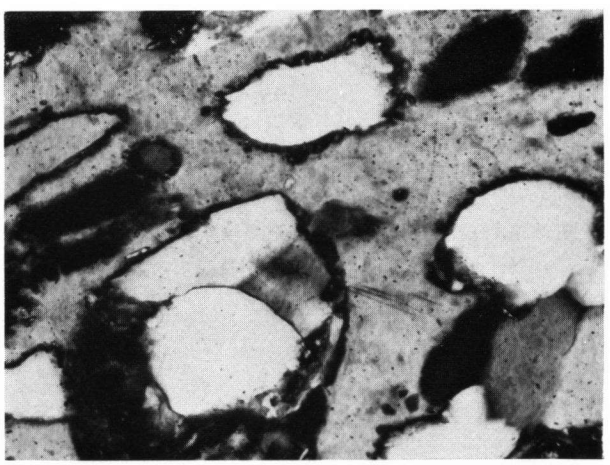

Fig. I-11. a. Corroded quartz inclusions in an albite metablast. The boundaries between the quartz grains are sharp (St. 141694, × 100).

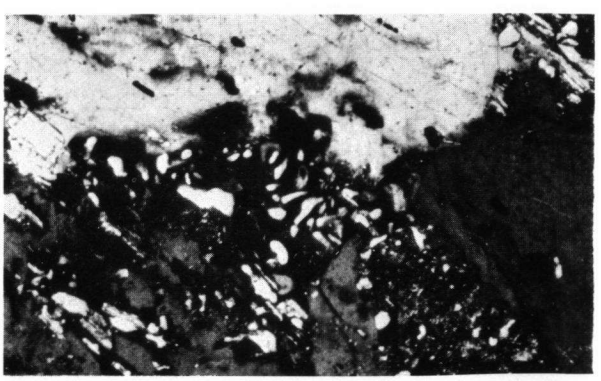

b. An incompletely albitized oligoclase metablast. The oligoclase relics still contain the characteristic quartz drops (St. 141694, × 75).

After the oligoclase metablastesis and just before F_2, the process of albitization as well as the development of albite metablasts started due to an important sodium metasomatism. The albites may have inherited the inclusions of oligoclase blasts with the exception of the small quartz droplets which completely vanished; the larger quartz grains show signs of resorption (Fig. I-11a). It is evident that in addition to a Na-metasomatism, albitization required the presence of some free silica. Those sections of the oligoclase blasts which are unaffected by albitization still carry the quartz droplets (Fig. I-11b) while the younger albite does not, but contains instead euhedral and often twinned rutile crystals in addition to the inherited inclusions. Albite metablasts enclosing rutile, garnet and zircon and often also micas, quartz grains and opaque minerals have also been reported by Floor (1966) from southern Galicia, as well as by graduate students working in the northern part of the "blastomylonitic graben". Some of the albites are twinned, generally along {010}; lamellar twins are rather scarce.

The occurrence of albiteblast-bearing paragneisses is a characteristic feature of the "blastomylonitic graben" (Floor, 1966, in southern Galicia, and Rubbens, 1963; Monster, 1967; Rijks, 1968 and van Tongeren, 1970, north of the present area). The albiteblast-bearing paragneisses are closely related to the alkaline orthogneisses, which provided the necessary Na for the albite blastesis.

Samples St. 141691 and St. 141692 are banded rocks, in which a weak second schistosity s_2 intersects the banding (s_1). In sample St. 141693 recumbent F_1-folds are clearly visible; F_2 resulted in an open folding with a weak crenulation cleavage (Fig. I-2).

Almost all the metablasts of the second group of paragneisses and only a few of the first group demonstrate an internal schistosity (s_i) with a variable orientation with respect to s_1 and s_2 as well as each other. Only in samples St. 141690 and St. 141693 is s_i partially oriented parallel to s_1; F_2 rotated some of the metablasts disrupting the parallel orientation.

It has been suggested (Avé Lallemant, 1965, p. 172) that the s_i of the metablasts are of pre-Hercynian origin. The rotations are caused by the successive Hercynian deformation phases (F_2 and F_3).

The oligoclase metablasts are generally xenomorphic and the micas (s_e)are bent around them.

Paragneisses with a hornfelsic appearance. – In the northern part of the area, very fine-grained linear paragneisses with a hornfelsic appearance (St. 141696) are exposed. Similar rocks have been reported by Monster further north. The extremely compact rocks have a granoblastic texture but the micas are to a great extent oriented. In a quarry, 200 m N of the road intersection at Val, this paragneiss is banded; the compact sub-vertical bands alternate with narrow mica-rich layers (St. 141695). The latter layers in turn are microbanded and may enclose isoclinal folds (Fig. I-4). In other localities it was found that a pronounced linear appearance of the rocks was caused by a weak s_2 crossing a barely visible banding (s_1). Laterally the paragneisses may grade into plagioclaseblast-bearing paragneisses.

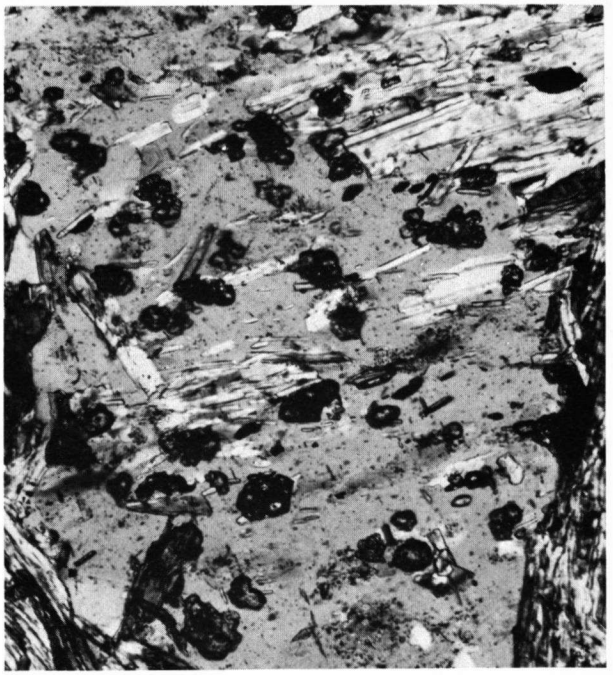

Fig. I-12. a. An albite metablast enclosing micas in parallel orientation (s_i) and resorbed garnets (St. 141693, × 80).

b. An adularia vein with chlorite vermiculae in albiteblast-bearing paragneiss, 2.7 km SE of Pte. Olveira, (× 500).

The "hornfelsic" paragneisses occur adjacent to the orthogneisses and thus the hornfelsic appearance of the former may be explained by contact metamorphic influences at the time of intrusion of the latter. But it seems more likely that the paragneisses owe their present texture particularly to their original quartzophyllitic character.

Besides differences in texture, the present rocks differ from the other paragneisses in that they are poor in *plagioclase* which furthermore is not metablastic. The rounded and frosted *zircons* are smaller compared with those in the metaquartzites and are slightly larger than the zircons in the plagioclaseblast-bearing paragneisses.

Metaquartzites. – Schists with a quartzitic composition are rather scarce in the central zone. The light-coloured, rather massive and planar rocks occur as bands of variable dimensions concordant within the paragneisses and schists.

East of Noya a larger zone has been found within the two-mica schists (see geological map). Mineralogically the rocks are very monotonous with *quartz* as the only main constituent together with varying amounts of *muscovite*. Quartz is generally highly undulose; in sample St. 141700 it has been flattened (F_2) almost perpendicularly to the main schistosity (s_1). Occasionally *feldspar* may be present in subordinate amounts.

The metaquartzites are characterized by the presence of relatively abundant, large *zircons* and *monazites* dispersed throughout the rock. The very fine-grained rocks have a granoblastic texture (Spry, 1968).

Graphite schists. – Intercalations of graphite schists, concordant with the regional schistosity, are scarce and small. Very narrow graphite bands, up to a few cm thick, may occur within the paragneisses; maximum dimensions of 0.5 × 2 m have been reported by von Metzsch (1964).

Sample St. 141702 is rich in muscovite; the thinly banded rock has been microfolded chaotically.

Very fine-grained *quartz* is always present as a main constituent. The quantity of *graphite* and *muscovite* is quite variable. A graphite-rich sample was investigated for microfossils in Strassbourg through the kindness of Prof. J. Cogné, but the results were negative.

Fig. I-13. A folded cummingtonite-bearing banded para-amphibolite. Some amphiboles in the fold crests are oriented parallel to the banding. Negative print; quartz and plagioclase are dark and amphiboles greyish (St. 141738, × 10).

Para-amphibolites. – A sedimentary origin can be assumed for only a few of the many amphibolites occurring in the metasedimentary rocks. A full account of all the amphibolites will be given on page 72.

Calc-silicate lenses. – Conformably enclosed in the para- and orthogneisses as well as in the migmatites and some granites, small and tough hornfelsic lenses have been encountered which after microscopic analysis appear to contain calc-silicate minerals and quartz. The grey-to-green very fine-grained to aphanitic lenses, with maximum dimensions of 20 × 50 cm, are finely layered due to differences in mineralogical composition. The composition of the different layers has been indicated in Table I-3.

It was found that biotite never appears together with pyroxene and hornblende. The central part of sample St. 141758 consists almost completely of pyroxene, while the outer rim is free of it. Sample St. 141754 was found enclosed in the biotite orthogneiss, 5 km SSE of Noya. It is mineralogically and texturally different from the other calc-silicates and possibly represents a product of assimilation or contamination; few similar rocks have been encountered elsewhere.

Mineralogy (*Table I-3*). – *Quartz*, highly undulose in some samples and unstrained (mosaic) in others, occurs together with basic *plagioclase* in the leucocratic layers.

Many lenses contain an almost colourless diopsidic *pyroxene*, which may be surrounded by *uralite* or *clinozoisite*. Variably coloured blue-green *hornblende* is often poikiloblastic and *garnet* occurs as atolls or more complex skeletons.

Other minerals are *biotite; opaque minerals;* "sedimentary" *zircon;* euhedral to subhedral *apatite; titanite; tourmaline* and *allanite*.

Biotite orthogneisses

The leucocratic and very fine-grained biotite orthogneisses owe their present texture mainly to a very strong deformation during F_1, which turned the pre-Hercynian granites into highly cataclastic linear and planolinear granite gneisses and mylonites. The subsequent Hercynian metamorphism caused a widespread metablastic recrystallization which resulted in the formation of aggregates of more or less optically oriented quartz, feldspars and biotite. Due to later deformations (F_2 and F_3), the effects of the primary recrystallization have been partially or completely obliterated. Many orthogneisses became mylonitic again, especially where F_3 was effective. The "second" mylonitization was most prominent near the western fault-zone and in the northeast. When present, the feldspar phenocrysts were reduced to small "augen" or completely crushed (Fig. I-15a and Plate III-d).

Quartz recrystallized in the stress-shadows of the eyelets and in the tension cracks of some porphyroclasts (St. 141718); in some cases, an almost completely recrystallized post-F_3 quartz occurs together with moderately optically oriented feldspar aggregates and micro-crystalline mortar zones consisting of quartz, feldspar and biotite.

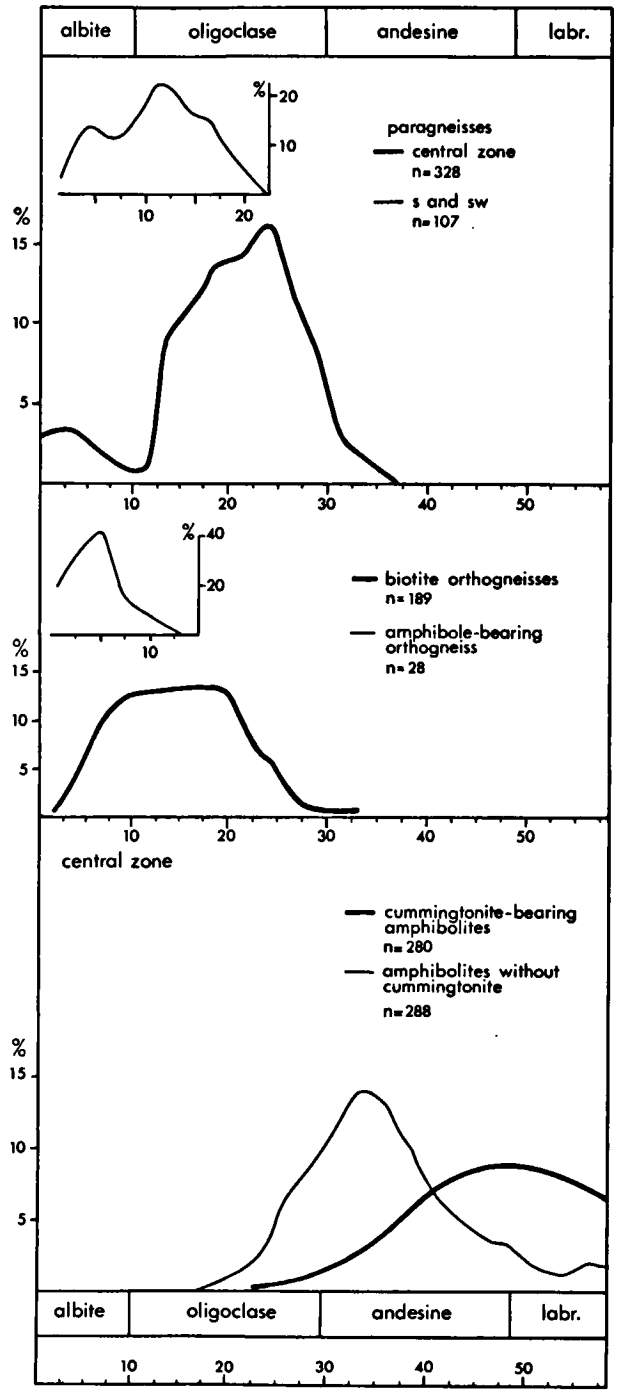

Fig. I-14. Anorthite percentage frequency curves of plagioclase in paragneisses, orthogneisses and amphibolites.

Near wrenchfaults and around boudinaged amphibolite lenses, the foliation of the gneisses may deviate. Especially in the area around Barquiña the subsequent tectonic activities were pronounced. Carlé (1945, p. 23) gave the following account of the rather intricate relations between orthogneisses and amphibolites: "Auf der Halbinsel von Barro, 1 km nördlich von Noya, enthält 155° streichender und 50° W fallender Biotit-gneiss teils concordant teils unregelmässig begrenzte, jedoch stets gleichmässig verschieferte Amphibolitschollen. Warscheinlich händelt es sich um einen nachträglich in seiner Gesamtheit verschieferten Intrusionsverband."

The biotite orthogneisses can be subdivided into linear, planolinear and augen-bearing varieties (Plate III). In addition, the biotite content of the orthogneisses is variable (Fig. I-16). Some types are quite leucocratic and linear (St. 141722, St. 141726) and may contain relatively large metablastic albites or plagioclase with a low An-content. These aplogranitic varieties and some intrusive aplites, pegmatites (Fig. I-17a) and relic quartz veins (as "rootless folds") are the scarce symptoms of relatively late-magmatic activities in the pre-Hercynian granite series.

The presence of a hornblende-biotite orthogneiss variety within the biotite orthogneiss as exemplified by a find near Noya is rather exceptional; similar rocks have been described by Floor (1966, p. 115). The hornblende-bearing biotite orthogneiss (Noya) is texturally (blastomylonitic) and mineralogically (plagioclase 20–24 % An) more closely related to the biotite orthogneisses than to the biotite-ferrohastingsite orthogneisses in the north (see p. 74).

Mineralogy (*Table I-2*). – *Quartz* is either completely crushed in zones or elongated and highly undulose with irregular outlines or mortar rims, or has partly or completely recrystallized into relatively coarse-grained mosaics (Plate IV-a and b).

The orthogneisses contain more *alkali feldspar* than *plagioclase*. Original alkali feldspar megacrysts were reduced to small eyelets or completely crushed during mylonitization. The individual grains often have mortar rims. The "augen" are often twinned according to the Carlsbad law; they may enclose small plagioclase crystals. Different types of perthite (see p. 95) and cross-hatching are always present.

Plagioclase (5–25 % An, see also Fig. I - 14) is often twinned along {010} and {001}, and weakly zoned. Simple twins are subordinate; however some of the multiple {010} twins may probably be regarded as secondary or deformation twins (Vance, 1961). Some plagioclases are metablastic and enclose quartz drops. Myrmekite and a small-scale albitization of alkali feldspar is present. Some biotite orthogneisses carry many relatively young albites, often simply twinned; it is a phenomenon that characterises most of the amphibole-bearing orthogneisses (Rubbens, 1963, Monster, 1967; see p. 74).

Biotite was finely crushed during mylonitization (F_1), but has recrystallized afterwards (metablastic recrystallization). Later deformations, especially F_3, have locally crushed the biotites again. Biotite is often partly altered into *chlorite*. *Muscovite* may appear in the orthogneisses close to the Hercynian two-mica granites in the E (St. 141721) and S. Zoned *allanite* is almost always present. The brown pleochroic crystals are partly or completely altered into orange-brown isotropic relics. *Epidote* may occur as secondary rims around allanite, in biotite and plagioclase. Other accessory minerals are *opaque minerals;* idiomorphic *zircon; apatite; fluorite; titanite; rutile; tourmaline* and *garnet* (Fig. I-25).

Investigation of heavy mineral concentrates revealed that the orthogneisses are generally free of *monazite* and *xenotime* in contrast to the other granites, gneisses and schists of the area.

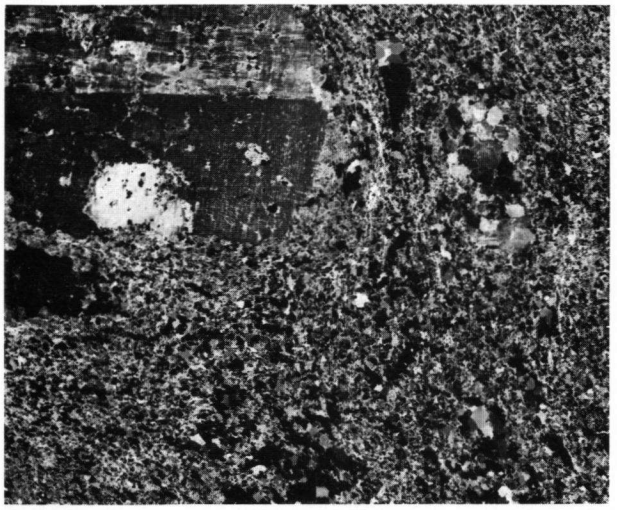

Fig. I-15. a. A twinned megaclast in aphanitic groundmass in which a cataclastic cluster of microcline and recrystallized (mosaic) quartz is visible. Biotite orthogneiss 2 km WSW of Pte. Beluso (× 4).

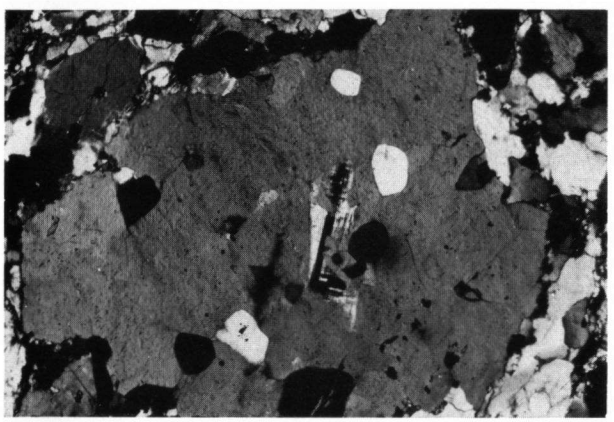

b. Albite metablast in per-alkaline orthogneiss (St. 109739). The relatively young albite encloses resorbed microcline and quartz grains (× 130).

St. 141727 is a sample of a blastomylonitic hornblende-biotite orthogneiss. *Hornblende* has the following optical properties: $2V_{\alpha} = 56°, 59°$; r > v strong; y = 1.695 ± 0.005, colour: intense blue-green.

Amphibolites

A characteristic feature of the central zone is the presence of numerous amphibolitic lenses. The paragneisses contain more amphibolites than the biotite orthogneisses, while the two-mica schists E of Noya have very few and the amphibole-bearing orthogneisses are completely devoid of amphibolites.

In places as many as 10–15 concordant lenses may be encountered within a 50 m tract perpendicular to the schistosity. Generally the width of the lenses is approximately 1 m; length-width ratios could only be measured in a few locations and they were found to vary between 20 and 100. The largest amphibolite exposure was found along the coast N of Barquiña (length > 300 m and width ≈ 15 m).

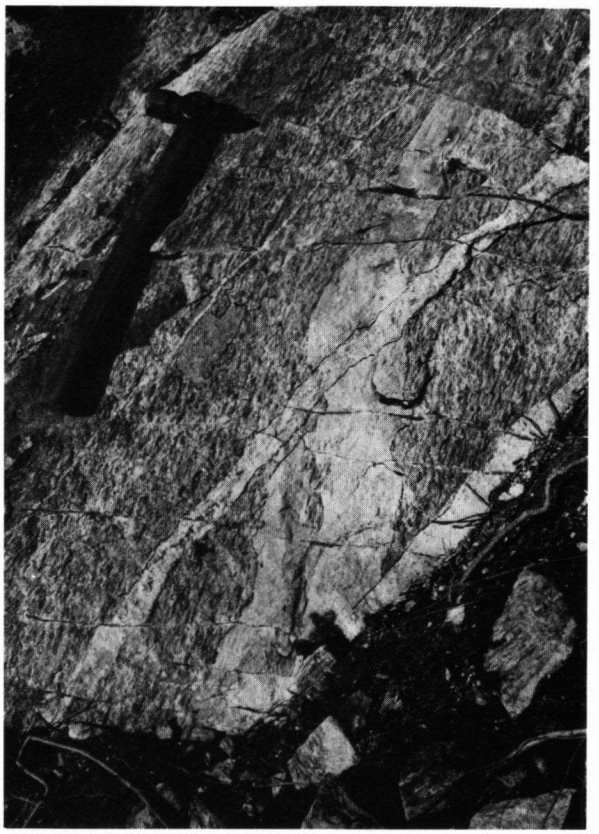

Fig. I-16. Planolinear orthogneiss (St. 141722) cut by a linear aplite gneiss (St. 141723) and Hercynian pegmatite and aplite (pre-F_3). A set of tension joints partly acted as dextral tearfaults.

The amphibolites are easily recognized in the field because of their dark green colour, an orange-brown weathering profile and a close joint system (i.e. many tension joints). The rocks are usually fine-grained, homogeneous and have a linear texture, although occasionally planar or hornfelsic varieties occur; some amphibolites have leucocratic eyelets up to 4 mm across. In the southern part of the area several amphibolites have a conspicuous greenish-grey colour. Thin section analyses revealed that these lenses contain large amounts of cummingtonite.

With a few exceptions it is extremely difficult to distinguish between para- and ortho-amphibolites both in the field and by thin section analysis, but an attempt has been made to do so.

Criteria that may indicate a sedimentary origin are e.g. a marked banding with compositional differences from one layer to the other, the striking similarity between the metablastic plagioclases of some amphibolites and the metablastic paragneisses (Floor, 1966, p. 169), the presence of graphite (Avé Lallemant, 1965, p. 153) or "sedimentary zircon", and a relatively high quartz and/or apatite content.

It is believed that most of the amphibolites have an igneous origin, especially those occurring in the biotite orthogneisses. In a few cases an intrusive relationship

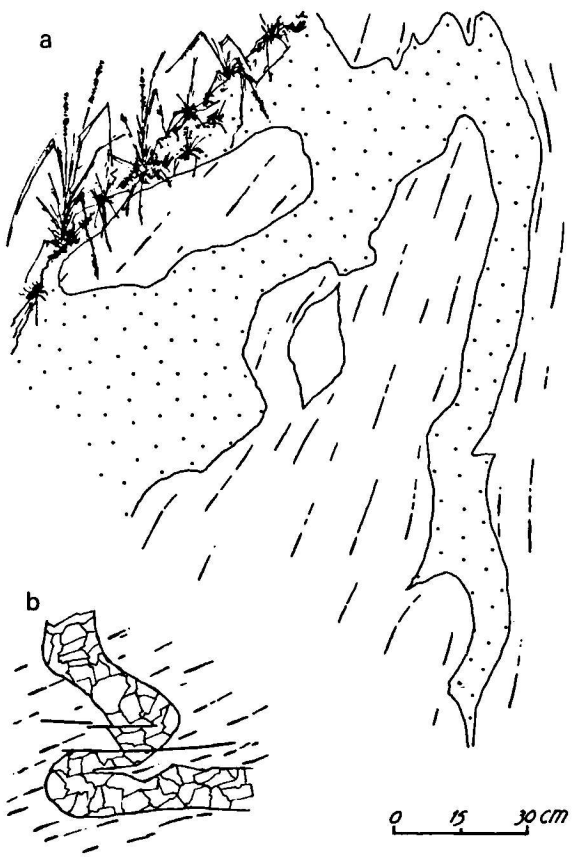

Fig. I-17. a. An intrusive relationship between an orthogneiss and an ortho-amphibolite (dotted), 1.9 km SE of Sierra de Outes (sub-vertical exposure). b. A folded old pegmatite in a planolinear orthogneiss near Noya. A N-S directed fracture cleavage (F_3) is present (sub-horizontal exposure). c. A banded garnet-bearing pegmaplite in a planolinear orthogneiss 1 km N of Barquiña. The photo shows a part of the undeformed pegmaplite.

could be recognized (Fig. I-17a and Avé Lallemant, 1965, p. 153), but generally the more competent amphibolites were boudinaged and transposed during the Hercynian orogeny, so that the genetic relationships are obliterated. The presence of a metaporphyritic structure is a clear indication that some of the amphibolites are metamorphosed basic dykes (Plate IV -c and d). The relic structure is either represented by leucocratic eyelets consisting of plagioclase grains (St. 141741 and St. 141745) or melanocratic clusters composed of hornblende (St. 141747 and St. 141748).

Mineralogy (including the para-amphibolites; see Table I-3). – *Quartz* is often present in subordinate amounts; the highest percentages (measured by point-counting) vary between 4% for some cummingtonite amphibolites to 9% for St. 141636, a banded para-amphibolite.

Plagioclase is always a main constituent in the amphibolites. It occurs dispersed throughout the rock and is often finely intergrown (St. 141744) with hornblende.

Metaporphyritic amphibolites contain leucocratic eyelets, which are composed of plagioclase grains that may enclose biotite flakes (St. 141745) or garnet (St. 141741).

In para-amphibolites the plagioclase may be concentrated in layers (St. 141736, St. 141738). Metablastic plagioclase is usually subordinate (St. 141735) or lacking, although it is abundant in sample St. 141742. The metablasts include small hornblende laths in parallel orientation, with s_i perpendicular to s_e. The plagioclases are inversely zoned and polysynthetic {001} and {010} twins are common. The anorthite content of the plagioclase in the cummingtonite-bearing amphibolites (30–>70 % An) is higher than that in the ordinary amphibolites (25–50 % An, Fig. I-14).

Blue-green hornblende is the most important constituent in all amphibolites with the exception of a few cummingtonite amphibolites (St. 141738). The quantity of hornblende in common amphibolites varies from 50–64 % (results of point-counting) and in cummingtonite-bearing amphibolites from 39–52 %.

Small and somewhat older laths of hornblende form the s_i pattern for some plagioclase metablasts; usually however the hornblendes are concentrated in bands and clusters or dispersed throughout the rock, always more or less oriented with [001] parallel or sub-parallel to the tectonic B_1-axis (F_1). Masses of very small euhedral to subhedral hornblende grains intergrown with xenomorphic plagioclase typify the compact and tough amphibolites with a hornfelsic appearance (St. 141744); they are probably metamorphosed basaltic dykes.

St. 141749 is almost a hornblendite and consists mainly of medium-grained hornblende poikiloblasts.

The intensity of the pleochroic colours (α: yellowish, β: olive-green and γ: blue-green) varies slightly; hornblendes of sample St. 141736 are pale blue-green (γ); $2V_\alpha = 71–82°$, $\gamma \wedge c = 16–20°$ and $\gamma = 1.663–1.679 \pm 0.005$.

Cummingtonite developed at the expense of hornblende and is an important indication of the decrease in pressure during metamorphism. Transformations of hornblende into cummingtonite are irregular (Fig. I-6), and only occasionally parallel to their crystallographic elements {001} or {100}. Relatively large crystals, oblique to the schistosity s_e, are frequent.

Cummingtonite is colourless, and has a higher birefringence than hornblende; $2V\gamma \sim 85°$, $v \gg r$; twinning is frequent. The cummingtonite-bearing amphibolites contain 3–18% cummingtonite. In sample St. 141738 hornblende is almost absent.

Biotite is usually a minor constituent or absent, but percentages up to 17 % have been counted upon occasion. The mineral, when dispersed throughout the rock, has a better parallel orientation with respect to s_e than hornblende.

Resorbed *garnets* are found in a few amphibolites (St. 141744). They are embedded in plagioclase (Fig. 1–5b) and are never in contact with hornblende. Data for n(Na) and a_0 (Fig. I-25) indicate that the composition differs from that of the garnets from the paragneisses.

A colourless diopsidic *pyroxene* has been encountered in sample St. 141736; the xenomorphic grains are concentrated in layers. $2V\gamma = 55–60°$, $r > v$ and $\gamma \wedge c = 40–44°$; a multiple twinning is present. The pyroxenes are partly surrounded by or intergrown with pale blue-green hornblende.

Titanite occurs as clusters or as euhedral crystals in variable amounts; when enclosed within hornblende, it often displays pleochroic haloes. Some amphibolites include *apatite* as large anhedral crystals or in bands.

Zircon, with a sedimentary appearance, has been found in St. 141736 and St. 141738.

Other minerals are *opaque minerals; rutile; graphite*, indicating a sedimentary origin, and secondary *muscovite, chlorite* and *epidote;* the latter mineral is often found in veinlets.

Amphibole-bearing orthogneisses

The group of amphibole-bearing orthogneisses distinguishes itself from the biotite orthogneisses by the absence of amphibolite lenses and by the fact that they generally crop out as isolated bodies. Their occurrence in the Galician "blastomylonitic graben" is restricted to the northern (Rijks, 1968, Monster, 1967 and Rubbens, 1963) and southernmost sections (Floor, 1966); the present area covers the southern extremities of the former.

The amphibole-bearing orthogneisses in the northern parts of the area can be subdivided into the biotite- ferrohastingsite orthogneisses and the astrophyllite-bearing riebeckite-aegirine orthogneisses.

After the metablastic recrystallization following F_1, the present group of orthogneisses was severely deformed by F_2 and F_3. Near important faults the gneisses were greatly altered and may have turned into cataclasites (St. 141734). The fabric of the gneisses is comparable with that of some of the aplogranitic biotite orthogneisses and is characterized by the presence of relatively large albites.

Biotite-ferrohastingsite orthogneisses. – NNE of Val, a tongue-shaped orthogneiss body is exposed consisting megascopically of a leucocratic amphibole-bearing orthogneiss, more or less as a border zone around a melanocratic amphibole-rich orthogneiss. The leucocratic variety has ferrohastingsite and biotite as ferromagnesian minerals, while the melanocratic variety contains a deep blue-green hornblende in addition to ferrohastingsite and locally biotite. In the leucocratic border facies, a few riebeckite-bearing intercalations also occur.

The fine-grained to aphanitic rocks are variably cataclastic. The presence of younger simply twinned albite porphyroblasts is a characteristic feature.

Mineralogy (*Table I-2*). – *Quartz* and alkali feldspar are present in variable amounts, but are generally main constituents in only the leucocratic varieties. Quartz is often absent in the melanocratic varieties.

Plagioclase is represented by albite. The clear, often simply twinned grains may enclose small particles of titanite, apatite, amphibole, quartz and occasionally corroded microcline.

Strongly coloured blue-green *hornblendes* may be present together with *ferrohastingsite*. The latter has a much smaller $2V_\alpha$, a greater dispersion and a higher refractive index than the common hornblendes. The following properties were found for ferrohastingsite in sample St. 141860: $2V_\alpha = 15–30°$; $r \gg v$; $\gamma = 1.710 \pm 0.005$, colour: dark blue-green.

Titanite is always present and may be a main constituent in some of the melanocratic varieties. The mineral occurs as individual crystals, clusters of small grains or streaks.

Opaque minerals are *magnetite* and *ilmenite;* the former is important in the highly altered orthogneisses. *Limonite* may also occur.

Allanite is generally changed into an orange-coloured isotropic alteration product which may still display the original zoning. Allanite is often surrounded by a pleochroic halo and by secondary *epidote*.

Relatively large *zircons* are present in significant amounts in the leucocratic varieties; they have a simple idiomorphic morphology.

Other accessory minerals are *apatite; fluorite* and *garnet*.

Per-alkaline orthogneisses. – The astrophyllite-bearing riebeckite-aegirine orthogneiss body, of which the southern extremities are exposed E of Pte. Olveira (Rubbens, 1963), is a medium-grained to aphanitic severely deformed rock and is mineralogically very similar to the Galiñeiro-type per-alkaline orthogneiss S of Vigo (Floor, 1966, p. 39). The successive Hercynian deformations affected all of the rock-components. Relatively large albite porphyroblasts have rounded outlines and are surrounded by mortar rims consisting of quartz, alkali feldspar, riebeckite, aegirine and astrophyllite. Along the mortar structures, alteration of the dark minerals and albitization of microcline took place.

In addition to the large single body, some small riebeckite orthogneiss intercalations (St. 141733) have also been encountered in the leucocratic ferrohastingsite orthogneiss border zone.

Mineralogy (*Table I-2*). – Strained *quartz* and *microcline*, both generally aphanitic with variable grain sizes, together form the groundmass. Many alkali feldspars are cross-hatched, while others enclose string and film perthite. Perthitization

often started from the grain boundaries. Myrmekite has not been encountered. Albitization around the grain boundaries is frequent. Some relatively young and large *albites* enclose corroded microcline (Fig. I-15b), as well as small grains of quartz, aegirine, riebeckite, astrophyllite, zircon and biotite. The albites are often simply twinned along {010}; incidental complex twins occur.

Riebeckite and aegirine were severely crushed by F_2 and F_3 and may have ragged outlines. *Riebeckite*, only idiomorphic to hypidiomorphic in basal section when enclosed in albite, has the following properties: α = dark prussian blue; β = light brown and γ = dark indigo blue; absorption: $\gamma \geqslant \alpha \gg \beta$; $\alpha \wedge c$ = very small and γ = b; basal section has negative elongation; the mineral displays a high dispersion and often an anomalous extinction. The properties correspond with those of *osannite* (Tröger, 1959).

Aegirine is weakly pleochroic in green and has $2V\gamma \approx 70°$ and $r < v$. The best examples of the fibrous *astrophyllite* are visible when this mineral is enclosed within albite.

The optical properties are: α = dark orange, β = yellow and γ = lemon yellow; $2V \approx 90°$ with $r < v$ strong.

Other minerals are: relatively large but crushed *zircon;* xenomorphic *xenotime; opaque minerals; fluorite; pyrochlore* and *biotite*. It is not impossible that the riebeckite gneiss intercalations occurring in the ferrohastingsite orthogneiss may contain a *sodic hornblende* with arfvedsonitic properties.

Fig. I-18. An andalusite schist inclusion in the medium to coarse-grained two-mica granite (Barbanza granite). The original mica schist has been completely metamorphosed into a tough andalusite granofels (Mt. Iroite).

Schists, paragneisses and amphibolites in the south and southwest

In the southern part of the area, west of the Río Coroño, non-migmatic metasediments are exposed which appear quite different from the paragneisses and schists belonging to the central zone. A separate treatment of these rocks is therefore warranted.

Apart from the andalusite schists, the predominant rock-types in this part of the area comprise mica- and tourmaline-bearing quartzitic schists, metaquartzites and graphite schists. The quartz-rich rock-types contain relatively large amounts of apatite and tourmaline. Some rocks were eventually almost completely tourmalinized. Only a few feldspar-rich metasediments have been encountered. The feldspars are almost always plagioclase metablasts. A very few conformable amphibolitic bands are present.

Fig. I-19. A banded muscovite-bearing metaquartzite 2.5 km WNW of Boiro. The recumbent disharmonic and isoclinal F_1 – folds are clearly visible.

In the southern part of the present area the rocks occur more or less in situ. This unit is bordered by a fault-zone to the east, by the syn-kinematic medium to coarse-grained two-mica granite (Barbanza granite) to the north and by the Caldas de Reyes granite, a post-kinematic granite to the south. Further north the rocks are found in the two-mica granite as many, sometimes large, inclusions (Mt. Iroite; Abelleira, Avé Lallemant, 1965).

Similar metasedimentary rocks (Fig. I-1) have been reported further north by Avé Lallemant (1965), de Graaff (1962) and Koster van Groos (1962), from the Barbanza Peninsula by von Raumer (1963) and to the south by Hensen (1965) and Vogel (1967). Possibly they may even be correlated with the zone of metasediments SW of Vigo and in northwestern Portugal.

Evidence of deformation and metamorphism

Nearly all rock-types under discussion demonstrate a marked banding (Plate V-a and b; Fig. I-19) which, in some cases, may have been an original sedimentary layering. The layers are generally very thin (1–5 mm) for the mica-rich rock-types, while the metaquartzites are more coarsely banded (up to several cm wide). Transitions from one layer or from one rock-type to another are generally abrupt. The rocks of the present series are not only different from the metasediments of the central zone in their mineralogical aspects, but also in structural appearance (Fig. I-20).

The present series was subjected to all Hercynian

orogenic phases and probably suffered no previous orogenic events. A strongly developed first Hercynian deformation (F_1) resulted in recumbent disharmonic and sometimes isoclinal folds (Fig. I-19; Plate V-a and b). The axial planes are generally parallel to the local layering (schicht-parallele Schieferungs-Fläche, von Raumer, 1963). With a few exceptions (some massive metaquartzites), the micas have recrystallized parallel to the axial plane. The present attitude of this important schistosity is sub-horizontal, while the fold-axes are variably oriented around a NW-SE axis.

A second Hercynian deformation (F_2) resulted from a similarly oriented stress-field but was less penetrative. F_2 barely affected the massive quartzitic rocks, but small open folds are found in the thinly laminated and mica-rich rocks, locally accompanied by a sub-vertical crenulation cleavage (Plate V-a). A third Hercynian phase of tectonic activity, again the result of a similar stress field, was even weaker and locally caused a further deformation producing a disruption of originally more coherent textures (the metablasts moved relative to each other). The older NW-SE structures were bent into a NNW-SSE or N-S position (Figs. I-20, I-21 and geological map).

The presence of a possibly Hercynian pre-F_1 deformation is suspected in only a very few locations (Plate V-b). Sample St. 141864, a tourmaline-bearing metaquartzite, was folded by F_1; the crest of this fold reveals the presence of an older lineation.

As in the rocks of the central zone, the Hercynian regional metamorphism of these metasediments culminated after the first deformation phase. In this case however the mineral assemblages are:
pelitic rocks: quartz + muscovite + chlorite; biotite + muscovite + andalusite + quartz; albite + muscovite + chlorite + quartz
basic rocks: blue-green hornblende + plagioclase (An 40 %) ± quartz

The regional metamorphic mineral assemblages are indicative of the highest grades of the greenschist facies or, according to Winkler (1967), the quartz-andalusite-plagioclase-chlorite sub-facies of the greenschist facies in the Abukuma low-pressure facies series.

The low-grade syn-kinematically metamorphosed rocks locally suffered a superimposed contact-metamorphism corresponding with the hornblende-hornfels facies and coinciding with the emplacement of the parautochthonous two-mica granites (Barbanza granite).

The second deformation immediately followed the emplacement of the two-mica granites, as will be discussed later; F_2 folded the mica-rich rocks, causing a local crenulation cleavage (s_2). Directly afterwards a new generation of andalusite poikiloblasts formed that grew in the newly formed cleavage planes. The latter generation of andalusite crystals is an unstrained post-kinematic type (Plate V-a); it has also been reported by Avé Lallemant (1965, p. 151) with respect to the schist inclusions near Abelleira, 3 km W of Esteiro.

Some quartz-bearing metapelitic inclusions in the Barbanza granite suggest even more extreme hornfelsic conditions, indicative of the beginning of the alkali feldspar-cordierite-hornfels facies (Winkler, 1967). Besides quartz, biotite, andalusite and sillimanite, both muscovite and alkali feldspar (metablasts) are co-stable (Fig. I-22; sample St. 141715).

The combination of the reaction 1 muscovite + 1 quartz ⇆ 1 alkali feldspar + 1 andalusite/sillimanite + 1 water and the phase transformation andalusite ⇄ sillimanite may require, according to Winkler (p. 70), a $P(H_2O) \geqslant 2000$ bar and a temperature of about 640 °C or, according to Fig. 1 of Hietanen (1967), a $P(H_2O) \geqslant 3500$ bar and a temperature of about 580 °C.

Thin section analyses show clearly that sillimanite grew mainly at the expense of biotite. However, alkali feldspar may also be produced during fibrolitization of biotite. Shelley (1968) has suggested the following reaction: 1 aluminous biotite + 2 quartz = 2 alkali feldspar + 1 sillimanite + 2 water + 5 iron oxide.

The presence of cordierite could not be proven in the hornfelsic inclusions, nor has von Raumer found any in the metasediments further west (von Raumer, 1963).

The process of retrogradation started after F_2 and was accelerated by F_3. Evidence of retrogradation includes a strong sericitization of andalusite, as well as chloritization of garnet and epidotization of hornblende (St. 141763).

Mica-bearing and tourmaline-bearing metaquartzites. – St. 141703 is a thinly banded (1–5 mm) muscovite-chlorite quartzitic schist (Plate V-a), clearly demonstrating a first Hercynian schistosity that was refolded by the second deformation causing a crenulation cleavage. Large post-kinematic (post - F_2) andalusite xenoblasts (Barbanza granite influence) developed in the cleavage planes.

The granoblastic *quartz* is very fine-grained. Very small *muscovite* laths occur dispersed throughout the quartzitic layers together with an almost colourless *chlorite* (non-anomalous greyish polarization colours) in the mica layers. *Sericite* occurs as irregular spots in the specimen and as rims around andalusite.

Tourmaline is almost always present in all types of metasediments. Locally, however, the rocks are highly tourmalinized, probably replacing (almost) all the pre-existing biotite.

St. 141704 is an apatite and tourmaline-bearing metaquartzite. Tourmaline is generally zoned with a clean and idioblastic core and a poikilitic and xenoblastic rim (Fig. I-23); the reddish-brown tourmaline crystals are perfectly oriented parallel to a lineation caused by F_2.

The size of the quartz grains in the quartz layers varies widely. The highly strained grains contain trains of small two-phase inclusions.

Apatite is also an important constituent of the tourmaline-bearing metaquartzites (Fig. I-23).

St. 141705 is a folded (F_2?) tourmaline schist, with layers of very fine-grained to microcrystalline quartz alternating with light brown poikiloblastic tourmaline layers. Secondary bluish-green tourmaline is also present.

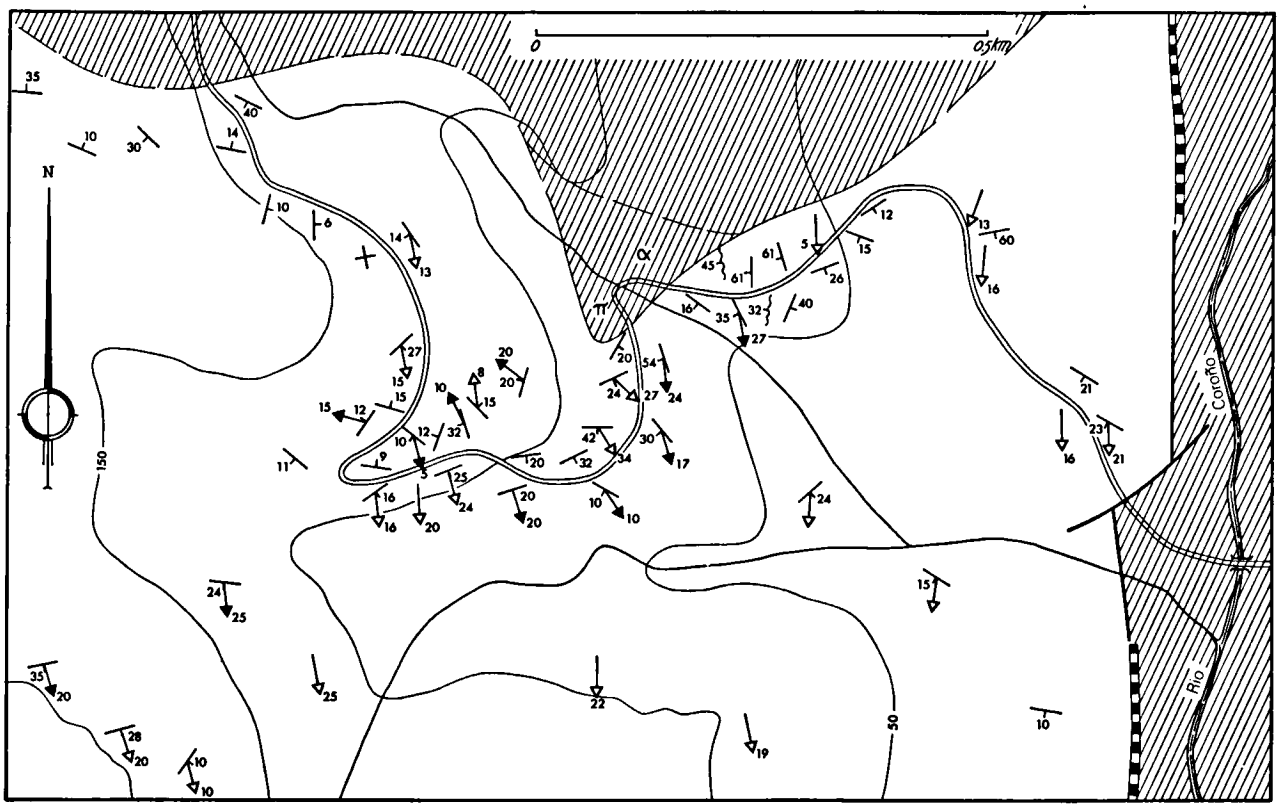

Fig. I-20. A structural detail-map of the metasedimentary rocks WNW of Boiro. The measurements represent F_1 – schistosities (main schistosities) and two F_2 – crenulation cleavages. The arrows indicate F_1 fold-axes (closed) and F_2–lineations (open).

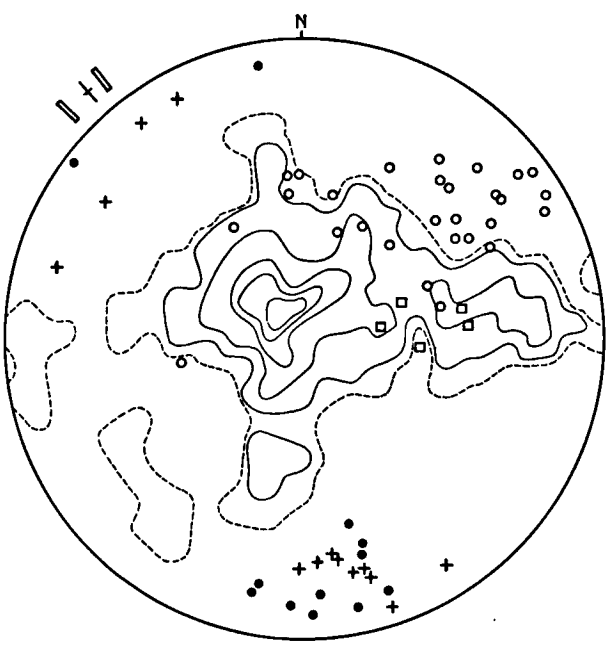

Fig. I-21. Lower hemisphere projections of the poles of the main schistosities (contoured), F_1 fold-axes (closed dots), F_2-lineations (crosses) and the poles of some crenulation cleavages (squares). The open circles indicate the poles of schistosity planes of the metasedimentary inclusion at Mt. Iroite. The direction of foliation of the surrounding Barbanza granite has also been indicated.
Contours at 2, 5, 8, 11 and 14% per 1% area (N = 92).

Graphite schists. – Many intercalations of graphite schists and graphite-bearing schists have been encountered. These rocks are generally very fine-grained and yield important structural information. St. 141707 and St. 141706 contain well-developed first-phase folds (Plate V-b).

In addition to *quartz* and *graphite*, the schists also contain variable amounts of *muscovite*, *tourmaline* and *biotite*.

A search for the presence of micro-fossils in two samples was negative (see also p. 70).

Magnetite-bearing schists. – The mineral *magnetite* has frequently been encountered in the present metasediments; sample St. 141708 includes *biotite* and *muscovite* together with large amounts of this mineral. The sub-idiomorphic grains are dispersed throughout the very fine-grained rock. Other minerals are sub-idiomorphic *apatite;* large rounded *zircons* (width up to 100 μ) and *monazites; tourmaline* and a little *feldspar.*

Andalusite-bearing schists. – Most of the schists crowded with andalusite occur close to the granite contacts or as xenoliths in the Barbanza granite as well as in the Caldas de Reyes granite.

The poikiloblastic late syn-kinematic *andalusite* crystals of samples St. 141709, St. 141710 and St. 141711 are highly sericitized; remnants of a chiastolitic cross are sometimes present.

Quartz may occur in thin bands alternating with *biotite* and *muscovite* parallel to the main schistosity plane (s_1). Sample St. 141710 contains remnants of an older possibly Hercynian deformation: trains of very small *opaque mineral* particles (mainly *graphite*) in parallel orientation.

The main schistosity was affected by a second deformation; sample St. 141709 clearly reveals the resulting crenulation effects.

Sample St. 141711 is an example of a garnet-bearing andalusite granofels where the schistosity can barely be recognized, except for a parallel orientation of some opaque mineral grains in the now completely sericitized andalusite poikiloblasts. The sample also contains large muscovite flakes which developed in the sericite masses.

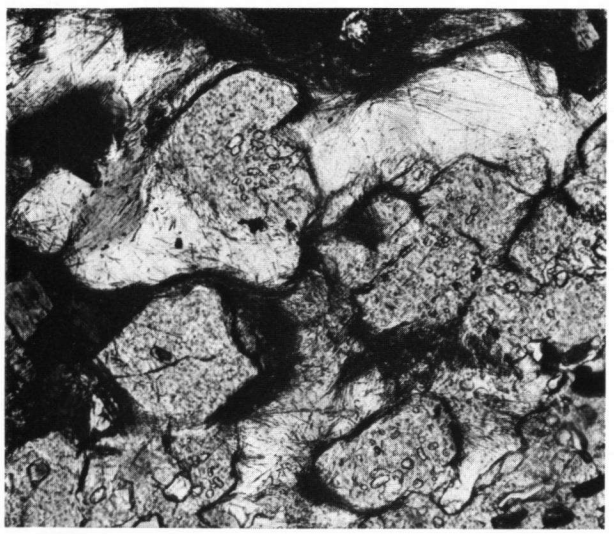

Fig. I-22. a. Phase transformation andalusite → sillimanite. Fibrolitic sillimanite surrounds poikilitic andalusite (St. 141715, × 100).

b. Metablastic alkali feldspar and fibrolitic sillimanite have grown at the expense of micas and quartz (St. 141715, × 100).

Apatite-, tourmaline- and magnetite-bearing paragneisses. – Sample St. 141712 is a muscovite-chlorite-magnetite-bearing metablastic paragneiss. *Muscovite* and the numerous *plagioclase* metablasts (albite-acid oligoclase) enclose trains and micro-folds of tiny mineral particles which probably belong to a deformation older than F_1 (Plate V-c).

Magnetite, often idiomorphic, seems to have grown during a relatively long period. The smallest crystals are often found as inclusions in the plagioclase metablasts together with small muscovite laths, while the larger crystals are more confined to the mica zones. *Apatite* is an important accessory.

Sample St. 141713 is quite similar to the former, but it contains less mica. Traces of a pre-F_1 deformation are present in *albite* metablasts and *muscovite*. *Apatite* and *tourmaline* sometimes appear as inclusions in the metablasts together with quartz and muscovite. Tourmaline has a bluish-green colour and is often zoned. Apatite occurs dispersed throughout the entire rock but is also concentrated in layers.

Sample St. 141714 is a banded apatite-tourmaline-magnetite-bearing paragneiss. Medium-grained *plagioclase* layers (3–20 % An) alternate with layers containing zoned bluish-green *tourmaline*, *magnetite* and *muscovite* or *apatite*. Magnetite and *biotite* are partly concentrated in the transition zones between the layers. Plagioclase blasts in the melanocratic layers show traces of an older deformation.

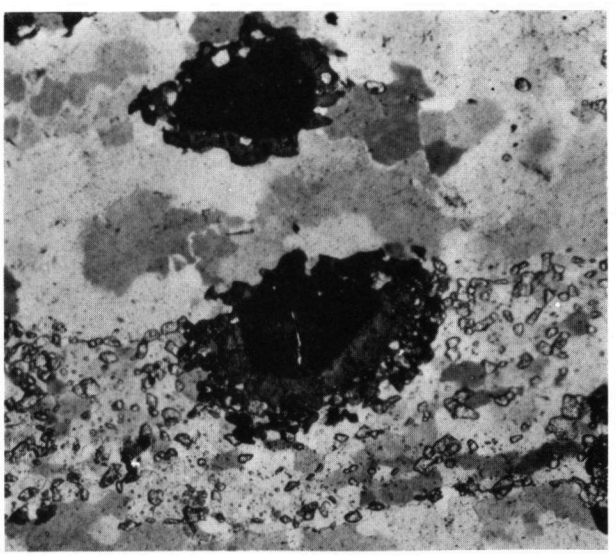

Fig. I-23. Tourmaline, idiomorphic core and xenomorphic rim, and anhedral grains of apatite, concentrated in layers (St. 141704, × 65).

Alkali feldspar- and sillimanite-bearing andalusite schists. – Samples St. 141715 and St. 141716 are banded schists with *andalusite* poikiloblasts which, in St. 141716, have grown post-kinematically with respect to the crenulation cleavage planes (s_2). *Sillimanite*-fibrolitic wisps have grown from biotite and andalusite (Fig. I-22a).

Alkali feldspar metablasts have inclusions of andalusite, quartz and small muscovite laths.

Some *biotite* and *muscovite* have grown perpendicular to s_1. *Plagioclase* (7–18% An, Fig. I-14) is subordinate and *quartz* is mainly restricted to layers.

Amphibolites. – In contrast to the central zone only a few amphibolites have been encountered in the metasediments in the SW. The concordant amphibolite intercalations are well-layered.

The amphiboles are blue-green *hornblendes* which, in sample St. 141750, have very deep pleochroic colours, $2V_x$ varying from 40–55° and strong axial dispersion ($r \gg v$).

Sample St. 141752 contains radially arranged hornblendes (max. length 0.8 mm; Fig. I-24); a similar amphibolite has been reported by Priem (1962) from Northern Portugal. Hornblende in sample St. 141751 is microcrystalline, but in sample St. 141750 many individual laths vary in length from 1–3 mm.

Fine to medium-grained *epidote*, occurring in lenses, is a main constituent in samples St. 141753 and St. 141750; sample St. 141753 is a retrograded epidote-quartz-chlorite rock with relics of hornblende. Other minerals are *plagioclase; quartz; opaque minerals;* subhedral and sometimes large *apatite; titanite* and *muscovite.*

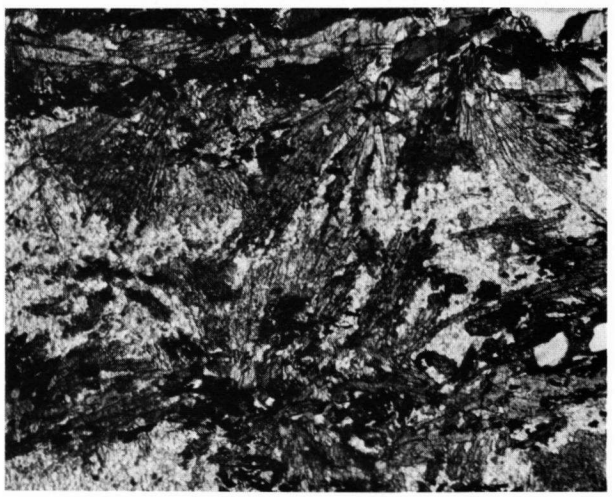

Fig. I-24. A banded amphibolite with blue-green hornblende rosettes oblique to the banding (St. 141752, × 40).

THE MIGMATIC ROCKS

At the present exposure level, the Hercynian regional metamorphism locally caused conditions which led to a widespread migmatization of quartzo-feldspathic rocks. Macroscopically different stages of mobilization (Mehnert, 1968) are clearly visible; laterally the overall picture is highly variable due to differences in the rate of migmatization and the original composition of the parent rocks.

The Galician migmatites have been treated in terms of Mehnert's genetic subdivision based upon the petrographic character of the newly formed components by Avé Lallemant (1965), Woensdregt (1966), van Zuuren (1969) and others. Although many of the migmatites originated by partial anatexis, a widespread infiltration of pegmaplitic and leuco-granitic material, formed closer to the heat-source during progressive mobilization, has also affected many lower-grade migmatites and non-migmatic country rocks. In acknowledgement of this complexity, the migmatites are named and represented on the geological map according to a nomenclature especially devised for western Galicia, see Table I-7. The classification is non-genetic but in the field as well as in the laboratory, the genetic relationships between paleosome and neosome have also been investigated whenever possible.

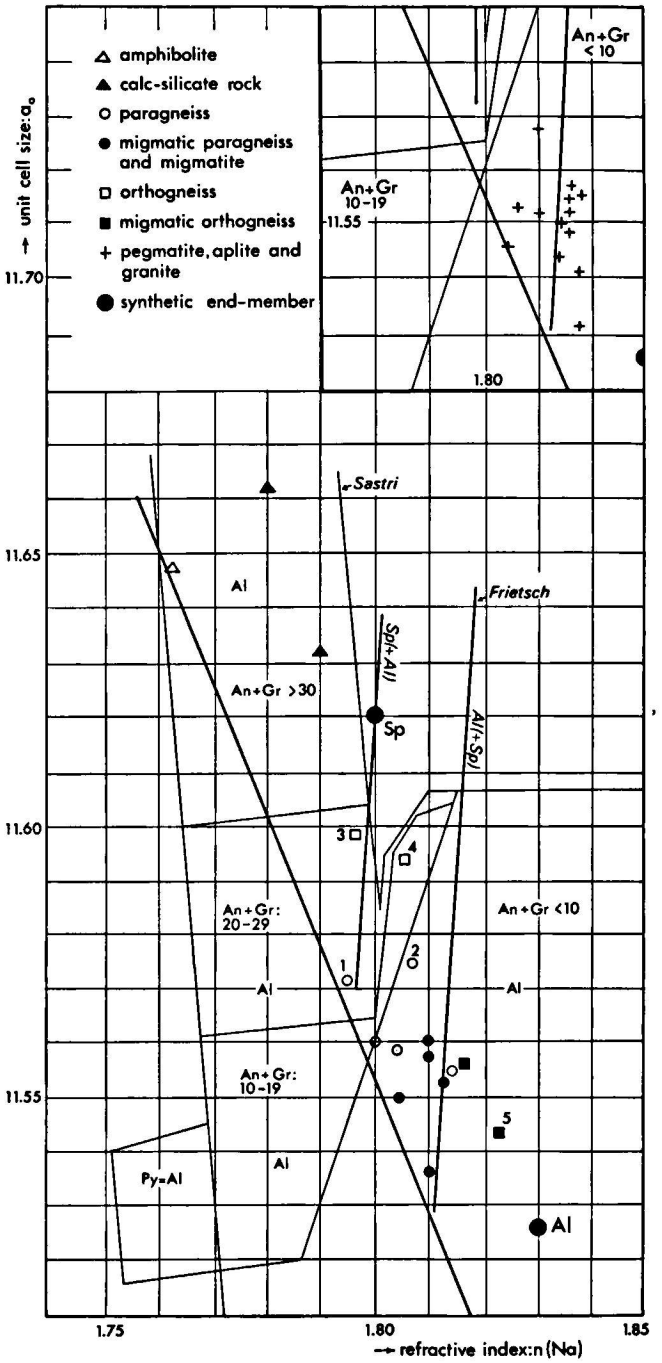

Fig. I-25. a_0 – n(Na) diagram for garnet according to Frietsch (1957) and Sastri (1958). Data from Arps, Avé Lallemant and ten Bosch.

Two groups of migmatites can be distinguished in the present area, i.e. migmatic metasediments and migmatic orthogneisses; the latter group can be subdivided into the migmatic biotite orthogneisses (originally blastomylonitic orthogneisses) and the migmatic coarse-grained augengneisses. A zone of migmatic metasediments carrying bodies of migmatic coarse-grained augengneisses as well as migmatic biotite orthogneisses occurs E of the central zone but separated from it by faults; another relatively narrow sub-meridional zone is exposed between the large western body of migmatic coarse-grained augengneisses and the megacrystal-bearing granodiorite intrusion. In the Río Coroño Valley both types of migmatites occur.

The ultimate products of anatexis, the palingenic granites, will be discussed with the intrusive rocks because they all are homogeneous, more or less par-autochthonous or allochthonous and often display intrusive relationships.

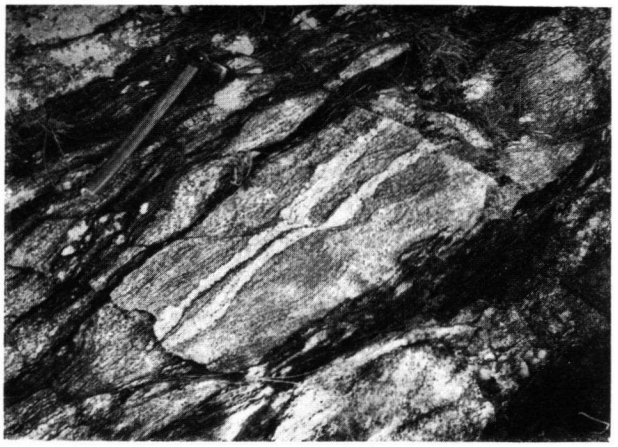

Fig. I-26. a. A migmatic gneiss enclosing streaks of less migmatized paragneiss and pegmatoid segregations (4 km E of Rianjo).

b. A nebulitic migmatite; the migmatite has reached a high degree of mechanical mobility (Mt. Pedride).

Evidence of deformation

The process of migmatization leading ultimately to a complete anatexis and the emplacement of the palingenic granites took place just before F_2. The influence of F_2 seems rather weak and it is difficult to discriminate between its effects and the various migmatic structures, which are the result of varying degrees of mobilization (Plate VI). The melanosomes are very often intensely but irregularly folded, but evidence of a new and consistent cleavage plane has not been encountered. F_2 is only responsible for the fact that the migmatic banding and the foliation of the melanosomes are roughly directed (N)NW-(S)SE. The granitic neosomes and the palingenic granites in the area under consideration generally display a slight parallel orientation of the micas (s_2).

The third deformation was in general only effective in the northern, western and southern parts of the area along restricted zones (Río Coroño Valley).

Migmatic metasediments

The migmatites of metasedimentary origin are mixed rocks, consisting of mobilisates (leucosomes) and melanocratic restites (melanosomes). Progressive mobilization of the different metasediments resulted in migmatites which differ in petrographic character and structure, while injection of or contamination with granitic or pegmaplitic material further changed and genetically complicated the overall nature of the rocks.

The migmatites are completely recrystallized rocks with an average grain size larger than that of the parent rocks. Most frequently encountered in the migmatic metasediments are rafted ("schollen"), veined, layered, folded, streaked ("schlieren") and nebulitic structures (Mehnert, 1968, p. 10 and 11; Plate VI). The migmatic metasediments are generally banded. Many of the low-grade migmatites are in fact recrystallized schists; they still have quartz lenses and bands. The higher-grade migmatites have leucocratic bands consisting of quartz and plagioclase, while alkali feldspar is subordinate or lacking despite the fact that sillimanite may occur as a main constituent.

Experiments on anatexis by von Platen and Winkler (Winkler, 1967) clearly indicate that alkali feldspar will appear in the metatect regardless of this mineral's presence in the parent rock, if the latter consists of at least quartz $\pm$ biotite $\pm$ muscovite $\pm$ plagioclase.

At the appropriate temperatures and pressures and

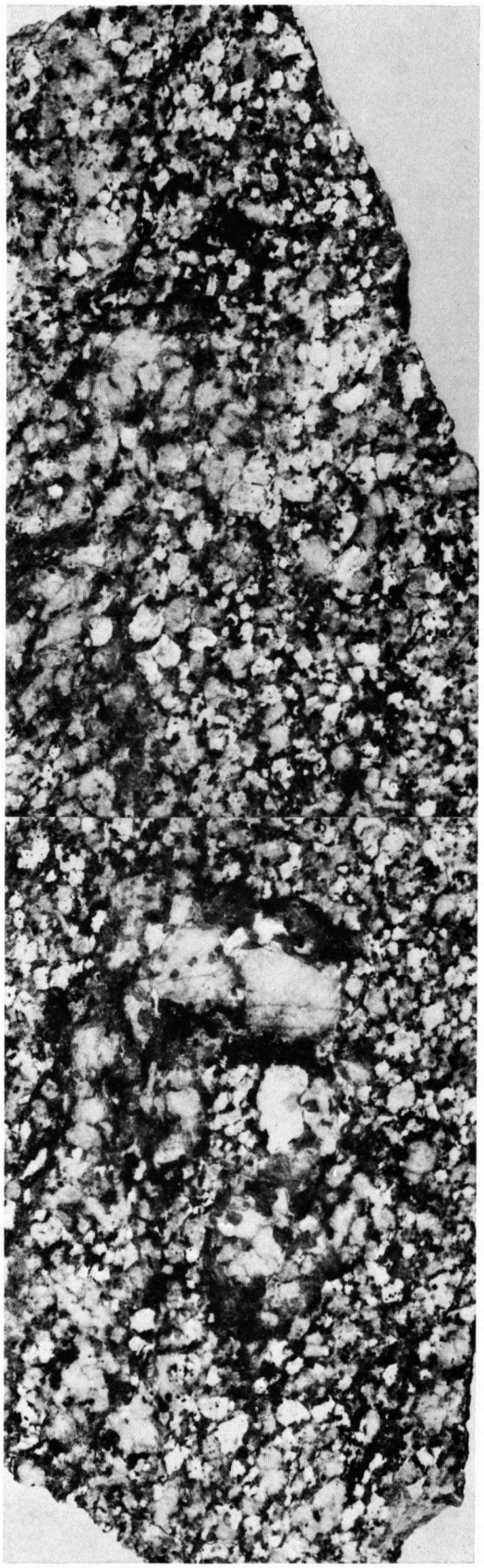

when enough excess water is present, anatexis of paragneisses or schists will produce eutectic melts consisting of quartz, plagioclase and alkali feldspar. The relative amounts of the newly formed components, however, depend upon such factors as original composition of the parent rock, An-content of plagioclase in the parent paragneiss, the presence of other ions in the water solution and $P(H_2O)$.

For the migmatites of the area under consideration, it is believed that many of the newly formed components, including most of the alkali feldspar, have migrated and accumulated into pegmatoid and granitoid neosomes nearby (within approximately one metre).

In a few cases migmatites were found containing relatively large and idiomorphic alkali feldspar crystals. In sample St. 141766, the leucosome with convex outlines next to the melanosome is bordered by dark rims of recrystallized biotite; here a venitic origin of the metatect is most probable (Plate VI-a; Mehnert, 1968, p. 248).

The mineral association sillimanite $\pm$ alkali feldspar $\pm$ garnet (almandine) is typical for various migmatites in the area; cordierite has not been encountered. The mafic restites of the migmatites, consisting of biotite, muscovite, sillimanite and garnet, are either very fine-grained masses or coarser-grained aggregates. Sillimanite, generally of a fibrolitic habit but occasionally idiomorphic (Fig. I-28), seems to have grown largely at the expense of biotite following the reaction of Shelley (1968)*; the rims around the corroded biotites are rich in iron ore. It remains a remarkable fact that so many low-grade migmatites in the immediate neighbourhood of sillimanite contain hardly any alkali feldspar.

When melting is more advanced or almost complete, the structure of the migmatites becomes streaky and nebulitic to nearly homophanous (Figs. I-26b and I-27) and the neosome has a leucogranitic composition rich in alkali feldspar. Such migmatites may be called diatexites and, depending upon the degree of homogenization, they can be subdivided into inhomogeneous and homogeneous diatexites (Mehnert, 1963 and 1968). Both types occur frequently in the area, but it is assumed that some of the diatexites formed as a result of the penetration of granitic and pegmatitic material. Field evidence indicates that many homogenized granitoid melts must have been capable of intrusion and that they penetrated less migmatized zones as anatectic granites, occasionally even as far as some of the non-migmatic rocks (central zone, NE of Noya and E of Boiro). The transitions in the field between the migmatites and the anatectic granites (homogeneous diatexites) may be gradual or

* see p. 68.

Fig. I-27. A granitoid migmatite enclosing pegmatoid patches (7 km NNE of Sierra de Outes, × 9/8).

abrupt. The gradual transition suggests either that the granitic material was formed in situ or that it has penetrated into mechanically mobile migmatites; the latter indicates an intrusive origin.

Mineralogy (*Table I-4*). – In the migmatic metasediments xenoblastic *quartz* occurs as lenses and bands (St. 141766, St. 141768) together with feldspar. Other types of quartz are: round or hypidiomorphic inclusions of quartz in feldspars, a characteristic feature of many migmatites (Mehnert, 1968, p. 255) (St. 141776) and corrosive quartz grains with convex contours towards feldspars and mica; sometimes clusters of small, round and irregularly shaped quartz drops are also enclosed in plagioclase (comparable with myrmekite) although no alkali feldspar is present in the immediate neighbourhood. In many migmatites quartz encloses numerous trains of two-phase inclusions (St. 141777).

Plagioclase is xenomorphic to hypidiomorphic and sometimes idiomorphic (Fig. I-29); it is often zoned. In the pegmatoid leucosomes the feldspars may be very coarse-grained. The average anorthite content varies between 15 % and 28 % for the lower-grade migmatites and between 5–20 % for the granitoid migmatites.

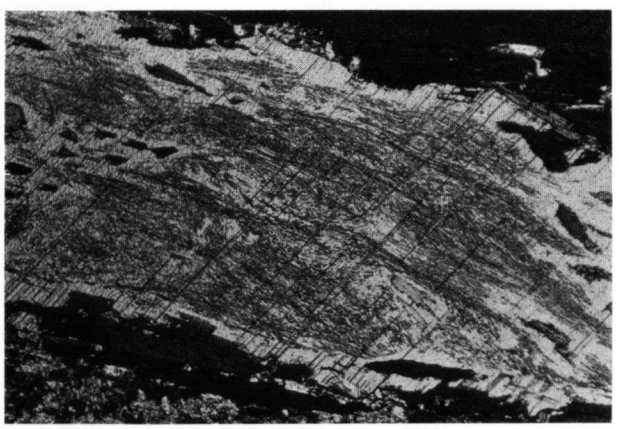

Fig. I-28. a. Fibrolitic sillimanite enclosed by younger cross-muscovite in a migmatic schist, 4 km NNE of Rianjo (× 30).

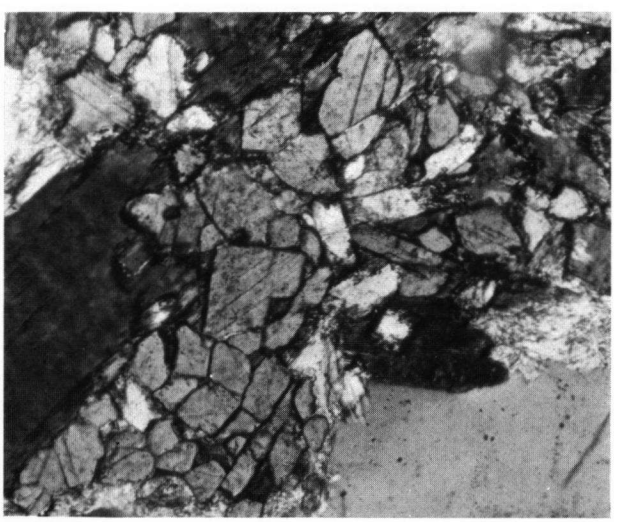

b. Idiomorphic sillimanite crystals have grown at the expense of biotite (St. 141773, × 150).

In the low to medium-grade migmatites the content of *alkali feldspar* is either low or it is completely absent. But in the granitoid migmatites (diatexites) this mineral is abundant.

Biotite and *muscovite*, generally recrystallized and more coarsely grained than in the parent rocks, is concentrated in melanosomes in most of the migmatites. Individual crystals are generally oriented parallel to s_e but cross-micas have also developed (Fig. I-28a).

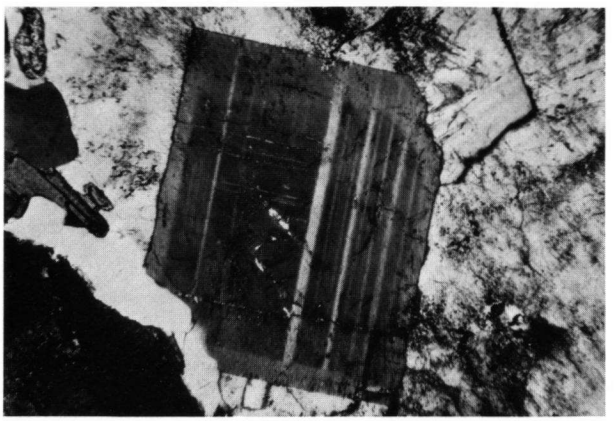

Fig. I-29. Idiomorphic zoned and twinned plagioclase (⊥ [100]) in pegmatoid leucosome (St. 141769, × 35).

Sillimanite, fibrolitic and idiomorphic, has replaced biotite or muscovite; the replacement took place after the recrystallization of the micas (St. 141767, St. 141772 and St. 141773). A later retrogradation transformed much of the fibrolite into sericite (St. 141768).

Other minerals are *andalusite; garnet; tourmaline; opaque minerals; zircon; monazite; xenotime; apatite; fluorite; rutile; anatase* and *brookite*.

Migmatic orthogneisses

Coarse-grained augengneisses. – In addition to the planolinear orthogneisses, coarse-grained augengneisses are a common feature in the northwestern part of the Hesperian massif (Parga-Pondal, 1956; Avé Lallemant, 1965; den Tex, 1966; Woensdregt, 1966; Floor, 1968).

The coarse-grained augengneisses of the area intruded as coarse-grained and megacrystal-bearing two-mica granites. Some alkali feldspar augen still bear traces of a zonal growth with regularly arranged plagioclase and biotite inclusions (Plate VIII-a; Frasl, 1954) and zoned perthite, while the zircons are oblong and idiomorphic. The intrusion of these pre-Hercynian granites may have been facilitated by the presence of the fundamental fault W of the central zone. The western augengneiss is part of a long intrusive body which continues some 25 km further north. The eastern bodies appear to once have been continuous and can be followed as far south as Redondela in southern Galicia (Fig. I-1).

During the Hercynian orogeny the leucocratic coarse-grained and megacrystal-bearing granites were first transformed into coarse-grained augengneisses (F_1). Then partial anatexis affected the augengneisses; it resulted in partially to completely recrystallized

amount of neosome	< 25 %	25–75 %		> 75 %
petrographic character of neosome	hydrothermaloid pegmatoid/pegmatitic (granitoid/granitic)	pegmatoid/pegmatitic granitoid/granitic	(pegmatoid/pegmatitic) granitoid/granitic	granitiod/granitic
persistance of foliation	strike of foliation persistent dip of foliation variable	strike of foliation persistent dip of foliation variable	strike of foliation non-persistent and variable; dip of foliation highly variable	strike of foliation non-persistent and variable; dip of foliation highly variable
examples of nomenclature	pegmatoid/granitoid migmatic *paragneiss/ orthogneiss*	pegmatoid/granitoid (para)gneiss *migmatite/* (ortho)gneiss *migmatite*	pegmatoid/granitoid (para)gneiss *migmatite/* (ortho)gneiss *migmatite*	migmatic *granite* (always inhomogeneous, otherwise: anatectic granite)
examples	Plate VI-a	Fig. I-26a	Plate VI-b and c Fig. I-31a	Fig I-26b; Fig. I-27 Fig. I-31b; Plate VIII-b
legend on geological map	basic colour corresponds with colour of parental rock; in addition: red lines parallel with regional foliation	basic colour: pale red (migmatite)		basic colour: pale red (granite)
		in addition: lines // regional foliation of which the colour corresponds with colour of parental rock	in addition :≈ ≈	
genetic nomenclature (a.o. Mehnert, 1968)	metatexite, metatexitic gneiss	metatexite, metatexitic gneiss; diatexite, diatexite gneiss	(metatexite) inhomogeneous diatexite	granitoid migmatite, inhomogeneous diatexite

Table I-7. Non-genetic classification of the migmatites (Mainly according to the Internal Report, no. 2, 1969, of the Dept. of Petr., Min. & Cryst., Leiden University).

rocks which differ in macroscopic appearance (Fig. I-31 and Plate VIII).

SE of Esteiro and E of Mount Iroite the augengneisses were re-transformed into very coarse-grained two-mica granites. In the southern and eastern parts of the area, gneissic migmatites resulted in which the augen were partly or completely reduced (St. 141782, St. 141783). On the coast 4 km E of Rianjo, the migmatic augengneisses vary greatly in appearance due to differences in grain size and in the relative number of alkali feldspar augen. In the eastern migmatite zones most of the partially mobilized augengneisses have a "schlieren" structure due to a high degree of mobility. North of Mount Bella the granitoid migmatites may contain remnants of the parent augengneiss: scattered augen in a granitic matrix (Fig. I-31b).

Where the influence of migmatization remained slight as in the northern part of the western body, the foliation (s_1) of the augengneisses indicated by the direction of the micas and the long axis of the feldspar augen is constantly directed (N)NW-(S)SE.

The phyllonitic appearance of the augengneisses (F_1), which locally disappeared due to migmatic recrystallization, was partly restored by F_2 and especially F_3 (Plate VIII-a).

The size of the augen varies; the largest oblong crystals are about 12 × 7 × 4 cm. The augen are enclosed within a coarse to fine-grained matrix of granitic composition.

The coarse-grained augengneisses have relatively few paragneiss inclusions, some of which show evidence of assimilation (St. 141785) and enclose alkali feldspar porphyroblasts and coarse-grained aggregates of quartz.

Large amounts of pegmaplitic and leucogranitic material, possibly augengneisses that were completely mobilized at deeper levels and have penetrated the coarse-grained augengneiss, occur especially W and SW of Noya. This together with the successive intrusions of relatively young parautochthonous two-mica granites and their apophyses has given the rocks an agmatic appearance (Fig. I-32). The rocks have been indicated on the geological map as "coarse-

Fig. I-30. Hypidiomorphic alkali feldspar from parautochthonous granite enclosing granophyric quartz (St. 141832, × 40).

grained augengneisses". Only the relatively large pegmatitic and leucogranitic exposures and the younger parautochthonous two-mica granites have been indicated separately.

Mineralogy (*Table I-4*). – The augengneisses have the mineralogical composition of a leucocratic two-mica granite and contain *quartz*, *plagioclase* (5–20 % An), *alkali feldspar*, *biotite* and *muscovite* as main constituents and *opaque minerals*, *zircon* (idiomorphic), *monazite*, *xenotime*, *apatite* (two generations: relatively large and sub-idiomorphic grains and needles in feldspars and quartz), *rutile*, *tourmaline*, *garnet* and *allanite* as accessories.

The feldspar augen are microclines, often twinned according to the Carlsbad law and enclose relatively small plagioclase crystals with rims of albitic composition, irregular quartz and biotite (sometimes oriented parallel to growth zones). Evidence of albitization, decalcification, perthitization and myrmekitization is common (Plate VII).

Quartz is usually xenomorphic but it may also be found as small droplets in feldspars. The presence of relatively young and corrosive quartz grains with convex outlines is a remarkable feature in some migmatic augengneisses (St. 141784).

The groundmass has a granitic composition; most of its constituents have been crushed (mainly F_3), especially around the large augen. The augengneiss on the eastern side adjacent to the SW fault-zone is mylonitic (F_3); quartz has completely recrystallized into a post-F_3 mosaic (St. 141781).

The complicated agmatic character of the migmatized coarse-grained augengneisses is clearly exposed along the coast of the Ría de Noya, between Portosin and Punta Boa (Fig. I-32 and von Raumer, 1963, Abb. 25) or Esteiro and Freijo (Avé Lallemant, 1965, Fig. 6).

The aplogranitic rocks vary greatly in macroscopic appearance due to differences in mineralogical composition, grain size and rate of deformation(s).

The rocks may include *biotite* in patches. *Muscovite*, *tourmaline*, *garnet* (Fig. I-25) and *apatite* are almost always present in relatively large amounts; *beryl* has also been encountered.

The presence of so many of the former minerals in the aplogranitic rocks cannot be reconciled with a pure anatectic origin. A widespread infiltration of the necessary elements from below must have taken place; in places it even affected the migmatic coarse-grained augengneisses causing the growth of tourmaline and garnet.

Migmatic biotite orthogneisses. – A few small and narrow lenses 750 m SW of Moimenta and a larger body 3.5 km NNE of Val are clear evidence of the existence of migmatic biotite orthogneisses. The rocks have granoblastic microfabrics with an average grain size larger than their non-migmatic counterparts in the central zone (Fig. I-33).

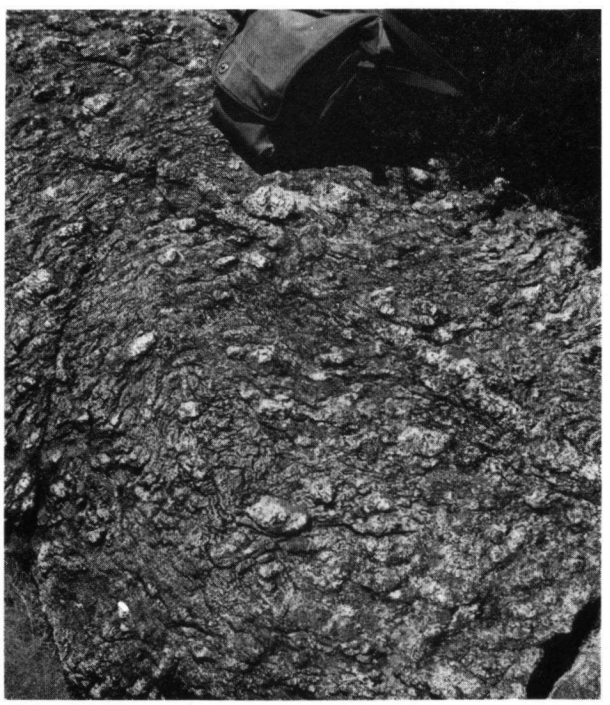

Fig. I-31. a. Migmatic coarse-grained augengneiss with a schlieren structure (4.5 km NE of Pte. Beluso).

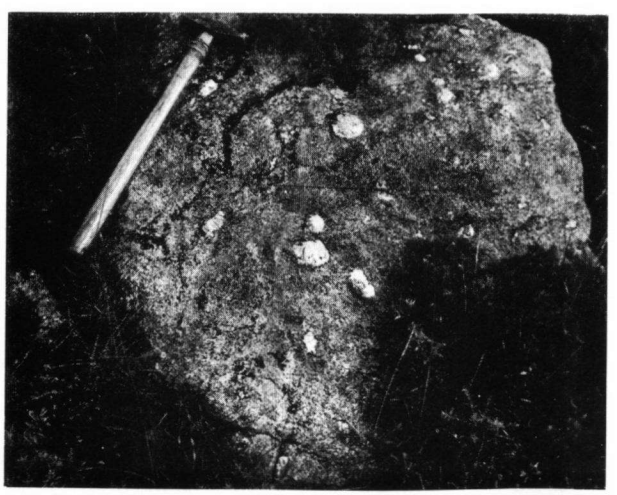

b. Augen relics within a granitoid migmatite (2 km N of Mt. Bella).

Mineralogy (*Table I-4*). – The more or less equidimensional *feldspars* contain round inclusions of *quartz*, although the quartz may also have corroded the feldspars. The An-percentage of *plagioclase* (10–30 %) has not changed during migmatization. As in many other granitic migmatites in the area, *garnet* may be an important constituent. Many idiomorphic grains (∅ 0.03–0.16 mm), dodecahedrons and other garnet crystals with regularly striated faces, probably resulting from an alternating development (Phillips, 1960), have been encountered (St. 141790).

In contrast to the non-migmatic orthogneisses, the present gneisses are relatively abundant in *monazite* and *xenotime*.

THE INTRUSIVE ROCKS (HERCYNIAN)

Syn-kinematic intrusives

The Hercynian syn-kinematic intrusives of the investigated area include all the rocks that were emplaced after F_1 and just before F_2; they can be divided into two rock-groups.

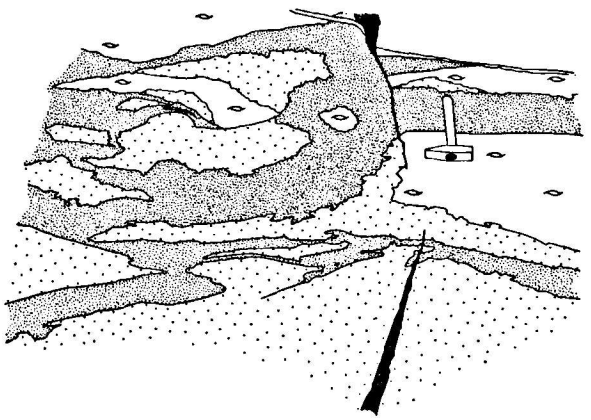

Fig. I-32. Agmatic character of the coarse-grained augengneiss on the coast 2 km NNE of Portosin. Dotted: aplogranite; closely dotted: medium to coarse-grained two-mica granite (Barbanza granite); dark: quartz vein.

The rocks belonging to the relatively early syn-kinematic megacrystal-bearing granodiorite comagmatic series were emplaced first; they consist of a main megacrystal-bearing granodiorite body, containing dioritic to granodioritic inclusions and an intrusive muscovite granite. They were followed by the second group, the syn-kinematic parautochthonous two-mica granites (the Barbanza granites, the Muros granites, the Banza granite, etc.). They are all palingenic granites, i.e. the ultimate products of complete mobilization at the appropriate levels which have intruded into higher levels. The late syn-kinematic megacrystal-bearing Ruña granite is probably the youngest of the second group. The emplacement of this granite most likely occurred between F_2 and F_3.

Structural aspects of the syn-kinematic intrusive rocks

The second deformation F_2 variously affected almost all of the syn-kinematic rocks in the area.

The alkali feldspar megacrystals of the relatively early syn-kinematic megacrystal-bearing granodiorites

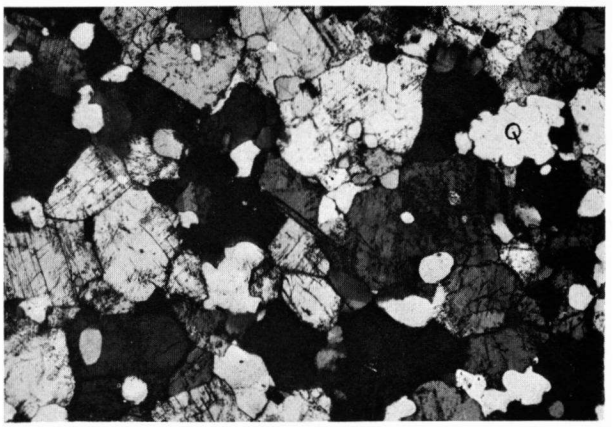

Fig. I-33. Granoblastic microfabric of migmatic biotite orthogneiss; note the characteristic habit of quartz (Q); drops and corrosive grains with convex outlines (St. 141790, × 25).

are oriented (N)NW-(S)SE, generally with their longest axis [001] in a sub-horizontal position (Fig. I-34a). This preferred orientation of the megacrystals is probably due to magmatic flow, but a slight reorientation of the megacrystals to their present position was induced by F_2; locally the regional orientation of the megacrystals deviates from the general trend of the intrusion.

In the syn-kinematic two-mica granites, a slight parallel orientation of the mica flakes due to F_2 may be present and is most clearly visible where F_3 was not active. The relatively large late-stage micas, a characteristic feature of many of the two-mica granites, were little affected by F_2 and are therefore considered to have grown mainly after F_2.

The third Hercynian deformation affected most of the rocks in the western part of the area and caused, along restricted zones, a phyllonitization of the coarser-grained rocks in particular, i.e. the megacrystal-bearing granodiorites and many two-mica granites. The megacrystal-bearing granodiorite is predominantly phyllonitic especially along the fault contact with the central zone.

Even the Ruña granite seems to have been influenced by F_3; the granite is deformed slightly and has some traces of phyllonitization. The approximately ENE-WSW directed compression yielded conjugate sets of sub-vertical slip planes and a sub-vertical B_3-axis (van Zuuren, 1969, p. 43).

A period of wrench-faulting and mylonitization are the latest tectonic activities attributed to F_3. A strong dextral shear along sub-vertical N-S directed slip planes caused further cataclasis and mylonitization of the phyllonitic rocks (Plate X-c); along approximately N-S trending joints and faults the rocks are generally brecciated or mylonitized. Phyllonitization, mylonitization, and wrench-faulting were greatest in the southwestern part of the area (Río Coroño Valley) and hamper accurate mapping. Many intrusive relationships have been obliterated, due to slip along the

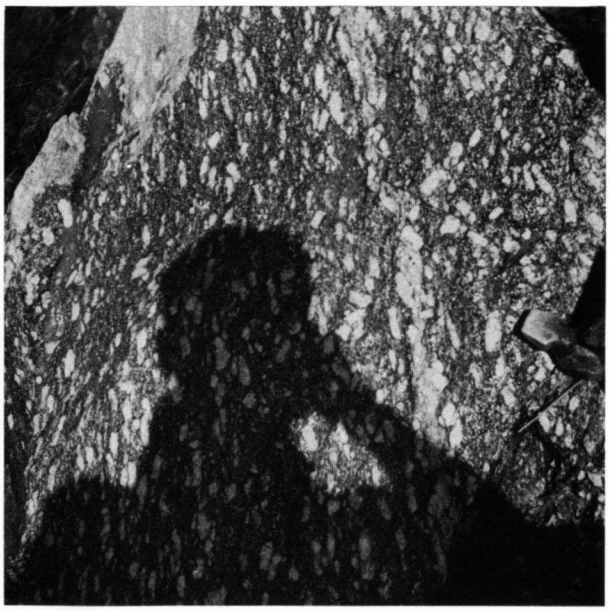

Fig. I-34. a. Megacrystal-bearing granodiorite 1.2 km SW of Moimenta. The alkali feldspar megacrystals are roughly NW-SE oriented.

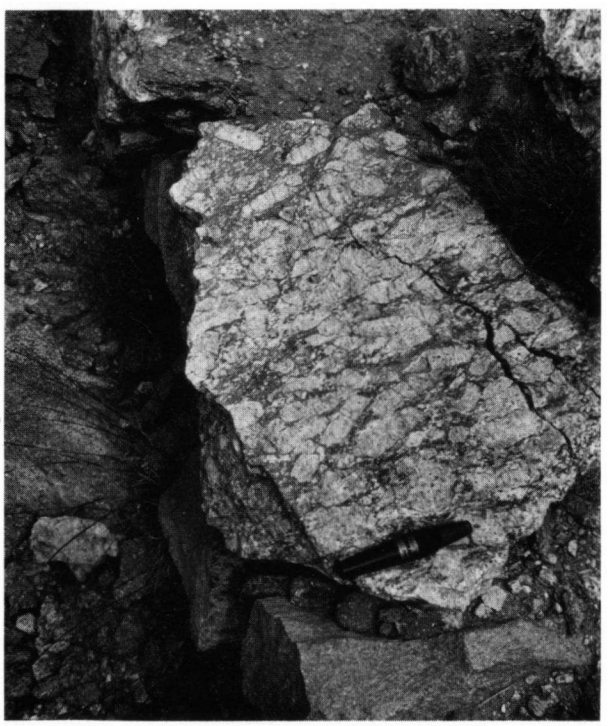

b. Accumulation of alkali feldspar megacrystals (St. 141806) in megacrystal-bearing granodiorite 2.3 km NNW of Moimenta.

contacts. Pseudo cross-beddings are not exceptional.

Late Hercynian phyllonitization, mylonitization and wrench-faulting are common features in certain zones in western Galicia and have been reported by Avé Lallemant (1965), den Tex (1966), den Tex & Floor (1967) and van Zuuren (1969), but they have not been encountered in southwestern Galicia (Floor, 1966).

The joint systems found in the area (see geological map) originated during F_2 and were partly reactivated during F_3. Many pegmatites, aplites and quartz veins intruded before and after F_3 along existing zones of weakness (von Raumer, 1963).

Megacrystal-bearing granodiorite series

Three main rock-types are regarded as belonging to this series, i.e. the megacrystal-bearing granodiorite s.s. which contains, in addition to xenoliths, many comagmatic inclusions with a predominantly granodioritic composition as well as veins and larger bodies of aplogranitic composition. The three rock-types occur, in the present area as well as in other parts of Galicia (Floor, 1966), in close association and are therefore tentatively regarded as products of a magmatic differentiation.

The megacrystal-bearing granodiorite intruded during a period of dilatation just before F_2 along the N-S trending fundamental fault-zone on the western border of the central zone. The map in Fig. I-1 shows that the present granodiorite extends southwards beyond Vigo and northwards some 43 km NNW of Noya. West of Moimenta, in the southern part of the area, the emplacement of the megacrystal-bearing granodiorite intrusion followed two fault-zones, i.e. the one adjacent to the central zone and the one continuing in a southern direction.

Along the faults east of the central zone, scattered diorite, granodiorite and megacrystal-bearing grano-diorite veins and bodies also penetrated the migmatic rocks.

Together with the comagmatic inclusions the main granodiorite contains numerous xenoliths (Plate X-a) i.e. para- and orthogneisses and amphibolites; 3.5 km NNW of Pte. Olveira, a large coarse-grained augengneiss xenolith was also found (Rubbens, 1963).

The orthogneiss xenoliths were not affected by the intruding magma, but many paragneisses and occasionally amphibolites show evidence of assimilation.

Various paragneisses recrystallized into granoblastic quartz-diorites, sometimes with feldspar porphyroblasts (mainly plagioclase; Plate X-a). With an increasing rate of assimilation, a distinction between paragneisses (xenoliths) and comagmatic inclusions (autoliths) could be established by studying the zircon crops. The results are quite revealing (see Chapter II and Arps, 1970).

Many veins and larger intrusive bodies of two-mica granite, generally concordant to accordant with regional foliation, penetrated the megacrystal-bearing granodiorite chiefly in the central and southern parts of the area; they were followed by pegmatites, aplites and quartz veins.

Dioritic and granodioritic cognate inclusions. – The cognate inclusions are generally more coarsely grained and poorly oriented compared to the dioritic and quartz-dioritic xenoliths (paragneisses and amphibolites). While most of the xenoliths are relatively small lenses, the autoliths are often much larger and may have irreg-

ular dimensions; the contact of the latter with the megacrystal-bearing granodiorites is often gradual.

Most of the autoliths were encountered in the northern part of the main intrusion, between Mt. Tremuzo and the Río Jallas. The inclusions are macroscopically equigranular. Most of the inclusions are biotite granodiorites, but several others may include hornblende in addition to biotite. At Suevos, 8 km NW of Sierra de Outes, and another locality 5.8 km E of Noya, hornblende-biotite diorites are surrounded by biotite granodiorites. The biotites of the former developed as large crystals (⌀ 5 cm) without orientation embedded in a matrix consisting mainly of plagioclase and hornblende (Plate X-b).

Mineralogy (*Table I-5*). The amounts of *quartz* and *alkali feldspar* may vary from 13.2 % and 10.1 % for hornblende-biotite granodiorites to 2.0 % and 3.8 % for biotite-hornblende diorites, respectively (von Metzsch, 1964) but variations in this composition may occur (St. 141792 versus St. 141793).

Plagioclase (25–70 % An for the hornblende-biotite diorites, 25–50 % for the biotite granodiorites) is quantitatively the most important constituent (43 %, Avé Lallemant, 1965); the hypidiomorphic crystals are almost always twinned (albite, Carlsbad-albite and pericline twins) and intensely zoned.

The amphibole is a common blue-green *hornblende* with $\gamma = 1.654 \pm 0.005$ and $2V_\alpha \approx 80°$, $r > v$ (St. 141792). Relics of an almost colourless diopsidic *pyroxene* may be found enclosed by hornblende (St. 141792).

Biotite is exceptionally large in samples St. 141792 and St. 141793; $\gamma = 1.638 - 1.640 \pm 0.002$ (St. 141792).

Titanite is always an important accessory. Zoned idiomorphic *allanites* are also a common feature; the partly or completely altered crystals are larger than those occurring in the paragneisses (and paragneiss xenoliths).

Perfect idiomorphic *zircons* are present in the granodiorites, while some of the diorites may almost completely lack this mineral. Other accessory minerals are *apatite; rutile; anatase; tourmaline; epidote; calcite* and *opaque minerals.*

Megacrystal-bearing granodiorites s.s. – Quantitatively the most prominent variety of the present series is a granodiorite with relatively large (up to 12 × 6 cm), oriented alkali feldspar crystals (Fig. I-34a).

The megacrysts are often twinned according to the Carlsbad law and contain relatively small, sometimes zonally arranged, inclusions of biotite and plagioclase (Frasl, 1954).

Along the eastern margin and near important faults, as well as in shear zones (F_3), the rocks are highly phyllonitized and mylonitized (Plate X-c) or may have turned into cataclasites and even kakyrites (Plate IX-a). Local differences in mineralogical composition and fabric have been traced. Near Suevos a small outcrop of the megacrystal-bearing granodiorite contains some hornblende (St. 141800). In some locations, the megacrystal-bearing granodiorites were found to grade into non-porphyritic granodiorites (St. 141798, St. 141802).

Leucocratic varieties (St. 141807), containing muscovite but relatively poor in biotite, are mainly restricted to the southern part of the area.

Accumulations of both biotite and alkali feldspar (Fig. I-34b) are not exceptional inhomogeneities. Another aberrant variety is a leucocratic coarse-grained biotite-muscovite granite (St. 141808), exposed at the coast 5 km SSW of Sierra de Outes. It may be regarded as a later product of magmatic differentiation (Avé Lallemant, 1965, p. 159).

Mineralogy (*Table I-5*). – All of the megacrystal-bearing granodiorites are more or less highly deformed (F_2 and F_3). Thin section analyses clearly reveal that the sharp edges of the alkali feldspars have crumbled off, while the surrounding minerals are crushed. Mortar and shear zones are always present. Most of the quartz recrystallized subsequent to F_3 into polygonal mosaics. The feldspars have been bent or are broken. The fissures parallel to the direction of maximum stress are filled up with quartz. Locally all the quartz has been squeezed out by tectonic action (F_3; Plate IX-a).

The *alkali feldspar* megacrystals are microclines, often twinned (Carlsbad law) with numerous inclusions of plagioclase, micas and quartz. Large-scale perthitization (exsolution perthite as well as replacement perthite), albitization and myrmekitization of alkali feldspar are always found.

Plagioclase (10–35 % An, but variable with composition) may also attain large dimensions, although always smaller than the alkali feldspar megacrystals. A relatively small generation of resorbed and partly altered (sericite, saussurite) crystals is enclosed in the alkali feldspar megacrystals.

Quartz is xenomorphic, strained, completely crushed or has recrystallized into aggregates. A few small pseudomorphs of high-temperature quartz are enclosed within feldspar.

Biotite, $\gamma = 1.638 - 1.640 \pm 0.002$ and $2V_\alpha = 5–10°$ (St. 802), has ragged outlines or is completely crushed.

Other minerals are *muscovite*, often secondary in feldspar or cross-muscovites in biotite; *chlorite; apatite*, idiomorphic grains with turbid cores, enclosing small zircons, and needles in feldspar and quartz; idiomorphic *zircon;* resorbed *monazite* and *xenotime; titanite; rutile* (sagenite in biotite); *tourmaline; garnet; allanite; fluorite; calcite* and *opaque minerals.*

Muscovite granites and aplites. – Two relatively large muscovite granite bodies together with many aplitic veins are the ultimate products of magmatic differentiation of the megacrystal-bearing granodiorite series. The rocks have variable grain sizes (Plate X-d) and the texture is generally phyllonitic or gneissic. The majority of the smaller veins occur in the neighbourhood of the larger bodies and near the contact with the central zone. A similar gneissic aplite has also been encountered in the central zone (St. 141812). Macroscopically garnet and tourmaline are often visible. Muscovite has a greenish tint; biotite patches may be present.

Mineralogy (*Table I-5*). The main constituents are *quartz, albite* and *alkali feldspar.* Resorbed patches of the latter are frequently found enclosed within albite. Many albites are relatively large and clear and have probably originated by albitization (St. 141811). Perthite is a common feature in the alkali feldspars, but myrmekite is absent.

Other minerals are idiomorphic and turbid *zircon; apatite*, idiomorphic or xenomorphic and needles; blue or greenish *tourmaline; beryl*, perfectly idiomorphic in sample St. 141812; idiomorphic *garnet;* beryl and garnet may enclose blue tour-

maline; *biotite; sillimanite* in muscovite; zoned *childrenite-eosphorite* (Avé Lallemant, 1965, p. 160); *anatase* and *opaque minerals.*

Parautochthonous and allochthonous two-mica granites

Western Galicia is characterized by the presence of many syn-kinematic two-mica granites, which obviously have originated by anatexis of the pre-Hercynian country rocks (see p. 79). Different generations of anatectic granites have been encountered in the area. Some scattered outcrops may possibly be considered autochthonous; they are generally inhomogeneous (Fig. I-27) and occur E of the central zone. But ultimately large amounts of granitic melt formed and, being capable of intrusion, penetrated into higher levels.

The most prominent parautochthonous and allochthonous (Buddington, 1959) granites west of the central zone are coarse to medium-grained two-mica granites (Barbanza granite: von Raumer, 1963; Avé Lallemant, 1965; Dumbría granite: Woensdregt, 1966), the somewhat younger medium to fine-grained granites (Muros granites: Avé Lallemant, 1965) and the still younger Ruña granite.

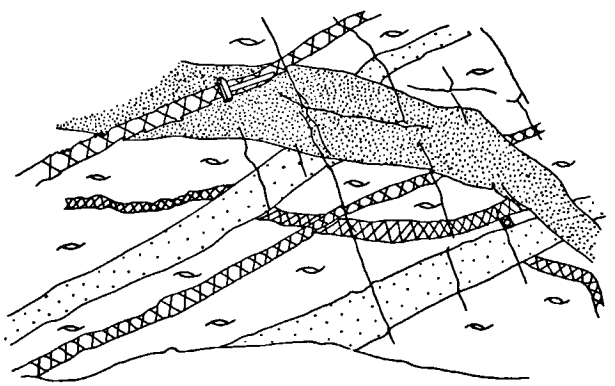

Fig. I-35. Intrusive relationships in the coarse-grained augengneiss on the coast, 2.5 km SE of Esteiro; dotted: fine-grained two-mica granite; closely dotted: medium to coarse-grained two-mica granite (Barbanza granite); the other veins are pegmatites.

East of the central zone the granites vary more widely in appearance; they are generally medium to fine-grained. The intrusive relationships are difficult to find due to the dense vegetation.

In the central and southern parts of the area, the two-mica granites and their corresponding apophyses have invaded the megacrystal-bearing granodiorite series, the coarse-grained augengneisses and even the paragneisses of the central zone ENE and NNE of Boiro.

A few small fine-grained two-mica granite veins have intruded into the western coarse-grained augengneiss series prior to the aplogranitic phase (St. 141786 and Fig. I-35).

Most of the present two-mica granites are similar in that they contain relatively young and large late-stage muscovites and to a lesser extent biotites as well (St. 141829 and St. 141833, respectively).

Mineralogically the granites are very much the same. The most important differences concern their textures, the relative amounts of the constituents and the frequency of their properties (feldspar megacrystals, myrmekitization, perthitization, late-stage micas; see also Capdevila & Floor, 1970).

Medium to coarse-grained two-mica granites (Barbanza granites). – Large quantities of these syn-kinematic granites intruded into the coarse-grained augengneiss and, mainly in the central and southern parts of the area, the megacrystal-bearing granodiorite. The western extremities of the present area include part of a batholith, which continues to the NW and N (Fig. I-1).

The granites are generally easily recognized in the field by their grain size (medium to coarse-grained) and by their texture which, in the investigated area, is often phyllonitic (Plate XI-b).

In the area around Esteiro and Mt. San Lois, and in some parts of the eastern extremities of the Sierra de Barbanza, the rocks are barely deformed. In the Río Coroño Valley, they are instead highly phyllonitic. Locally the granites contain megacrystals ($\leqslant 4$ cm) of alkali feldspar (Mt. Iroite).

On closer examination these granites vary somewhat in composition (Avé Lallemant, 1965, p. 163) and may be inhomogeneous within a single hand-specimen (Plate XI-b).

Petrogenetically the granites can be divided into a relatively early variety, poor in biotite and possibly slightly more deformed (F_2), and a later biotite-muscovite granite, with biotite $\leqslant$ muscovite (Plate XI-a). These types were called the muscovite-rich and the biotite-rich types, respectively, by Avé Lallemant (1965, p. 161). Clear intrusive relationships were found at the coast, 2 km SSW of Esteiro, where the muscovite-rich types occur as inclusions of restricted size within the biotite-muscovite variety, which is regionally more important.

The mineralogy of the present group of granites will be treated together with that of the other two-mica granites.

Medium to fine-grained two-mica granites (Muros granites, Banza granite, eastern and southern two-mica granites). – Large amounts of relatively young, medium to fine-grained two-mica granites are exposed in the areas W of Esteiro, between Abelleira and Muros. Avé Lallemant (1965, p. 161) distinguished between three generations of these "Muros-type" two-mica granites, i.e. a medium-grained variety and a relatively young fine-grained variety with small inclusions of a granite with an even finer grain. 8.5 km SW of Portosin, the Muros-type medium to fine-grained granites were also encountered by von Raumer ("feinkörniger Granit", p. 11).

The Muros-type granites occurring W of the central zone in rather minor amounts may possibly be corre-

lated with the majority of the two-mica granites E of the central zone. Evidence that may warrant a correlation are grain size, the presence of relatively large muscovite and often large biotite flakes and the relatively insignificant amounts or absence of (Avé Lallemant, 1965, p. 162) myrmekite. Furthermore it should be noted that some fine-grained granite inclusions were found in the southern extremities of the Banza granite, a medium-grained two-mica granite body 4 km N of Sierra de Outes (Plate XI-c).

The few relationships among the eastern granites which could be observed indicate that medium-grained varieties, with small megacrystals ($\leqslant 2$ cm), were intruded by later medium to fine-grained and equigranular or weakly porphyritic varieties (samples St. 141837 and St. 141838 respectively).

With the exception of the western part of the Banza granite, the eastern two-mica granites are not phyllonitic.

The anatectic two-mica granites in the S are quite similar to the eastern granites. They are generally medium to fine-grained, equigranular and non-phyllonitic (St. 141836 and St. 141832).

Mineralogy (*Table I-6*). – *Quartz* (ca. 30–40 % for the medium to coarse-grained granites, a little less for the medium to fine-grained granites; results of point-counting by Arps, 1965 and Avé Lallemant, 1964) is xenomorphic and strained or recrystallized after F_3 into polygonal or mosaic aggregates. In mortar zones quartz has been completely reduced together with feldspar and micas. Other varieties of quartz are the small, round and sometimes hexagonal inclusions in feldspar (pseudomorphs after high-temperature quartz), myrmekite quartz, granophyric quartz in alkali feldspar (Fig. I-30) and relatively late quartz. Where the feldspars have been broken, quartz may have filled up the tension cracks (Plate IX-c).

Alkali feldspar (ca. 17–27 % for the medium to coarse-grained granites and 27–35 % for the medium to fine-grained granites) is xenomorphic to hypidiomorphic. Megacrystals may also be present. In the phyllonitic granites the grains may have rounded outlines and mortar rims. Cross-hatching and different generations of perthite are always present. The alkali feldspars, frequently twinned according to the Carlsbad law, are generally larger than the plagioclases and may enclose small plagioclases, micas and quartzes.

Most of the *plagioclases* (ca. 17–35 % for the medium to coarse-grained granites and 14–22 % for the medium to fine-grained granites) are albites or acid oligoclases (western Barbanza and Muros-type granites). In the eastern granites, there is a greater variation in the An-content of plagioclase and the individual grains are sometimes extensively zoned (normally or irregularly). Primary and deformation {010} twins are always present, but only a few according to the Carlsbad law.

Plagioclase is idiomorphic to hypidiomorphic when next to quartz and alkali feldspar. Some crystals in the eastern granites may attain the size of megacrystals; small and resorbed crystals may be enclosed within alkali feldspar. Albitization is widespread; some albites enclose patches of microcline. The best examples of decalcification are visible in plagioclases enclosed within alkali feldspar. Myrmekite is generally present in varying amounts but less than in the megacrystal-bearing granodiorites (see also Capdevila & Floor, 1970).

Of the micas *muscovite* is quantitatively more important than *biotite*, 10–16 % and 2–12 %, respectively; both minerals are always present. In the biotite-poor Barbanza-type granite variety, the percentages of muscovite and biotite vary between 10.3–16.6% and 1.2–5.7%, respectively (percentages determined by point-counting, Avé Lallemant, 1965).

The results of refractive index determinations for γ of biotite were: St. 141824, $\gamma = 1.644 - 1.647 \pm 0.002$; St. 141833, $\gamma = 1.648 - 1.652 \pm 0.002$ and St. 141831, $\gamma = 1.646 - 1.648 \pm 0.002$.

Roughly two generations of muscovite and sometimes also biotite can be distinguished. The relatively older muscovites are smaller and grew more or less together with biotite; the late-stage muscovites (lepidoblasts) belong to the second group (Plate IX-b).

The late-stage micas are supposed to be the result of epimagmatic processes (den Tex & Floor, 1967). They have ragged outlines and some may enclose fibrolitic sillimanite and biotite. Some muscovites have symplectitic rims, consisting of muscovite intergrown with quartz, when next to alkali feldspar (St. 141834) probably representing the arrested breakdown of alkali feldspar according to the equilibrium reaction Ms + Q $\leftrightarrows$ Alk fsp + Sill + H_2O. In other samples (St. 141786) muscovite has a fibrous appearance, which is attributed to the growth of muscovite at the expense of sillimanite (+ alk. feldspar). Small secondary muscovites occur within feldspars parallel to their cleavages.

In comparison with the smaller micas, the lepidoblasts are poorly oriented or not oriented, though they may have been bent under the influence of F_3 (Plate IX-b).

Zircon is dispersed throughout the rock or is enclosed by the micas and apatite. Clusters of small and slender idiomorphic, though resorbed crystals may be found together with *monazite* and *xenotime*.

Roughly two generations of *apatite* can be distinguished. A relatively large and more or less equidimensional generation, often enclosed by the micas and displaying turbid cores that include zircon crystals, and a generation of small, slender prisms dispersed throughout the leucocratic main constituents, mainly alkali feldspar.

Rutile occurs as sagenite in biotite and idiomorphic prisms; very thin needles (most probably rutile) are often found within quartz.

Other accessory minerals are *fluorite; titanite; anatase;* greenish-blue and brown zoned *tourmaline; garnet; allanite; sillimanite; chlorite; sericite* and *opaque minerals.*

Pegmatites, aplites and quartz veins. – After the emplacement of the two-mica granites, numerous pegmatites, aplites and quartz veins, in successive generations intruded into all pre-existing rocks, especially in the central and southern parts of the area. The apophyses can be subdivided into one series that intruded before F_3, some of them even before F_2 (St. 141844, St. 141845), and another after F_3 (Fig. I-17c). Most of the intrusions follow the direction of the pre-existing joint systems and faults, or run parallel to the regional foliation. The network of dykes is locally very intricate. Some of the largest pegmaplites may reach lengths of a few kilometres, while dykes with widths of over 10 m are not exceptional. Locally pegmaplitic bodies were formed (2.3 km NW of Boiro, 1.2 km S of San Finx, etc.).

The majority of the apophyses are economically barren. The Sn-W bearing dykes seem to belong to the

	more or less circular with sharp contacts	more or less irregular with sharp contacts	dimensions in km	contact metamorphism	uniform intrusion	composite intrusion (ring intrusion)	compositional changes towards the border	presence of related granite products	apophyses	presence of xenoliths	(narrow) chilled margin	coarse-grained	medium-grained	strongly porphyritic; large phenocrysts	weakly porphyritic	muscovite	biotite	amphibole	major stoping, including piecemeal stoping	ringfracture stoping	effects of shouldering	↑ references ← characteristics
Caldas de Reyes granite	—	+	18 × >40	+		+		+		+	+	+			+	+	—	(+)		+		von Raumer, 1963; ten Bosch, 1964
Pando granite	+		5 × 3.5		+		—		—	—	+	+	+		—	+	—		+			de Graaff, 1962; Avé Lallemant, 1965
Pindo granite	+		13 × >10			+					+	+				+	(+)			+		de Graaff, 1962; Woensdregt, 1966
Arbos granite	+		6 × 5		+		+		+	—		+		+		+	< +		+		—	von Raumer, 1963; Arps, 1965
Ruña granite	—	+	19 × 8		+			+	—	+			+	+		+	< +		+			Koster van Groos, 1962; Woensdregt, 1966

Table I-8 Some characteristics for one late syn-kinematic and four post-kinematic granites in the southwestern part of the province La Coruña.
+ present, important property — subordinate, minor property

post-F_3 group of apophyses and are generally not deformed. The mineralized dykes of San Finx seem to be older than the Arbos post-kinematic two-mica granite. The emplacement of the latter granite slightly tilted the southwestern part of the NE-SW trending dykes. On the other hand, directly S of Moimenta, a relatively young N-S trending ore-bearing dyke occurs within the Arbos granite.

Macroscopically the minerals *muscovite*, *garnet* and *tourmaline* are generally found in the pegmatites and aplites. *Beryl* is another characteristic mineral, although more exceptional. Some pegmatites contain large *biotite* flakes instead of or in addition to muscovite (St. 141849).

The quartz veins are usually massive and vary in width. A few are zoned and have *muscovite* and *sulphide ores* in the centre. Some of the quartz which penetrated into faults has crystallized into palisades (2.2 km SSW of San Finx).

Mineralogy (*Table 1-6*). – *Alkali feldspar* in pegmatites displays a replacement perthite (albitic veins with lamellar {010} twins) which is generally macroscopically visible. In sample St. 141853 alkali feldspar encloses graphic quartz. Albitization is present in some aplites; myrmekite is absent.

Plagioclase is generally of albitic composition. Albite may enclose patches of alkali feldspar (St. 141850). Plagioclase laths in aplite (St. 141846) are not oriented but a preferential alignment, owing to flow, is visible in pegmatite sample St. 141852.

Quartz is either not equigranular and is strained with irregular outlines, or it is crushed in mortar zones, or it has recrystallized into polygonal aggregates. Frequently there are numerous trains of two-phase inclusions. In some samples late quartz has been corrosive.

Other minerals are *biotite; muscovite*, sometimes greenish (St. 141851); *garnet;* bluish and brown *tourmaline;* turbid *zircon;* idiomorphic and xenomorphic *apatite; fluorite; rutile; beryl; opaque minerals* and others.

Late syn-kinematic two-mica granite (*Ruña granite*). – The

Ruña granite, which crops out in the northwestern part of the area, is a megacrystal-bearing two-mica granite (Plate XII-a). The medium-grained granite has alkali feldspar megacrystals up to 2×3 cm; they are oriented NW-SE, which is probably the result of either magmatic flow (Koster van Groos, 1962) or solidification under a weak compressional stress (F_3?). The granite has cut through the medium to coarse-grained two-mica granite, the western migmatic rocks and the megacrystal-bearing granodiorite series.

Locally the granite may include many xenoliths of all types of older rocks; the western extremity has been cut off by the outer ring of the post-kinematic Pindo biotite granite (Koster van Groos, 1962; de Graaff 1962; Woensdregt 1966).

Bodies of younger more finely grained megacrystal-bearing two-mica granite, with alkali feldspars up to 1×2 cm, have been encountered by Koster van Groos within the Ruña granite.

Mineralogy (*Table I-6*). – The megacrystals of the Ruña granite varieties are microclines, often twinned (Carlsbad law) and display traces of a fine zonal growth, which encloses small plagioclases and biotites (Frasl, 1954).

The *alkali feldspars* are cross-hatched and may show perthitization, mainly replacement perthite. Some of the albitic plagioclases enclose patches of alkali feldspar; furthermore there is little or no albitization and myrmekitization.

Plagioclase has an albitic composition; *quartz* is highly strained and encloses fine *rutile* needles as well as numerous two-phase inclusions.

The *micas* have ragged outlines and are often deformed. Late-stage muscovites have been reported by Koster van Groos (1962). Biotite (St. 141839): $\gamma = 1.642—1.648 \pm 0.002$.

Other minerals are *zircon*, idiomorphic, zoned and resorbed; *monazite; apatite; titanite; anatase; chlorite* and *opaque minerals*.

Post-kinematic intrusives

The post-kinematic intrusives comprise all rocks emplaced after F_3, and include a megacrystal-bearing two-mica granite (Arbos granite), a biotite granite (Pando granite), a weakly porphyritic, locally amphibole-bearing, biotite granite (Caldas de Reyes granite), pegmatites, aplites, quartz veins, granite porphyries, lamprophyres and olivine dolerites.

The rocks are not deformed and occur discordant with regard to the pre-existing rocks and structures. The biotite granites belong to the Traba-type granites (Parga-Pondal, 1956) which include the granites of Traba (15 km SW of Lage), Pindo (30 km NW of Noya) and Porriño-Monçao (E of Tuy; Floor, 1966) and may be correlated with the coarsely porphyritic biotite granites of northern Portugal (the "younger granites": Schermerhorn, 1956a; Oen Ing Soen, 1958, 1960 & 1970; Priem, 1962; de Boorder, 1965; Floor et al, 1970). The biotite granites often have a characteristic reddish colour.

The mode of emplacement of the granite stocks was piecemeal stoping or, on a larger scale, major stoping (Billings, 1945; Oen Ing Soen, 1960 & 1970). The rising magmas caused little or no disturbance of the regional structures, although the granites are clearly discordant; important epi-crustal tensional forces therefore must have existed. Ultimately the stoping magmas fractured and fragmented their roofs. The Caldas de Reyes granite, at its present exposure level, clearly exemplifies the latter process. In contrast, the other granites contain only a very few small xenoliths. This may be explained either by the fact that the sections of these granites now exposed lay deeper or by the fact that fragmentation during stoping was only subordinate.

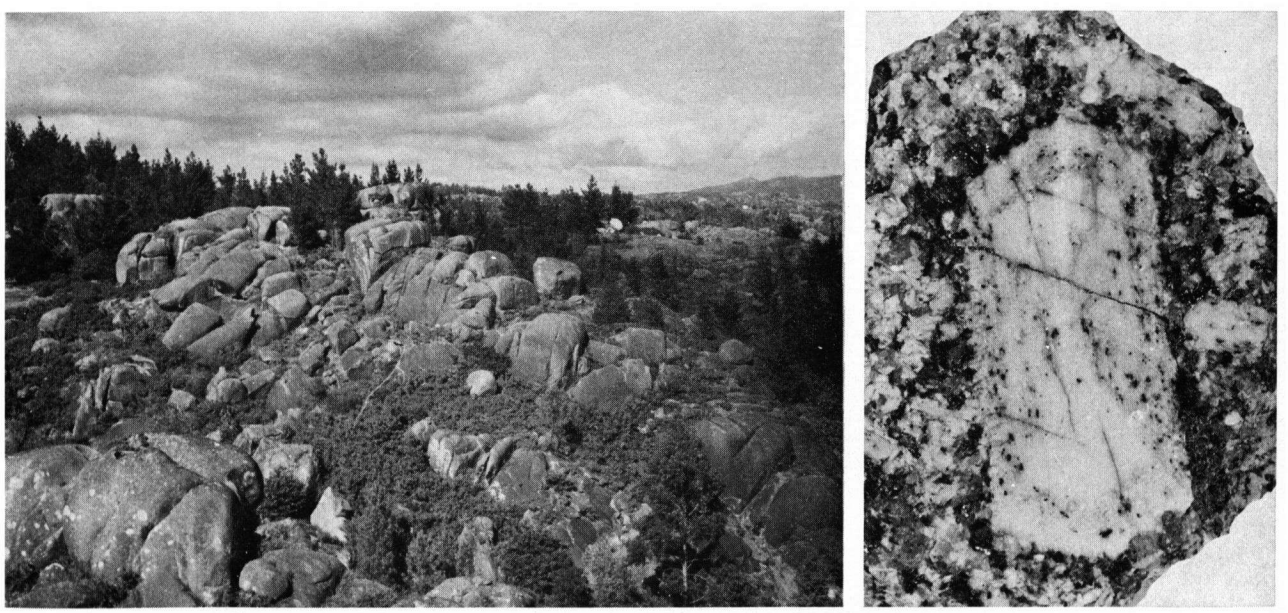

Fig. I-36. a. The post-kinematic Arbos granite; view from Moimenta facing east. b. An alkali feldspar phenocryst from the Arbos granite showing oriented inclusions of biotite (Frasl's) and a well developed 'hour-glass' structure. The biotites in the inner part of the crystal attach only to the (110) faces.

The post-kinematic granites have joint systems with an hexagonal symmetry, superimposed upon the most important older (regional) lineaments of weakness which they inherited (Arps, 1965; Avé Lallemant, 1965).

Table I-8 lists the most important characteristics of the post-kinematic granites of the area; the Pindo granite and the late syn-kinematic Ruña granite are also included. In Fig. I-40 the normative values for Q, Ab and Or have been plotted (see also p. 95).

Arbos granite. – The Arbos granite (Moimenta granite, von Raumer, 1963) is a very coarse-grained megacrystal-bearing two-mica granite, cropping out between Noya and Boiro (Fig. I-36a and Plate XII-b). The granite cuts through the rocks of the central zone, the eastern migmatic complex and the megacrystal-bearing granodiorite series. A few small xenoliths were encountered within the granite body. At the border of the dome-like intrusion, the granite grades into a medium-grained biotite-muscovite granite (SE and S) or a muscovite granite. After the emplacement of the granite, some aplites (occasionally porphyritic, St. 141857) and quartz veins followed; they were all found to be barren with the exception of a dyke S of Moimenta that has been mined for tin. The northern and northeastern borders of the granite may carry some sulphidic ore minerals.

The megacrystals of the granite may reach dimensions up to $2 \times 5 \times 10$ cm; they are generally twinned according to the Carlsbad law and contain small inclusions of plagioclase and biotite parallel to the growth zones of the alkali feldspar hosts (Fig. I-37; Frasl, 1954). Frequently an hour-glass structure is found with the enclosed biotites attached chiefly to the {110} faces (Fig. I-36b; Schermerhorn, 1956b; von Raumer, 1963).

Mineralogy (*Table I-6*). – The Arbos granite is much more coarsely grained than the Ruña granite. There is less mica; *biotite*, with $\gamma = 1.648 - 1.652 \pm 0.002$ (St. 141855), is almost completely transformed into *chlorite* which encloses secondary anatase crystals (Fig. I-38). *Muscovite* is slightly pleochroic.

Plagioclase is hypidiomorphic and has an albitic composition. *Alkali feldspar* displays exsolution and replacement perthites, the latter may accentuate the crystal growth zones (Fig. I-37). Myrmekite and albitization are either subordinate or not present. *Quartz* is slightly undulose.

Other minerals are *zircon*, idiomorphic, zoned and resorbed; *apatite; fluorite*, with violet pleochroic halos due to irradiation; *anatase; brookite; monazite* and *opaque minerals.*

Sample St. 141856 is a muscovite granite (border variety) containing some *garnet;* quartz is slightly idiomorphic.

Some of the aplites are clearly porphyritic and carry visibly idiomorphic feldspars, but the thin section of St. 141857 also reveals the presence of many idiomorphic quartz crystals (pseudomorphs after high-temperature quartz).

Pando granite. – A medium to coarse-grained biotite granite has intruded into the western part of the area, a few kilometres N of Esteiro (Plate XII-c).

Fig. I-37. Photomicrograph (crossed nicols) of an alkali feldspar phenocryst of the Arbos granite showing small biotite and plagioclase inclusions zonally arranged; their largest crystal faces are not always precisely attached to the growth zones of the host. Different generations of perthite, including a replacement perthite which started at the growth zones, are clearly visible (negative print, × 4).

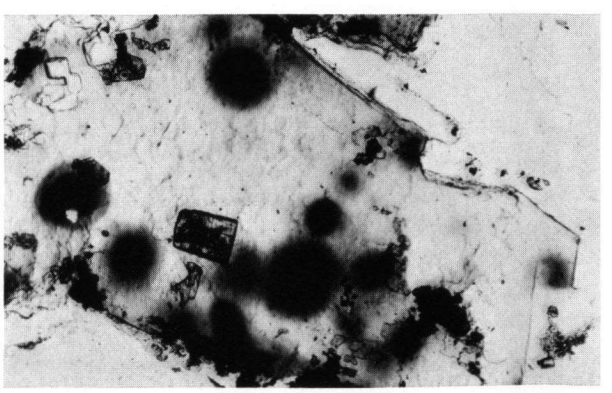

Fig. I-38. Photomicrograph of a chlorite in the Arbos granite enclosing idiomorphic secondary anatase crystals that originated during chloritization of biotite (St. 141854, × 75).
Note the idiomorphic outlines of biotite.

Avé Lallemant (1965, p. 164) in a discussion of the mode of emplacement of the Pando granite suggested the possibility of a "ring-fracture stoping", but this in fact should be regarded as a special form of major stoping (Oen Ing Soen, 1960). The granite contains few xenoliths.

Locally the granite is porphyritic or it may enclose bodies of a much more finely grained biotite granite (de Graaff, 1962; St. 111720). Apophyses are very scarce.

Mineralogy (*Table I-5*). – The main constituents are *quartz* (18–29 %; results of point-counting, Avé Lallemant, 1965 and de Graaff, 1962), xenomorphic and slightly undulose with occasionally high-temperature crystal forms (enclosed in alkali feldspar); *alkali feldspar* (35–43 %), hypidiomorphic or xenomorphic, cross-hatched and perthitized; and *plagioclase* (23–38 %), hypidiomorphic, normally zoned with a core of acid oligoclase and a rim of albite, twinned according to the albite, Carlsbad and pericline laws. Small crystals are often enclosed in alkali feldspar. Albitization, myrmekitization and decalcification are common (Avé Lallemant, 1965, Plate V-Fig. 4).

Small booklets of *biotite* are macroscopically visible. For biotite (4–6%), $\gamma = 1.656 - 1.660 \pm 0.002$ (St. 141816 and St. 141817).

Other minerals are idiomorphic, zoned and resorbed *zircon;* idiomorphic and zoned *allanite; apatite; fluorite; titanite; opaque minerals* and the alteration products *chlorite* and *muscovite* (sericite).

Caldas de Reyes granite. – At the southern end of the peninsula of Pesqueira, ca. 3 km S of Boiro and near the outlet of the Río Coroño, the northern border of a coarse-grained slightly porphyritic biotite granite is exposed (Plate XII-d).

In contrast to the other biotite granites in western Galicia, the main type of the present granite includes locally a little amphibole and is crowded with inclusions of all kinds.

Xenoliths of almost all previously described rock-types of the area occur in highly variable dimensions. Many of the xenoliths consist of more than one rock-type and the interrelationships are sometimes clearly visible.

Closely associated with the Caldas de Reyes granite are a fine-grained porphyritic biotite granite and a medium-grained porphyritic biotite granite; both types are probably older.

The northwestern border of the granite body has been mapped by von Raumer and the southern part by Vogel and Rengers (see also Floor, 1968). At the contacts of the granite with the low-grade metamorphic rocks at the outlet of the Río Coroño, there is evidence of a contact metamorphism causing the growth of andalusite in the metamorphic rocks. Along certain joints the granite has been highly epidotized.

Mineralogy (*Table I-5*). – The mineralogy of the Caldas de Reyes granite is comparable with that of the Pando granite.

Quartz, alkali feldspar, plagioclase and *biotite* are the main constituents. Biotite is dark brown and green and sometimes intergrown with a dark green ferrohastingsitic *amphibole* with a very small optical angle.

Other minerals are *muscovite;* large idiomorphic and zoned *allanite;* idiomorphic *zircon; monazite; apatite; fluorite* and *opaque minerals.* Secondary minerals are *chlorite, sericite* and *calcite.*

Secondary *epidote* is a main constituent in the epidotized parts of the granites, where it is idiomorphic and highly pleochroic in yellow (St. 141815).

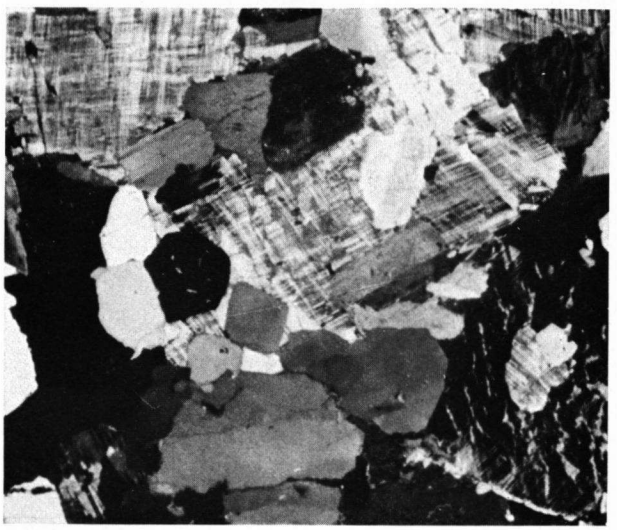

Fig. I-39. Caldas de Reyes granite: Quartz pseudomorphs after high-temperature quartz enclosed by microcline (St. 141813, × 10). Microcline also encloses a corroded plagioclase crystal with an albitic rim.

Granite porphyries. – The granite porphyries were encountered in all the principal rocks of the area with the exception of the post-kinematic granites. The dykes may have intruded along deep-reaching tension joints and faults that were the result of a regional updoming which coincided with the post-kinematic intrusions (Oen Ing Soen, 1960 & 1970). Most of the dykes seem to have restricted lengths; however there is one granite porphyry more than 5 km long with a width of ca. 2–5 m (NE of Pte. Beluso).

The granite porphyries are brownish yellow. The contacts are sharp; they have closely spaced joint systems.

Macroscopically phenocrysts of *quartz, feldspar* and *biotite* are often visible, especially on weathered surfaces.

Mineralogy (*Table I-6*). – Phenocrysts are *quartz* with high temperature crystal forms, sometimes corroded, *alkali feldspar,* often cross-hatched and perthitized, and to a lesser extent *plagioclase* and *biotite.*

Idiomorphic plagioclase may be enclosed within alkali feldspar. In sample St. 141859, the feldspar phenocrysts have "symplectitic rims" of quartz and feldspar (post-crystalline exsolution).

The groundmass consists largely of the same minerals. Other minerals are idiomorphic *zircon; apatite; rutile* (sagenite); *anatase; epidote; chlorite; muscovite* and *opaque minerals.*

Hornblende lamprophyres. – Like the granite porphyries, some scattered mafic dykes have been found in all the rocks of the area except the post-kinematic granites. Generally these dykes are considered to be the youngest intrusive rocks in western Galicia (Floor, 1968) and northern Portugal (de Boorder, 1965).

Mineralogically the fine-grained lamprophyres are spessartites; they are chiefly restricted to the northern part of the area. The darkly coloured and narrow dykes have intruded along important faults and joints.

Mineralogy (*Table I-5*). – The only phenocrysts are brown or brown and green zoned and often twinned *hornblendes.* The groundmass consists of hornblende; normally zoned *plagioclase* (30–54 % An); highly pleochroic *epidote; quartz; biotite; titanite; rutile; sericite; calcite* and *opaque minerals.*

Olivine dolerites. – On the coast of the Ría de Noya y Muros, 1.7 km NNE of Portosín, an olivine dolerite crops out between the high-tide and low-tide levels. Pebbles of this dyke have been found as far away as Barquiña in the Quaternary terrace deposits.

A similar dolerite is assumed to exist upstream in the Río Beluso Valley; heavy mineral samples from the river sediment contain a high percentage of titanaugite (Arps, 1969), which can also be found in the bottom sediment of the Ría de Arosa (Koldijk, 1968).

Mineralogy (*Table I-5*). – The medium-grained rock contains large amounts of idiomorphic to hypidiomorphic *plagioclase* (34–72 % An), which is normally zoned and twinned according to the albite and Carlsbad-albite law and displays an ophitic texture.

Phenocrysts of zoned and often twinned violet *titanaugites* may enclose *olivines*, which are sometimes idiomorphic. Relatively large and idiomorphic *magnetites* generally occur together with dark-brown *biotite.*

Other minerals are *apatite; analcime* (Harker, 1962); *calcite; chlorite; serpentine; sericite* and within a cavity, the zeolite *thomsonite.*

CONCLUDING REMARKS

Accessory minerals

The results of a detailed study of accessory zircons are discussed in the next chapter. A separation technique has been applied that guarantees optimal recovery of all accessory minerals (see p. 98). Thus it could be proven that minerals such as *monazite* and *xenotime* are present in varying amounts in almost all of the rocks of the area with the exception of the non-migmatic blastomylonitic orthogneisses and most of the cognate diorite and granodiorite inclusions of the megacrystal-bearing granodiorite intrusion series. Both minerals are always highly corroded. They sometimes appear to have grown together with zircon, partly or completely enclosing it (Plate XVI-j).

All the Hercynian two-mica granites contain secondary *anatase* (Fig. I-38) as well as some *brookite.* In general both minerals are perfectly euhedral; anatase may also form clusters (Plate XVI-l and m).

Pleochroic haloes in biotite, hornblende, tourmaline, muscovite and occasionally fluorite are quite common in almost all of the rocks of the area; the most prominent examples were found in the intrusive granites and granodiorites. The accessories recognised as causing the haloes are zircon, monazite, pyrochlore, titanite, allanite and apatite. Many haloes are composed of a darker inner ring and an outer concentric ring of weaker intensity (Fig. I-38). The dark haloes are the result of radiation (α-rays) originating from radioactive elements in the crystal lattice of many accessories. Each α-emitter induces a halo with a more or less characteristic diameter (Priem, 1962). Measurements of single as well as composite haloes in biotite from the post-kinematic Pando granite indicate that Po-214 is probably the emitting nucleus, which produces haloes with a radius of ca. 33μ and Rn-222, Po-218, Po-210, Th-224 and Th-228 are the emitting nuclei responsible for the haloes with radii between 17μ and 23μ (Rankama, 1954, p. 128). Haloes with similar radii were measured in blue tourmaline of a gneissic aplite (St. 141812).

Garnet

Two physical properties of garnets, i.e. cell dimension (a_0) and refractive index n(Na), have been measured in order to obtain some information on their composition. The data are plotted in a combined Frietsch-Sastri diagram for pyrope-almandine-spessartite garnets.

As Frietsch has already pointed out, no accurate information can be obtained with his diagram but "it is possible to distinguish a number of fields in which garnets of more or less similar composition occur" (Frietsch, 1957, p. 49).

Sastri constructed a more detailed pyralspite diagram in which the subordinate endmembers andradite and grossular play a role. According to Sastri (1958), his diagram(s) "provide accurate characterization of garnets."

The data for the garnets from various rocks of the present area can clearly be divided into several groups. The garnets from amphibolites and calc-silicate rocks differ from all the others; garnets from the biotite orthogneisses, paragneisses and migmatites are restricted within certain areas, although the last two partly coincide. The garnets of probably pre-Hercynian origin enclosed in the metablasts of the albiteblast-bearing paragneisses (no. 1 and no. 2, Fig. I-25) differ slightly, according to the present diagram, from those of Hercynian age. The migmatic biotite orthogneisses contain garnets which differ from those belonging to the non-migmatic orthogneisses (no. 3, no. 4 and no. 5). Sample no. 3 is a garnet from a biotite orthogneiss located close to the contact with an amphibolite. The garnets from Hercynian granites, aplites and pegmatites are closely grouped in the same part of the diagram as the garnets of the migmatites.

Albitization

Two manifestations of albitization in the rocks of the present area are summarized below.

Firstly, the oligoclase metablasts of the plagioclaseblast-bearing paragneisses close to the amphibole-bearing orthogneisses were partly or completely albitized (Fig. I-11). A causal relationship between the albite porphyroblasts and the amphibole-bearing orthogneisses is assumed; the albite metablasts are believed to have grown as a result of sodium metasomatism. Similar albiteblast-bearing paragneisses have been reported by Floor (1966) in the southern part of the "blastomylonitic graben" and by several other graduate students working in the northern sector of the graben (Monster, 1967; Rijks, 1968 and van Tongeren, 1970). Porphyroblastic albite-schists have been described in the Complex of Santiago (van Zuuren, 1969) and further eastward around the southern margin of the Ordenes Complex. Here, however, the albite porphyroblasts have developed into greenschists and have not replaced older plagioclase metablasts.

Secondly, albitization of alkali feldspar is frequently found in many intrusive granites and granodiorites of the area. During albitization, which is generally considered to be a process of autometasomatism, alkali feldspar is replaced by albite; the process starts at the grain boundaries of alkali feldspar with the surrounding minerals, as well as at the contacts with inclusions and cleavage planes.

The newly-formed albite has convex, and only occasionally hypidiomorphic, contours directed toward alkali feldspar (Plate VII-a). The process seems to proceed synchronously with myrmekitization and (replacement) perthitization.

Myrmekite

When myrmekitization occurs in the rocks of the area, it is always a process of replacement of alkali feldspar; the cauliflower-shaped myrmekite points toward alkali feldspar. The shape of the enclosed quartz varies with the direction of cut. It also seems probable that the very thin wormlets recrystallize into larger droplets as myrmekitization proceeds (Plate VII-b).

Perthite

All the various types of perthite (Alling, 1938; Avé Lallemant, 1965) have been encountered. The relative abundance varies with the rock-type and generally agrees with the observations of Capdevila & Floor (1970). The perthites can be divided into exsolution perthites and replacement perthites. The esxolution perthites are finer and generally do not continue to the border of the alkali feldspars (Avé Lallemant, 1965, Plate V – Fig. 2) nor do they trespass the Carlsbad twin-planes. The replacement perthites are much coarser and have irregular outlines. They are often twinned (Plate VII-a; Avé Lallemant, 1965, Plate V – Fig. 3) and generally start to grow at the grain boundaries and cleavage planes.

Conclusions based on the normative Q-Ab-Or data

The data for normative quartz, albite and orthoclase from the late syn-kinematic Ruña granite and the post-kinematic Arbos, Pando and Caldas de Reyes granites have been plotted* in a Q-Ab-Or diagram (Fig. I-40). The experimental results of von Platen (1965), Tuttle & Bowen (1958) and Luth et al. (1964) for the normative Ab/An ratios as well as the position of the cotectic lines and granite ternary minima with respect to pressure changes have been added to the diagram.

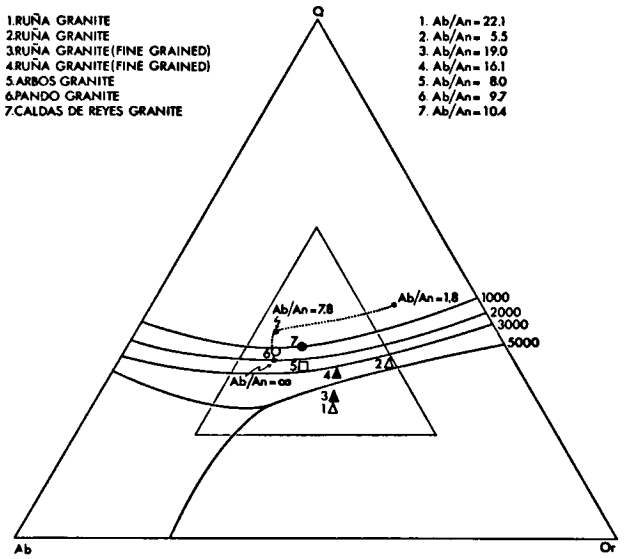

Fig. I-40. Q-Ab-Or diagram for the Ruña granite, the Arbos granite, the Pando granite and the Caldas de Reyes granite. The range of normative Q+Ab+Or varies between 80–89 %. The solid lines in the diagram represent the cotectic lines of the system Q-Ab-Or at Ab/An = ∞ and $P(H_2O)$ of 1000, 2000 and 3000 bars (Tuttle & Bowen, 1958) and at 5000 bars (Luth, et al., 1964). Dashed line indicates the shift of ternary minima at 2000 bar but with different Ab/An ratios (von Platen, 1965). The inner triangle indicates the compositional field of granites (Tuttle & Bowen).

The data for the granites under consideration indicate that the Arbos, Pando and Caldas granites were probably emplaced under epizonal conditions as suggested by Oen Ing Soen (1960 & 1970) for the origin of the "younger" granites in northern Portugal. The allochthonous Ruña granite probably crystallized under epi-mesozonal conditions. Another important aspect of the position of the granite ternary minima is its dependence on the normative Ab/An ratio of the granites (von Platen, 1965); these ratios vary considerably for the Ruña granite but follow roughly the experimentally determined shift in the granite ternary minima with different Ab/An ratios. Furthermore it is

* The data for the Arbos and Caldas granites are from von Raumer (1963); those for the Pando and Ruña granites are from de Graaff (1962) and Woensdregt (1966 and pers. comm.).

probable that an extra shift in the data of the Ruña granite in the direction of orthoclase was caused by an abundance of certain volatiles in the magma.

When the data from some nearby syn- and post-kinematic granites (Woensdregt, 1966, Fig. 3) are compared with the present diagram, it appears that the data for the syn-kinematic two-mica granites as well as the post-kinematic granites are concentrated in separate groups and underline the above-mentioned differences.

GEOLOGICAL HISTORY OF THE AREA

The rocks of the area have been treated in three groups, i.e. the non-migmatic rocks, the migmatic rocks and the intrusive rocks. The non-migmatic rocks occur in the central zone, part of a sub-meridionally trending "blastomylonitic graben" (den Tex, 1966; den Tex & Floor, 1967), in the SSW of the area, and as inclusions in a medium to coarse-grained two-mica granite batholite (SW and W). All the non-intrusive rocks have undergone the same Hercynian metamorphism but at different levels in the orogen. During the Hercynian both levels were brought into juxtaposition. The intrusive rocks, treated as a separate group, all* belong to the Hercynian orogeny and were emplaced during the successive orogenic phases (Appendix II).

The oldest rocks of the area are the paragneisses, schists and para-amphibolites located in the central zone. Though subjected to the successive Hercynian deformations and a regional metamorphism, some metasedimentary rocks still bear traces of a probably pre-Hercynian deformation and metamorphism.

For example, some paragneisses and schists contain resorbed relics of staurolite enclosed in (Hercynian) andalusite; in addition there are the relics of garnet enclosed in plagioclase metablasts in some paragneisses (Floor, 1966) or enclosed in the plagioclase of some amphibolites (Figs. I-5a, I-5b, I-10 and I-6).
Examples of a pre-Hercynian deformation are possibly the folded F-folds observed in the tough, very fine-grained paragneisses in the north (Fig. I-4) as well as the trains of elongated quartz grains present as s_i within plagioclase metablasts (Floor, 1966).

During a period of acid plutonism in the Upper Ordovician (460 to 430×10^6 years ago; Rb-Sr whole rock analyses, Priem et al., 1970), the metasedimentary series were intruded by coarse-grained megacrystal-bearing two-mica granites, biotite granites and peralkaline granites. Between the latter two intrusion series, the biotite granites and surrounding metasediments were invaded by numerous basic dykes. The intrusion of the pre-Hercynian granites took place along roughly N-S directed lineaments of weakness.

Three deformation phases during the Hercynian orogeny were active in the area under consideration; the direction of compression was always (E)NE- (W)SW. The first deformation (F_1) was very active; all the pre-existing metasediments, amphibolites and dykes were folded sharply, the biotite granites and peralkaline granites were flattened and transformed into granite mylonites, and the coarse-grained megacrystal-bearing two-mica granites became coarse-grained augengneisses (phyllonitic). F_1-folds are still found in many metasedimentary rocks and some amphibolites (Figs. I-2, I-4, and I-13).

The original position of s_1 is difficult to establish for the rocks of the central zone; there are some indications that s_1 was a sub-horizontal foliation plane (Fig. I-2). At present, however, the position of s_1 is usually sub-vertical.

The granite mylonites of the central zone have sharp linear and planolinear structures which are very consistent throughout the "blastomylonitic graben" (Plate III), even beyond the present area. It seems feasible to suppose that two successive deformations are responsible for these structures, i.e. probably F_0 and F_1.

The metasedimentary rocks in the S and SW, now in juxtaposition with the migmatites, represent an even higher tectonic level of the Hercynian orogen than the rocks of the central zone and in fact these schists together with the medium to coarse-grained para-autochthonous two-mica granites (Barbanza granite) SW and W of the area represent a structural unit that originated after F_2.

The original position of s_1 in the metasediments of this unit was clearly sub-horizontal (Fig. I-19); traces of an F_0 have also been encountered (Plate V-b). F_1 was followed by a phase of Abukuma-type plutono-metamorphism (Floor, 1966; Oen Ing Soen, 1970). The metasediments in the S, the rocks of the central zone and the migmatic rocks represent different levels of this low-pressure metamorphism.

The mineral paragenesis of the rocks in the south-western part of the area belongs to the quartz-andalusite-plagioclase-chlorite sub-facies of the green-schist facies and for the rocks of the central zone, reaches the sillimanite-cordierite-muscovite-almandine sub-facies of the cordierite-amphibolite facies (Winkler, 1967).

A subdivision of the rocks into zones of increasing grade of metamorphism is not really possible, but the relative abundance of the minerals andalusite and sillimanite in the paragneisses and schists and of cummingtonite in the amphibolites towards the eastern margin and the southern part of the central zone indicate an increase in temperature and a decrease in pressure, to the E and S (Fig. I-7).
The granite mylonites of the central zone recrystallized into blastomylonites. A metablastic growth of oligoclase is characteristic for many paragneisses (Plate II-a en b). A subsequent albitization of the oligoclase metablasts from paragneisses around the amphibole-bearing orthogneisses occurred; the replacement is obviously the result of sodium metasomatism (Fig. I-11, Plates I-b and II-c).

* The olivine dolerites seem to be the only exception; they are probably of Cretaceous origin (Floor, pers. comm.).

The migmatic complex consists of rocks of metasedimentary origin, migmatic orthogneisses and migmatic coarse-grained augengneisses; in fact all the augengneisses are more or less migmatic (Fig. I-31, Plate VIII-b). Large-scale anatexis ultimately led to the formation of aplogranitic and granitic melts which were often capable of intrusion into higher less-mobilized levels. The aplogranites are almost autochthonous to parautochthonous and are located within the coarse-grained augengneisses (Fig. I-32). They may be regarded as products of mobilization of the latter rocks, although the melts must have been enriched in certain elements which resulted in the growth of minerals such as beryl and tourmaline. The anatectic granites are considered to be autochthonous, when they occur as irregular bodies in the migmatites without intrusive relations. The majority of the anatectic granites, however, is parautochthonous to allochthonous (Oen Ing Soen, 1970). The emplacement of the anatectic granites caused a further thermometamorphic growth of andalusite in some schist xenoliths, transforming the rocks into andalusite granofelses (Fig. I-18). Sillimanite, garnet and sometimes even alkali feldspar may occur within the schist xenoliths (Fig. I-22). The latter minerals indicate that the alkali feldspar-cordierite hornfels facies has been reached (Winkler, 1967).

During a short period of crustal tension that reactivated the N-S trending fundamental fault on the western side of the central zone, two important events occurred. First, the rocks of the central zone directly adjacent to the fault subsided; the subsidence along the fault was so great that it induced, some kms eastward, synthetic faults in the paragneisses and schists.

Second, the fault went so deep that it must have tapped a deep-seated magma chamber; dioritic and granodioritic magmas were then able to intrude into higher levels. Most of the magma was emplaced W of the central zone as a large oblong body (central and northern part of the area), and some penetrated into the migmatites (southern part of the area). E of the central zone, in the central part of the area, small amounts of granodioritic material were emplaced in the migmatites along several eastern faults. The granodioritic series consists of three members of comagmatic origin. The main intrusion is a megacrystal-bearing granodiorite with many dioritic and granodioritic cognate inclusions as well as numerous para- and orthogneiss xenoliths. The youngest members of the series are the two muscovite granite bodies and many aplogranitic dykes (Fig. I-34 and Plate X).

Shortly afterwards, but during the same period of tension, the majority of the anatectic two-mica granites followed. The group of parautochthonous to allochthonous two-mica granites includes: a relatively early medium to coarse-grained two-mica granite (Barbanza granites: von Raumer, 1963; Avé Lallemant, 1965; Dumbría granite: Woensdregt, 1966) cropping out in the western part of the area. This granite consists of a main biotite-muscovite granite variety which locally may enclose bodies of a biotite-bearing muscovite granite variety (Plate XI-a). The intrusion of medium to fine-grained two-mica granites then followed. This granite consists of three members (Muros granites, Avé Lallemant, 1965); they can probably be correlated with the eastern and southern anatectic two-mica granites (Plate XI-c). A common feature of all two-mica granites is that they often contain late-stage muscovites (Plate IX-b), which grew during a period of muscovitization that followed the solidification of the granites. The emplacement of the palingenic granites was concluded (before F_2) with the intrusion of many apophyses.

The second Hercynian deformation (F_2) was not strong and penetrated only locally. The presence of a sub-vertical crenulation cleavage (s_2) has been encountered in the metasedimentary rocks of the northern part of the central zone and in the SW and W (Figs. I-2 and I-3, Plate I). In the central and southern parts of the central zone, s_2 and s_1 are sub-parallel and can only occasionally be distinguished as two separate entities. The influence of F_2 on the Hercynian migmatites and syn-kinematic intrusives also varies greatly. A marked parallel orientation of the alkali feldspar megacrystals of the megacrystal-bearing granodiorite resulted from F_2, while the mica flakes of the two-mica granites display a slight preferred orientation. The late-stage muscovites in the latter granites seem to have suffered little from F_2 (Plate IX-b). Shortly after F_2 the third deformation (F_3) followed. Many granitic rocks in the western and northeastern parts of the area were severely deformed along narrow zones that transformed the rocks into phyllonites and even mylonites (Plate VIII-a, IX-c, X-c and XI-b). Phyllonitization and mylonitization were greatest in the S.

The phyllonitic rocks owe their structure to a E(NE)-W(SW) directed compression that induced slip along a sub-vertical conjugate set of planes, striking roughly NNE-SSW and WNW-ESE. Dextral slip along the N-S to NNE-SSW striking planes was more intense and locally even converted the rocks into mylonites. Also attributed to F_3 is a large-scale block faulting. Part of the movements took advantage of the pre-existing sub-meridional faults; the rocks directly adjacent to these faults became mylonitic. Other strike-slip movements occurred along pre-existing joints, dextral along NE-SW striking joints and sinistral along NW-SE striking joints.

The emplacement of the Ruña granite, a late syn-kinematic megacrystal-bearing two-mica granite, most probably followed F_2 but preceded F_3, since the granite bears some traces of a phyllonitization. A weak preferred orientation of the alkali feldspar megacrystals is probably the result of magmatic flow (Plate XII-a). The subsidence of the non-migmatic metasedimentary rocks in the S and SW and a part of the Barbanza granite batholite into juxtaposition with the migmatites is tentatively placed between F_2 and F_3, during a period of temporary relaxation. Many pegmatites, aplites and quartz veins intruded, mainly along faults and joints, before as well as after F_3. The

intrusion of a post-kinematic megacrystal-bearing two-mica granite (Arbos granite) and two coarse-grained biotite granites (the Pando and Caldas de Reyes granites) together with a few granite porphyries and hornblende lamprophyres are the latest Hercynian magmatic activities of the area under consideration (Fig. I-36 and Plate XII). The Rb-Sr whole rock isochron age of some post-kinematic biotite granites from northern Portugal and western Galicia indicates that the intrusions took place $280 \pm 11 \times 10^6$ years ago.

As in northern Portugal, it is believed that the location of the intrusions is closely related to the effects of preceding tectonic events and that the granites were emplaced where important faults and master joints met (Carlé, 1945; Oen Ing Soen, 1960 & 1970). Furthermore it has been suggested by Oen Ing Soen that a causal relationship existed between a regional uplift and the rise of the granitic magmas. The very few olivine dolerites are probably of Cretaceous age.

CHAPTER II

ZIRCON IN GRANITES, GNEISSES AND METASEDIMENTARY ROCKS OF THE AREA AROUND NOYA

INTRODUCTION

Investigations of heavy accessories, especially zircon, were initiated to obtain more information about origin, genesis and the petrogenetic relationships for the numerous granitic and metasedimentary rocks of the present area. A separation technique has been applied by which, in addition to zircon, other heavy accessory minerals were also recovered; they have been mentioned in the mineralogical descriptions in the former chapter.

The present zircon investigations cover crystal morphology, general mineralogical descriptions, fluorescence properties and chemical composition.

Quantitative analyses of certain elements present in various zircon samples were obtained with an electron microprobe (Geoscan); they were carried out by Dr. P. Maaskant at the Institute of Earth Sciences of the Vrije Universiteit, Amsterdam.

The fluorescence properties of the zircon crops were investigated in cooperation with Dr. P. van Gijzel at the University of Nijmegen. Additional information about zircon morphology was obtained with the scanning electron microscope (Stereoscan) at the Central Laboratory TNO, Delft.

Statistical calculations based on length-breadth measurements of zircons were carried out with an IBM electronic computer at the Centraal Reken Instituut, Leiden.

The program was prepared by Mr. K. J. Roberti of the Geological Institute in Leiden.

Mineral separation technique

To obtain the highest possible recovery in a short time at relatively low cost, rising current elutriation is used as a phase in the mineral separation technique. The type of elutriator used (Fig. II-1) is based on a model by Harris (1965). The method has been thoroughly tested and the results will be published separately. The complete separation procedure is indicated in Table II-1. The rising current elutriator is used after wet sieving; only the fraction $<150\mu$ passes through the elutriator in at least two subfractions, $<75\mu$ and 75–150μ respectively.

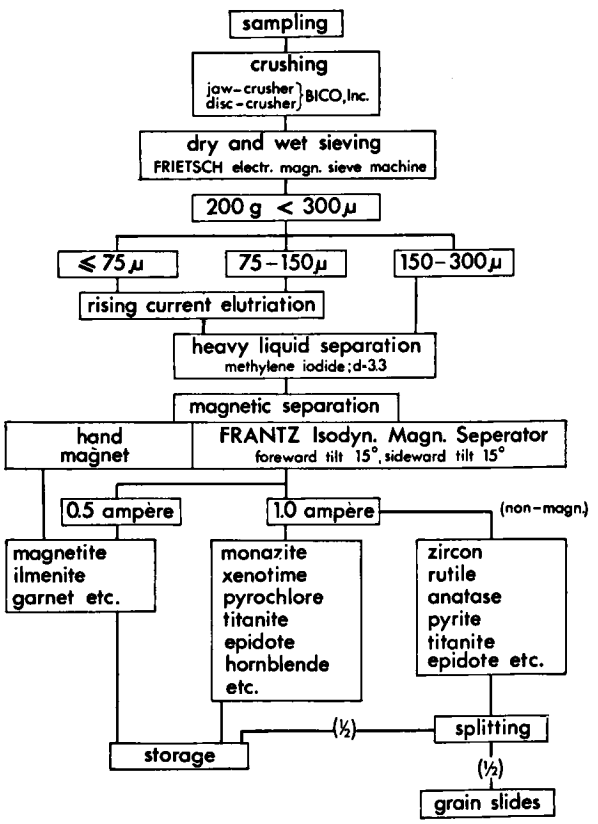

Table II-1. Flow diagram for the mineral separation technique.

Rising current elutriator. – In an article by Harris on the "water tower method", a brief description of his elutriator is given. Using these data, a slightly modified apparatus was constructed. The whole system in its present state is shown in Fig. II-1. The glass parts were made by Mr. C. J. van Klink, glass blower at the Kamerlingh Onnes Laboratory at Leiden.

Use of the elutriation system. – After sieving, the two finest fractions, i.e. <75μ and 75–150μ, pass through the elutriator one after the other. The samples are mixed with water and are put into funnel E_1; a pinch of Calgon (a water softener) and a few drops of Teepol (detergent to lower the surface tension of the water) are added.

Tap to A is opened and container A_1 is filled; the water level is kept constant by the insertion of tube A_3. Then A_4 and regulator D_1 are opened to allow the water to rise through the elutriator via B_1, B_2 and B_3; it is then discharged into C_2. When C_2, a settling reservoir, is filled the excess water will leave the system via C_3 and C_4.

The amount of water passing through the column is regulated with D_1 and can be "measured" on scale D_3; the position of the meniscus (head) in tube D_2 varies with the amount of water (discharge in cm^3 per sec) passing through the system. After adjusting the head in D_2 to a discharge suitable for the concentration of one of the fraction sizes, the concentration procedure is started by switching on E_2, a mixer, and slightly opening the tap of E_1. The sample gradually passes through B_6 and enters the elutriator via B_5. In B_2 the sample is split: a part is discharged into C_2 and a relatively small part settles at the bottom of the column (B_4). When the whole sample has passed through the elutriator, a concentrate rich in heavy minerals is collected. The whole procedure, including cleaning afterwards, takes about 15 minutes. The discharged part of the sample is once again passed through the rising current elutriator. For further details of the concentration procedure, the reader is referred to Harris (1965) and a forthcoming article by the present author.

The concentrates from both sample fractions which have settled at the bottom of the column are then collected, washed with acetone and dried. After 5–10 minutes the concentrates, about 20–30% (by weight) of the original sample, are put in a pear-shaped funnel with methylene iodine ($d \approx 3.3$) to carry out the final heavy liquid separation. The heavy minerals are collected, washed with acetone, dried and now passed through the magnetic separator to separate the minerals with different magnetic susceptibility (Rosenblum, 1958). At 0.8 Ampere and a sideward and forward tilt of 15°, the non-magnetic minerals, such as zircon, pyrite, anatase, brookite, titanite, etc. are separated from the magnetic minerals (magnetite, ilmenite, garnet, monazite, xenotime, etc.).

Methods of investigation and registration

The heavy mineral crops were not treated with acids and therefore the non-magnetic concentrates may, in addition to zircon, also include the above-mentioned minerals; the presence of these minerals did not complicate the zircon studies.

About one-half of each concentrate was mounted on slides with Canada balsam, while the rest was used for other studies. The zircon crops have been investigated in several ways.

The mineralogical properties of the zircons mounted on the slides were studied and the results of 11 samples selected from a total of 65 samples from different rock-types have been listed quantitatively in Table II-2.

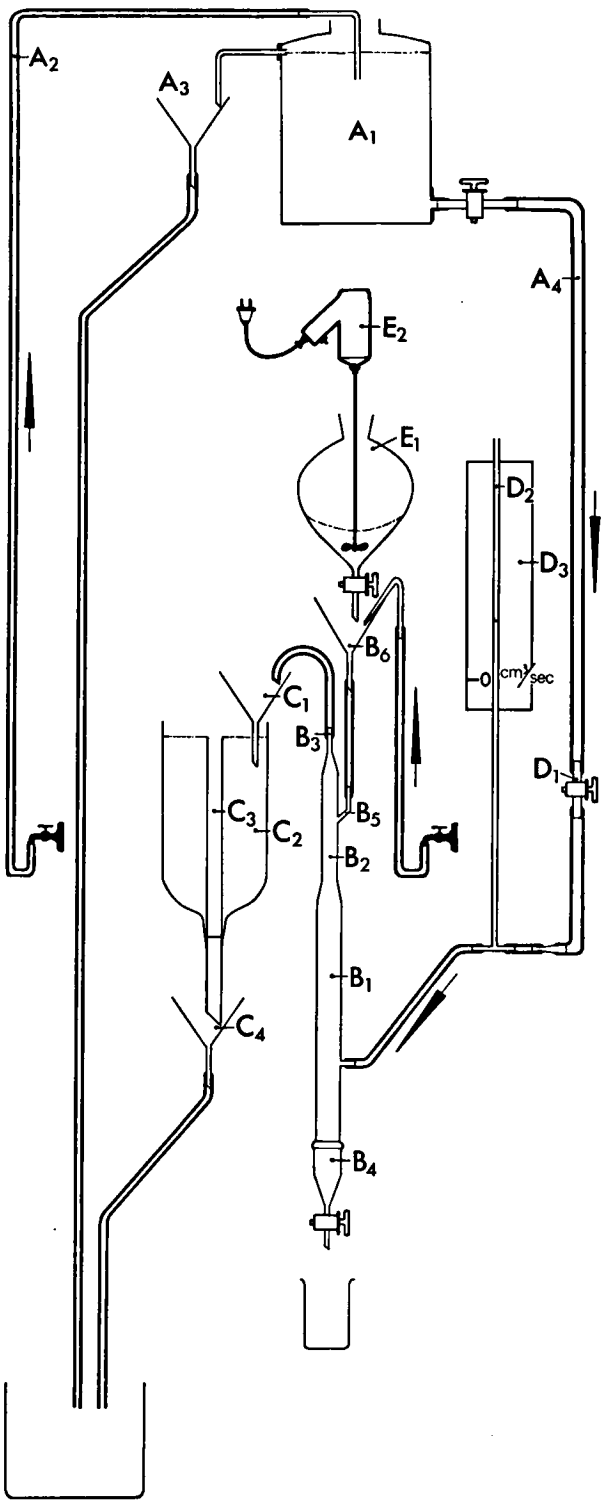

Fig. II-1. The rising current elutriation system. Explanation of symbols in text.

The investigation of the crystal morphologies received extra attention. The grain slides offer some information on crystal morphology but even more on contours, which more or less inevitably inspires the observer to carry out length-breadth measurements. If the crystals on the slides are clear, it is generally possible to draw some conclusions about the recurring crystal forms. It was found, however, that loose grains mounted on spindles and studied under reflected light offer even more information on the crystal forms of the zircon grains. Aberrant morphologies can also be studied better in this way.

Additional information on crystal morphology was obtained with the aid of the scanning electron microscope (Stereoscan). The results of the investigation of zircon crystal morphology are schematically indicated in Table II-3.

Finally the fluorescence properties of several zircon crops (loose grains) were investigated and some electron microprobe analyses were carried out.

The crystal forms were compared with the zircon habits from Goldschmidt's "Atlas der Kristallformen" (Goldschmidt, 1923) and those published in recent Russian articles (Zavjalova, 1966; Krasilnikova, 1966, Liakhovitch & Balanova, 1966; Yushkin et al., 1966).

The indices of the crystal forms that are used in this paper refer to a body-centered lattice (Mason & Berry, 1968); the notations differ from those based on a face-centered lattice (Fig. II-2).

Angle measurements with the goniometer were carried out by Mr. J. H. Slegtenhorst of the Geological Institute (Leiden) for two samples, each with zircons in a different habit. His measurements confirmed the visual evaluations of the present author, although it was found that a differentiation between {301} and {201} is really only possible by accurate measurements. In a few cases angle measurements according to Frasl were carried out (Frasl, 1963).

The length, breadth and elongation ratio graphs of the 12 selected zircon samples have been added to complete the morphological character of the zircon crops. One hundred unbroken crystals were measured according to the "ribbon counting" technique (Kalsbeek, 1962; van Harten, 1965) with the aid of photos taken at random from the grain slides.

The statistical parameters (Larsen & Poldervaart, 1957; Kalsbeek & Zwart, 1967) that are very often used in literature to characterize zircon populations are listed in Table II-6. The modes of length, breadth and elongation frequencies have been added to the list; the modes are graphically the highest points of the frequency curves and indicate which grains predominate in a population. Zircon populations always tend to be skewed with modes that are smaller than the means.

RESULTS OF INVESTIGATIONS

An attempt has been made to characterize the various petrogenetic important properties of the zircons occurring in the many rock-types of the area quantitatively by investigating either 50 or 100 grains from 11 selected samples (Table II-2).

Not all the zircons of the crops are well-developed

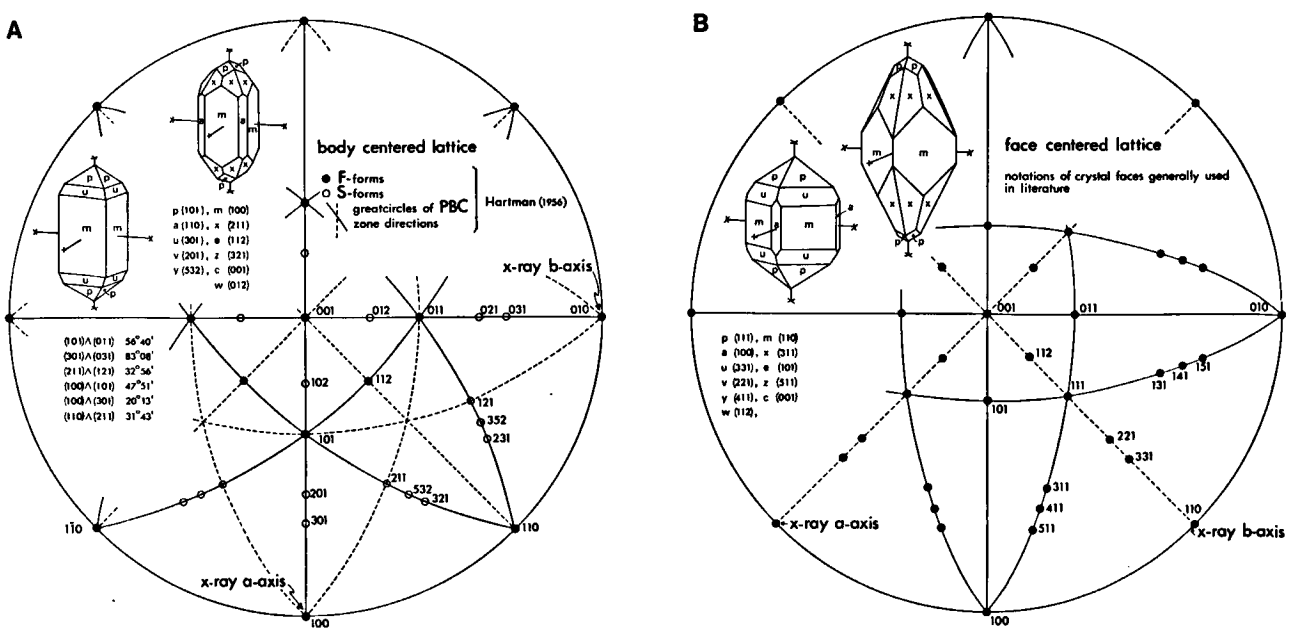

Fig. II-2. Stereographic projection of the main crystal faces and growth-zones of zircon crystals. The diagrams refer to a. body-centered lattice and b. face-centered lattice (the old morphological setting).

ROCK-TYPE			PRE-HERCYNIAN			HERCYNIAN							
						syn-kinematic					post-kinematic		
						magm. series			anatectic				
			2 coarse-grained augengneiss	3 biotite orthogneiss	4 biotite-ferrohast. orthogneiss	5 granodiorite cognate inclusion	6 meg-bearing granodiorite	7 muscovite granite	8 two-mica granite (Barbanza)	9 two-mica granite (Eastern)	10 meg-bearing two-mica granite (Arbos)	11 biotite granite (Pando)	12 amphibole-biotite granite (Caldas)
sample number			781	717	860	795	861	809	824	838	855	816	863
weight of zircon crop in mg per 200 gram sample			30.1	13.9	282.4	160.0	23.8	6.2	15.0	42.0	20.0	71.8	84.2
number of countings			100	100	50	50	50	25	50	50	50	50	50
crystal morphology	crystal forms	{100} ± {110}	91	99	84	98	90	88	86	96	96	92	94
		{101} ± {201} ± {301} ± {211}		72	82	24		76			78	82	84
		{211} ± {101}	89	19		62	84	4	92	92	12	2	10
	approximate size	{101} ⩾ {211}	2	17		44	22			4	8		4
		{101} < {211}	72	1		16	56	4	78	80		2	2
		all pyramid faces ⩾ all prismatic faces	54	29	58	20	54	44	54	32	22	28	18
		all pyramid faces < all prismatic faces	27	41	14	58	26	24	12	46	56	50	38
	unbroken crystals		65	63	56	52	64	52	56	58	56	54	42
	broken or incompletely developed	simply broken, damaged	21	24	24	30	22	36	34	32	36	22	40
		fragment	5	8	20	14	12	4	10	10	8	16	18
	crystal forms completely lacking		1	1				4					
	aggregates		8	4		4	2	4				8	
asymmetric outlines, aberrant crystals			7	26	12	30	24	8	30	8	10	4	26
resorption due to magmatic or metamorphic processes			62	79	60	8	82	100	88	72	84	72	20
zoning not neccessarily throughout the crystal		fine and regular	16	23	4		4	4	32	2	42	10	16
		coarse, sometimes irregular	14	17			24		22	42	30	54	6
		resorbed core, zoned rim	12	5			12		16	8	8	18	4
inclusions		„sedimentary" zircon core	6	2			4		8	2	22		
		crystal and phase inclusions	69	73	96	48	66	96	36	64	28	40	94
outgrowth, overgrowth			2	7			14		14	8	6	10	4
hindered growth			10	1	4	10			10	8			10
colour	colourless		52	34	18	62	6		2	16	16	14	60
	yellow		27	16	10	34	20	4	8	30	22	2	
	pink and brownish		21	50	72	4	74	96	90	54	62	84	40

Table II-2. Quantitative data of morphological and mineralogical aspects of zircon crops from 11 selected rock-types of the area around Noya. Number of countings is indicated in the table; the quantitative data are recalculated on a basis of 100 grains per sample (sample numbers are indicated without the prefix St. 141).

crystals; on the contrary often there are only a few. Generally a relatively large but variable number of crystals are broken, irregularly developed, rounded, resorbed, show evidence of hampered growth, etc.

The breakage of zircons may be the result of rock cataclasis, imperfect crystallization (St. 141734 a per-alkaline orthogneiss), metamictization, etc.; rock crushing does not seem to be an important cause with the exception of a few highly elongated crystals (Larsen & Poldervaart, 1957). The presence of "early-broken-later-healed" zircons was established more than once and indicates that these crystals have survived mechanical crushing (Plate XV-f).

The total weight of the zircon crops belonging to the rocks of the area is very different. The largest amounts have been encountered in the per-alkaline orthogneisses (ca. 0.21 weight %) and to a lesser extent in the biotite-ferrohastingsite orthogneisses and hornblende-biotite orthogneiss. With the exception of some hornblende-rich diorites the cognate inclusions of the megacrystal-bearing granodiorite magmatic series contain many more zircons than the main granodiorite, while the muscovite granite is very poorly populated. The paragneiss inclusions occurring in the granodiorite include, like all paragneisses of the area, relatively few zircons (ca. 0.01 weight %).

The amount of zircon in the Hercynian palingenic granites is highly variable but generally rather small. The post-kinematic biotite granites contain numerous zircons which is in contrast to the post-kinematic two-mica Arbos granite (Table II-2).

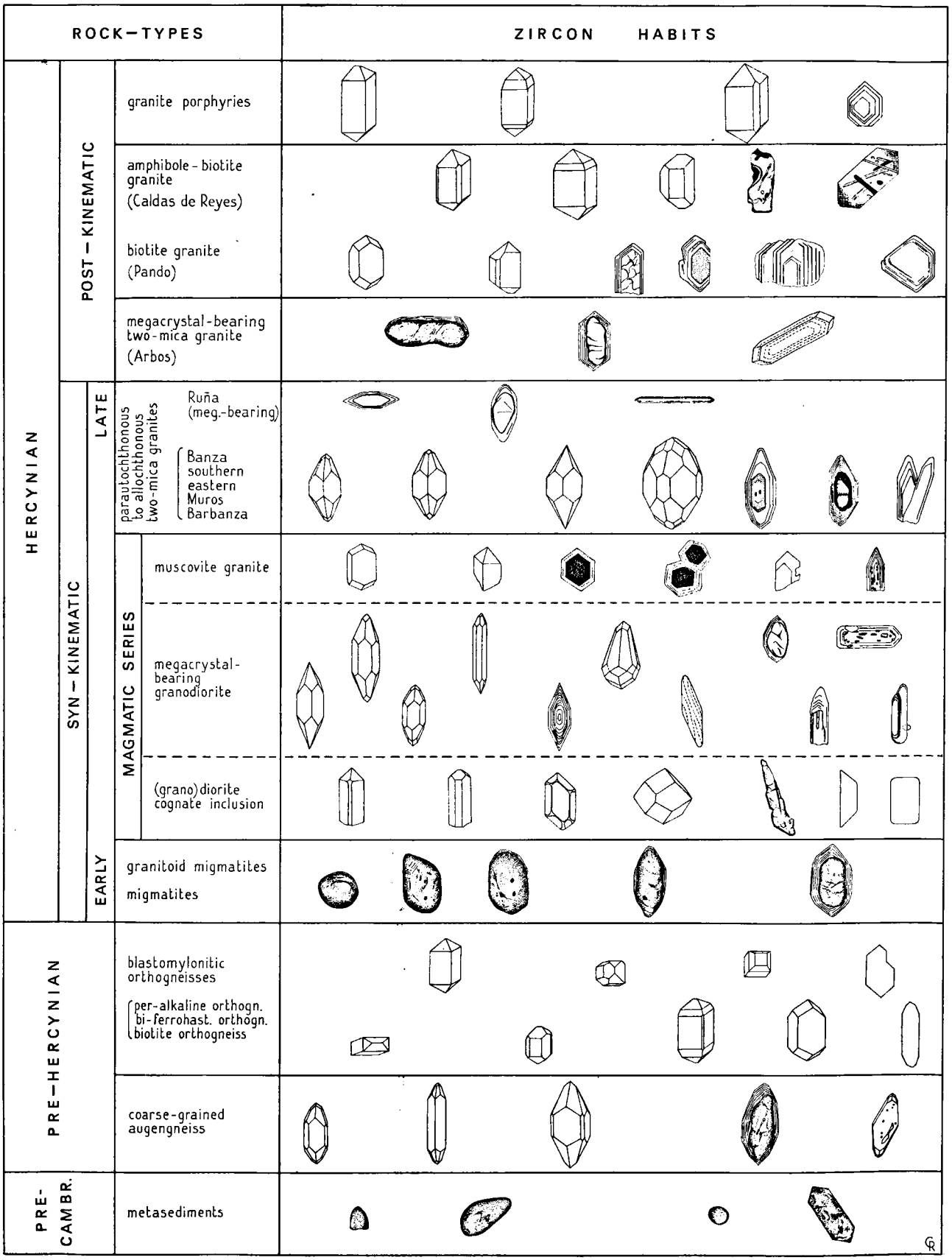
ROCK–TYPES
ZIRCON HABITS
HERCYNIAN
POST – KINEMATIC
granite porphyries
amphibole - biotite granite (Caldas de Reyes)
biotite granite (Pando)
megacrystal-bearing two-mica granite (Arbos)
SYN – KINEMATIC
LATE
MAGMATIC SERIES
paraautochthonous to allochthonous two-mica granites
Ruña (meg.-bearing)
Banza
southern
eastern
Muros
Barbanza
muscovite granite
megacrystal-bearing granodiorite
(grano)diorite cognate inclusion
EARLY
granitoid migmatites
migmatites
PRE–HERCYNIAN
blastomylonitic orthogneisses
per-alkaline orthogn.
bi-ferrohast. orthogn.
biotite orthogneiss
coarse-grained augengneiss
PRE-CAMBR.
metasediments

Morphology of the zircons

In general the morphology of zircons in rocks can vary greatly (Goldschmidt, 1923; Hartman, 1956) although there is a strong preference for certain forms to develop (Poldervaart, 1956; Hoppe, 1962 & 1963; Frasl, 1963; Kalsbeek & Zwart, 1967). Hartman (1956) derived a theoretical relationship between crystal structure, in terms of periodic bond chains or PBC's, and the morphology of zircon. He calculated that "the theoretical habit" agrees closely with many of the observed habits as quoted in the literature: a combination of the forms m{100} and p{101}. The crystal forms generally occurring in the zircon crops are schematically presented in Table II-3.

With regard to the zircon habits, the rocks of the area can be roughly divided into two morphological groups. The zircons of the rocks belonging to the first group have the forms m{100} and p{101} or a{110} and p{101} or m{100}, a{110} and p{101}. The form u{301} may also occur in addition to m{100} and p{101} and occasionally also v{201} or c{001}. The form x{211} is generally absent, and when it is present it is usually very subordinate.

Rocks belonging to this group are:

1. The pre-Hercynian blastomylonitic orthogneisses.
2. The muscovite granite of the Hercynian megacrystal-bearing granodiorite series.
3. The Hercynian post-kinematic megacrystal-bearing two-mica granite (Arbos).
4. The Hercynian post-kinematic biotite granites (Pando and Caldas de Reyes).
5. The granite porphyries.

The zircons of the rocks belonging to the second group are characterized by the presence of x{211} as an (the) important form. Most of the crystals of this group show the combination of x{211} with p{101}, m{100} and/or a{110}.

In some samples p{101} seems entirely absent, leaving the crystal shapes very sharp; on very close examination, however, p{101} generally turns out to be present. Once in a great while the form e{112} is encountered.

Rocks belonging to this group are:

1. The pre-Hercynian coarse-grained augengneiss.
2. The Hercynian megacrystal-bearing granodiorite (main body).
3. The Hercynian syn-kinematic palingenic two-mica granites (types: Barbanza, Muros, Banza, eastern and southern granites).
4. The late syn-kinematic Ruña granite.

In connection with this subdivision, the following should be noted:

a. This subdivision does not mean that forms typical of the second group, i.e. x{211}, might not occur in the first group or vice versa. In fact they often do, though they are a minority and the development of x{211} is subordinate in the first group.

b. The dioritic and granodioritic cognate inclusions belonging to the megacrystal-bearing granodiorite series contain many zircons of both groups, or in other words: the form x{211} is generally no longer subordinate and is found in a variety of sizes.

c. The rocks of the first group can be further subdivided. The biotite orthogneisses are generally devoid of u{301} and v{201}, while x{211} is often subordinately present. The amphibole-bearing orthogneisses seem to reflect the opposite.

The post-kinematic amphibole-bearing biotite granite (Caldas granite) contains more zircons with x{211} than the Pando biotite granite.

d. The crystal shapes of the zircons of both groups are often asymmetric of aberrant (Plate XVIII-m). It is not unlikely that this is the result of a hampered growth. Most of the asymmetric crystals have a pseudo-monoclinic (Plate XIV-i) or pseudo-rhombic (Plate XV-a) shape. The latter crystals when examined in the direction of [100] or [010] give the impression that the form c{001} is present. An inspection under reflected light of loose zircons mounted on a spindle offers much information on asymmetric or aberrant growth. It is clear that these shape deviations may influence the results of the statistical breadth and elongation frequencies when they occur too frequently. Consequently the curves of the granodiorite autoliths (Fig. II-3, sample 5) should be evaluated with some care.

e. When length, breadth and elongation frequencies of the zircon crops are investigated, as often reported in literature, it should be stressed that these investigations only cover a part of the petrogenetic aspects of zircon crops. In fact often it is merely the rate of aberrant growth in the direction of [001] which is evaluated.

f. The present investigations include some information on the approximate sizes of the main crystal forms relative to each other, i.e. the forms m{100} and/or a{110} with respect to x{211} and/or p{101}, and x{211} with respect to p{101} (Table II-2).

The size of m{100} of the zircons belonging to the first group is generally larger than a{110}. The form x{211} of crystals belonging to the second group is often the largest. The size of the forms u{301} and/or v{201} is always smaller than m{100}.

Length, breadth and elongation frequencies (see Table II-6 and Fig. II-3)

The majority of the frequency curves are unimodal and slightly skewed to the right. The latter property is a general feature of zircon frequency diagrams when a linear scale (abscissa) is used (Smithson, 1939; Poldervaart, 1956; Hoppe, 1963). The shape of the curves not only depends on the total number of count-

Table II-3. Crystal morphology and other characteristics of zircons from the rocks of the area around Noya.

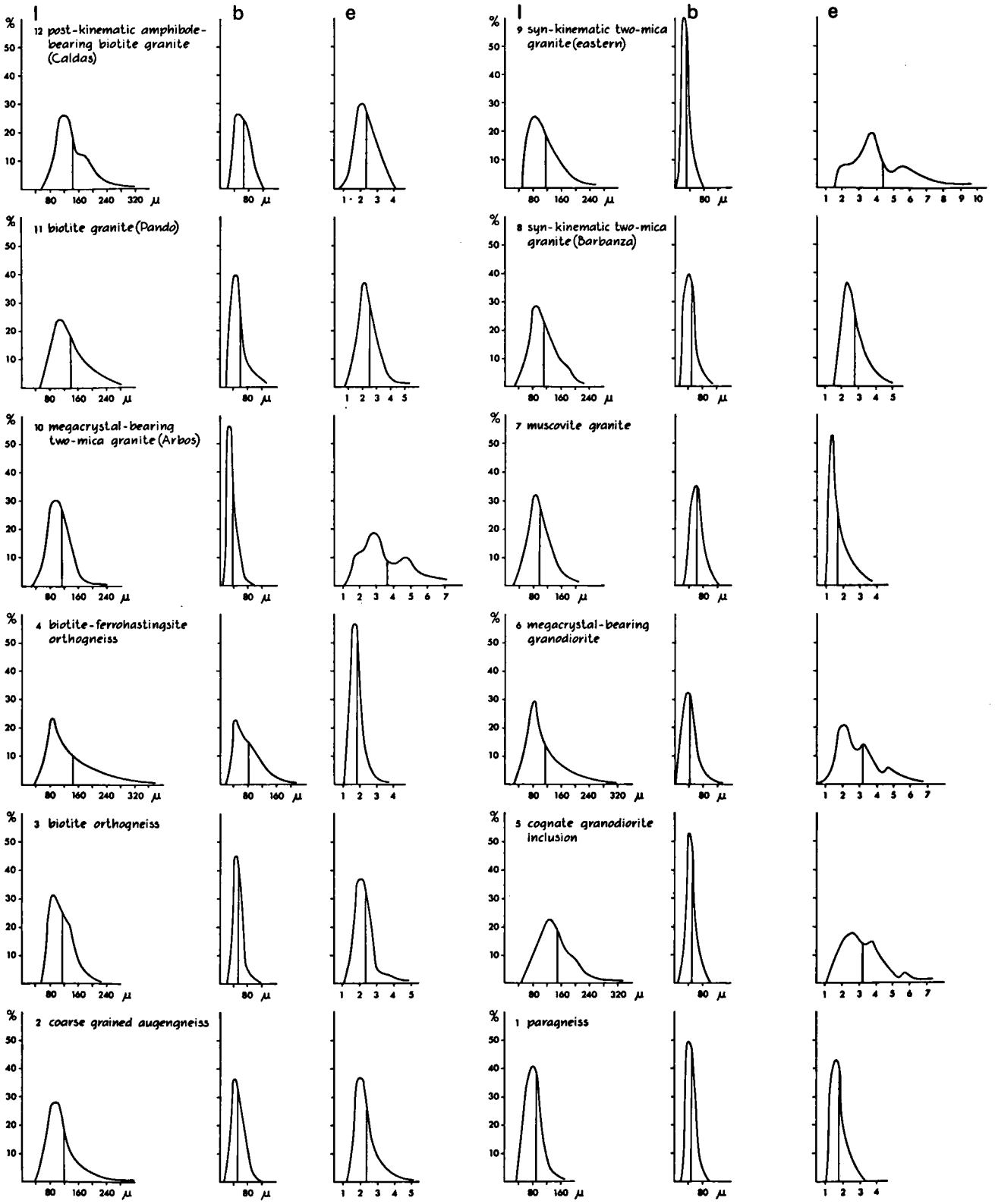

Fig. II-3. Length, breadth and elongation frequency curves of zircon populations from 12 selected samples (see Tables II-2 and II-6).

ings, but also on the range of the intervals within which the data fall.

For the samples under consideration length, breadth and elongation frequencies were obtained at regular intervals of 24μ, 16μ and 0.5, respectively.

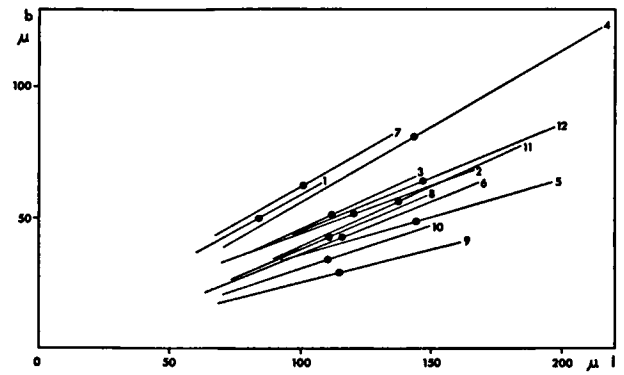

Fig. II-4. Reduced major axis of zircon populations from 12 selected samples (see Tables II-2 and II-6). The ends of the RMA are the intersections ($\bar{l} \pm S_l$) and ($\bar{b} \pm S_b$).

Polymodality of the elongation frequencies might indicate the presence of more than one zircon generation (Poldervaart, 1950; Veniale, et al., 1968). Many zircons of the Hercynian two-mica granites, the megacrystal-bearing granodiorite and the pre-Hercynian coarse-grained augengneiss display an interrupted growth and enclose a rounded zircon core. These zircons generally have a lower elongation ratio and when the population contains in addition many markedly elongated crystals, the combination of both effects may result in bi- or polymodality as the elongation frequency curves of zircons from the megacrystal-bearing granodiorite (no. 6 of the selected samples), the eastern two-mica granite (no. 9) and the megacrystal-bearing two-mica granite (Arbos, no. 10) seem to suggest. On the other hand the zircon frequency curves of the coarse-grained augengneiss (no. 2), the (Barbanza) two-mica granite (no. 8) and the (Pando) biotite granite (no. 11) are unimodal although the zircons display growth phenomena similar to that mentioned above.

The zircons belonging to the dioritic and granodioritic cognate inclusions of the megacrystal-bearing granodiorite magmatic series are generally very incompletely developed, especially in sample St. 141796 (Plate XV-g). Furthermore many zircons of sample no. 5 have aberrant crystal forms. The measurements of the unbroken grains show that the zircons are slender and have highly variable lengths.

The mean elongation ratios of all the samples are rather low, the modes are even lower. Despite the presence of many large zircons in the amphibole-bearing orthogneiss (no. 4) the modes of length, breadth and elongation are more or less the same compared with the biotite orthogneiss (no. 3). The majority of the zircons from the post-kinematic biotite granites are relatively large with a moderate mean elongation.

In Fig. II-4 the reduced major axes (RMA) of the zircon populations have been plotted (Larsen & Poldervaart, 1957). The RMA is an approximation of the growth trend of the zircon populations; it is a straight line that passes through the coordinates ($\bar{l}$, $\bar{b}$) with a slope $a = S_b/S_l$ (see Table II-6) and it forms an angle α with the abscissa ($tg\alpha = a$). The more elongated the crystals, the smaller α is (samples 5, 9 and 10 in contrast to samples 1, 4 and 7).

The correlation coefficient $r(1 \leqslant r \leqslant 0)$, indicating the relative dispersion of the l/b data round the RMA, has also been computed. When $r=1$ the correlation is perfect and when $r=0$ the correlation is absent. Samples 5, 9 and 10 demonstrate the highest dispersion of the measurements around the RMA and the data of samples 4 and 11 are only slightly dispersed; this was to be expected after evaluating the elongation frequency curves.

Resorption

The data in Table II-2 clearly indicate that resorption has thoroughly affected most of the zircon crops. Resorption may lead to a rounding off of the crystal edges; the resorbed crystal surfaces are sometimes smooth and brilliant (Plate XV) but generally they are pitted (Plate XIII-c and d) or grooved (Plate XIV-e and i) and have a dull appearance.

Resorption may have taken place during magmatic crystallization (Spotts, 1962; Hoppe, 1963); it resulted in a rough zonal growth when crystallization and resorption alternated. If magmatic resorption started relatively late during the crystallization of the zircons, the crystals are characterized by a resorbed core and a coarsely zoned rim. The two types of magmatic resorption characterize most of the zircons in the granitic rocks (samples 2, 3, 6, 8, 9, 10 and 11).

Metamorphism may also have corroded the zircons, probably being important only when the grade of metamorphism was sufficiently high and when metamorphism occurred under wet conditions (Marshall, 1969).

Zoning

As mentioned above, a crystallization which was irregularly interrupted by resorption resulted in an irregular and coarse zoning (zonar gestörtes Wachstum, Hoppe, 1963; Zonarbau mit Rekurrenzen, Frasl, 1963). But the zircon crystals may also display a fine and sharp zonal evolution. This type of zoning in contrast to the former seems to indicate that each period of growth was followed by a period of stagnation, which apparently was not followed by resorption.

The inner morphology of the zoned crystals may reveal exactly the same shape as the contours (Plates XIII-e, XIX-d and i) but this is not always the case. It sometimes appears that the inner forms, consisting of p{101} and m{100} or a{110} and probably a very small x{211}, gradually evolved into the outer morphology with a very small p{101}, a large x{211},

and m{100} and/or a{110}. Such an evolution is not exceptional for zoned zircons belonging to the second group of zircon morphologies (Plate XVI-b).

Zoned zircons belonging to the first group, which have the outer forms p{101}, m{100} and/or a{110}, may sometimes display an inner morphology where m{100} and/or a{110} are very subordinate (Plate XVIII-p).

Inclusions

Inclusions are present in a great many crystals of all the zircon crops, but they often differ greatly in nature. Usually the inclusions are subhedral to rounded grains of zircon, rutile, apatite, magnetite, biotite etc. In some crops, liquid and/or gaseous inclusions and "negative" crystals occur (the cognate inclusions, the Caldas de Reyes granite and the granite porphyries). The inclusions may occur in the centre of the host or in the border zones (Plate XIII-f); they may be zonally arranged, lie parallel to the crystallographic c-axis or they may seem to lie completely disoriented, although upon closer examination the inclusions are usually oriented parallel to some crystal face ("Einschlussregelung nach der Korngestalt", Frasl, 1963). (Plates XIII-h, XVI-c, XVIII-d and g).

Another type of petrogenetically important inclusion is the "pre-granite" zircon inclusion often encountered in the migmatites and in the autochthonous, parautochthonous and allochthonous palingenic granites, and to a lesser extent also in the intrusive granites (see later).

Growth hindrance

Zircons with partly irregular outlines, which are usually the result of a hampered crystal growth, frequently occur in the cognate inclusions, the Caldas de Reyes granite (plate XIX-m) and the granite porphyries (Hoppe, 1963). A few have been encountered in each investigated zircon sample.

Outgrowths and overgrowths

Both phenomena are often seen on the zircons from igneous and metamorphic rocks. Overgrowth may have developed during later stages of crystallization, sometimes after a period of strong resorption (Pando granite, Plate XIX-g), but in many other cases, as the migmatites and the palingenic granites of the area clearly demonstrate, they partly or completely grew around pre-migmatic or pre-granite zircons (Plate XVII-f, g and i; Plate XVIII-f and Plate XIX-a and b). Thin or irregular outgrowths and overgrowths may lack recognizable crystal forms.

Zircon aggregates

Composite crystals or aggregates of zircon crystals are not uncommon for any zircon crop derived from the rocks of this area (Plates XIII-g, XVI-f and XVII-k). Usually the aggregates are optically continuous, especially the composite crystals that have clustered together in an early stage of crystallization. Some aggregates consist of xenotime and zircon (Plate XVI-j).

rock - type / characteristics		granodiorite cognate inclusion	megacrystal granodiorite	muscovite granite
zircon, weight%		ca. 0,09%	ca. 0.012 %	< 0.002%
crystal forms	majority	a {110} ; m {100} ; p {101} ; x {211} ----|	x {211} ; m {100} a {110} ; p {101} ----|	p {101} and m {100} or a {110}
	subordinate	u {301} ; c {001}	----> +e {112} ? ; c {001}	----> + c {001}
nature of crystal faces, edges		variably resorbed smooth and brilliant sharp as well as rounded edges	often resorbed; often grooved and dull minority with sharp edges	heavily resorbed pitted and dull
elongation etc.		variable ; $\bar{e}$ = 3.14 ; many elongated and aberrant crystals	variable ; $\bar{e}$ = 3.21 many elongated crystals	equidimensional; $\bar{e}$ = 1.68
zoning		not present	often present	see Table II-3
inclusions		present: mainly small; many phase inclusions	present: small and large	clouded core
colour		colourless	brown tanned	brown
fluorescence colour		> 95 %: yellow orange - brownish orange	> 85 % orange - brown (see Table II-5)	greenish or brownish, cloudy
other accessories d ⩾ 3,3		titanite, rutile	monazite, xenotime, garnet	garnet, anatase

Table II-4. Zircon characteristics for the main rock-types of the megacrystal-bearing granodiorite magmatic series. Dashed lines indicate that a small amount of the crystals from one rock-type may be present in a later type.

Metamictization

As a result of the structural breakdown of the lattice caused by radiation (α particles) of radioactive elements present in the crystal (U, Th, Rare Earths), the crystal becomes metamict. Zircons with a higher content of radioactive elements may become metamict in a shorter time (Gastil, et al., 1967). The process causes an increase in volume, which is apparent as microcracks on the crystal surface (Plate XIX-h) and a decrease in density and refractive indices.

Completely metamict zircons have not been encountered in the zircon crops of the area, but it was often found that crystals with large and distinctive cores have zoned rims with a low birefringence; these rims are partly metamict (Plate XIX-g). Almost all zircons of the muscovite granites (no. 7) are rather highly metamict.

Colour

The zircon colours that were most frequently found are transparent, yellowish, and various shades of brownish. Table II-2 gives a good impression of the colour distributions within the crops. The colour of the zircons may depend on the total original amount of U and Th and the age of the crystals (Gastil, et al., 1967). The yellowish, reddish and brown crystals are an indication of a relatively high content of Th, U etc.

Zircons from the metasediments

The largest average grain size for zircons belonging to the different types of metasediments occurs in the metaquartzites (St. 141700 and St. 141699). Smaller grains are found in the metagreywackes (St. 141692) and metapelites (St. 141684). The total amount of zircon is also highest for the metaquartzites (ca. 0.05 weight %, St. 141699).

The average zircon size for sample no. 1 (St. 141696) falls between those of the metaquartzites and the metapelites.

As was expected, most of the grains are distinctly rounded (no. 1: $\bar{e}=1.75$) and have pitted surfaces (Plate XVII-a). In addition, however, a few perfect euhedral crystals also occur; these crystals may have entered the original sediment from nearby or as inclusions in other minerals.

It was found that in the zircon crops of the metasedimentary rocks of the area, no metamict grains were present; all the grains have a high birefringence. This fact must be explained by the sorting effect of the mechanical transport which the fragile zircons apparently did not survive and an internal radiation damage which did not destroy the zircons after deposition.

Zircons from the members of the megacrystal-bearing granodiorite magmatic series

It seems evident that the zircons of these co-magmatic rock-types (see p. 86) demonstrate a tendency toward a morphological evolution (Tables II-2 and II-4).

The morphology of the zircons of the (grano) dioritic cognate inclusions often shows a more simple development than those of the main intrusion. The form x{211} varies in degree of development but is usually smaller, and the prismatic faces are generally the largest faces of the crystals, which is also seen in the elongation ratios. The biprismatic dipyramidal crystals with large x{211} forms characterize crops of the main intrusion; they occur together with more elongated crystals and aberrant grains with the same faces as well as crystals which are more characteristic for the cognate inclusions (Fig. II-3 and Plate XVI).

The crystals of the muscovite granites and aplites are very simple and have an extremely low elongation ratio; these crops may also include a few crystals which are comparable with the zircons of the main intrusion.

The crystals of the cognate inclusions are often incompletely developed (Plate XV-i) but they are usually smooth with brilliant crystal faces. The crystal edges may be sharp or highly resorbed (Plate XV-a, b and i), while the zircons of the main intrusion are generally resorbed with rather dull crystal faces; the zircons of the muscovite granite have dull and pitted faces.

Another important difference is the presence and the nature of zoning. The zircons of the main body are usually coarsely zoned and may enclose a resorbed core. The zircons of the cognate inclusions are unzoned; those of the muscovite granite have a large turbid core and a relatively clear rim. The differences in colour from transparent (cognate inclusions) and transparent to brownish (main intrusion) to dark brown (muscovite granite) seem to indicate a progressive increase in the uranium and thorium content in the zircons of more or less the same age (Gottfried et al., 1959; Forbes, 1969). All the characteristics of the three co-magmatic products have been summarized in Table II-4.

The above-mentioned evolution tendency indicates that a relationship exists between the crystal forms observed and the physico-chemical conditions in which they crystallized.

It has been suggested (Yushkin et al., 1966; Forbes, 1969 etc.) that factors such as alkalinity, content of free quartz, etc., might influence zircon morphology and the variety of shape. Poldervaart (1956) has briefly discussed the views of some petrologists concerning the origin of long prismatic zircons and their attempt to interpret the long prismatic habit in terms of physico-chemical conditions.

Generally crystal morphology, i.e. the existence or lack of certain forms, will depend upon internal and external factors.

The most important internal factor is the crystal structure.

External factors are pressure, temperature, degree of disequilibrium (such as supersaturation), the supply of crystallizing constituents and the presence of foreign material (Hartman, 1956 & 1969).

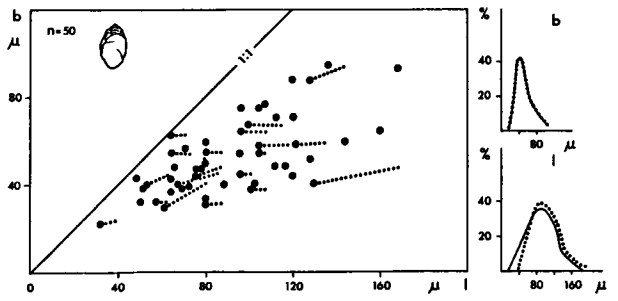

Fig. II-5. a. Dimensions of zircons from the restite (melanosome) of a migmatite (St. 141776; an inhomogeneous diatexite). The closed dots indicate the measurements of the sedimentary zircons and the interrupted lines the size increments. The length and breadth frequency curves are included.

b. Dimensions of zircons from the granitoid metatect of the same migmatite. Closed circles indicate the sedimentary zircon cores, the closed squares are zircons without overgrowths. The open circles are the regenerated zircons and the open squares euhedral zircons without cores. The length-breadth-elongation frequency curves of the sedimentary zircons (full) and the regenerated and newly grown zircons (dashed) are included.

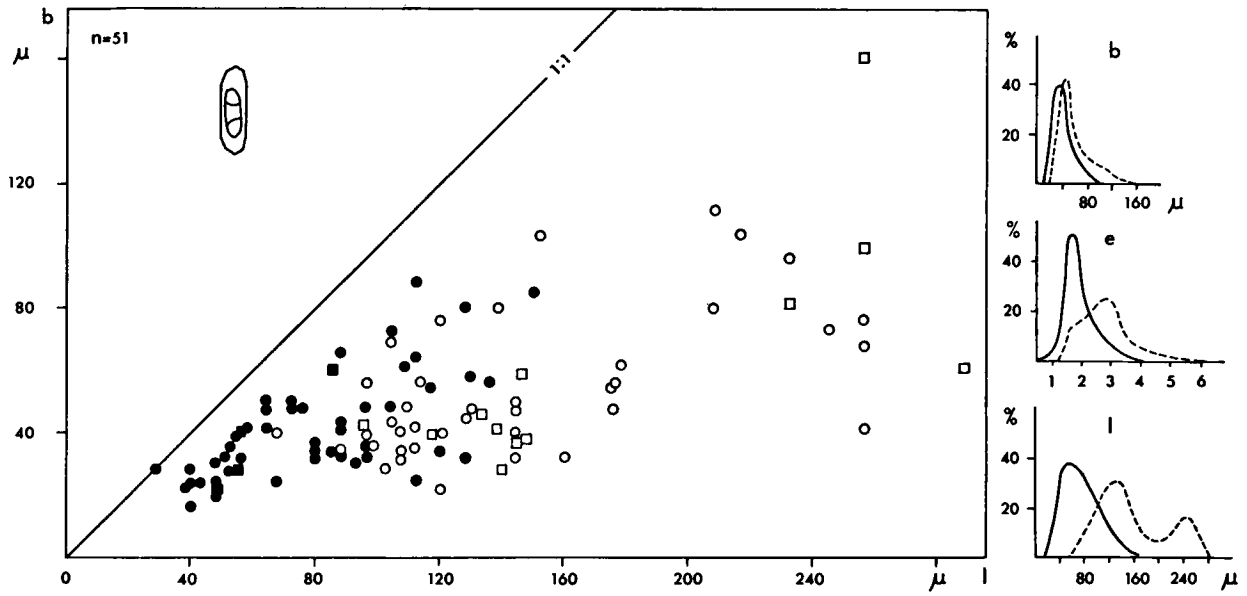

Zircon in migmatites

At first sight the initial stages of anatexis do not seem to have affected the zircons of the metasedimentary rocks. But in comparison with zircons from non-migmatic rocks, the surfaces of zircon grains from low-grade migmatites (metatexites, Mehnert, 1957 & 1968) are smooth and brilliant. Upon closer examination very thin and incomplete overgrowths are found on many grains (Plate XVII). An inhomogeneous migmatite consisting of restites and newly-formed pegmatoid metatect has yielded zircons which are more or less similar in shape for both migmatic components; the only difference is that the total number of zircons is smaller in the metatect.

As anatexis proceeds the overgrowths become more important and may even completely envelop the host crystal. In a length-breadth diagram (Smithson, 1939) the dimensional data for zircons belonging to two components of a migmatite (an inhomogeneous diatexite, Mehnert 1963 & 1968) have been plotted. To the data for the zircons of the restites, the rates of growth increment are added where they occur (Fig. II-5a).

The zircons from both migmatite components demonstrate perfectly the successive stages of the regeneration of the zircons. About 68% of the zircons of the granitoid metatect enclose pre-granite zircons (Fig. II-5b and Plate XVII); an autochthonous origin of the granitoid seems quite evident (Poldervaart & Eckelmann, 1955).

At a higher stage of homogenization of the autochthonous granites, the number of newly grown crystals without sedimentary cores increases. The crystallizing conditions in the present area, however, were such that the majority of the newly-formed crystals are coarsely zoned and many may enclose resorbed cores. Differentiation between the latter type of zircons and those enclosing pre-granite zircons may be very difficult.

The zircons from the migmatic orthogneisses have also suffered resorption; the crystal edges are a little more rounded and the faces more smooth and brilliant than the crystals of the non-migmatic orthogneisses. The less stable grains may have been affected to a greater extent; zircon stability will be reduced by metamictization, zoning and the presence of inclusions and fractures (Marshall, 1967 & 1969).

In addition to the resorbed crystals, the zircon crops

of the migmatic orthogneisses also contain grains with outgrowths (Plate XIII-k) and aggregates.

All the above-mentioned examples indicate that the ultimate conditions of metamorphism, which caused a widespread anatexis of the pre-existing rocks, were also favourable for a regeneration of the zircon crystals (Marshall, 1969).

Preliminary electron microprobe analyses

The results of the analyses are listed in Table II-7, three to five zircon crystals have been measured from each sample; no metamict crystals were present. The analyses indicate that no important differences exist among the various samples of different origin and age. Only the zircons from the biotite-ferrohastingsite orthogneiss deviate in that they have the lowest average hafnium content and accordingly the highest Zr/Hf ratio. The concentrations of aluminium and the radioactive elements are low; the iron concentration is lowest for the zircons of the orthogneiss. The granite porphyry, being representative of the latest Hercynian magmatic activities in the area, contains the highest U and Th content. No relationship could as yet be detected between crystal morphology and chemical composition.

Table II - 5

fluorescence colour → / rock-type ↓	yellow	brownish yellow	brown	brownish orange	orange	orange yellow	green	others
granite porphyry	9		22	44	13	7	5	
megacrystal-bearing granodiorite	2		2 10	44 70	42 17	10 3		
cognate inclusion	3			55	17	25		
biotite-ferrohast. orthogn.	8	9	9	33		41		
biotite orthogneiss			31	21		46		
coarse-grained augengneiss	18 11	 2	9 11	11 13	51 45	11 18		
metaquartzite	18	27	21	7	3	24		
two-mica schist	17	18	14	24	2	6		9

Table II-5. Distribution of primary fluorescence colours for some zircon samples. One hundred grains per sample were counted by 'ribbon-counting'.

Fluorescence of the zircons

The primary fluorescence properties of some loose zircon concentrates have been investigated using a Leitz Ortholux fluorescence microscope. A high pressure mercury vapor lamp was used as UV light source; approximately 365 nm "longwave" UV light was chosen for excitation of the fluorescence.

The investigations were carried out in cooperation with Dr. P. van Gijzel, first at the Geological and Mineralogical Institute in Leiden and later in his laboratory in Nijmegen (Katholieke Universiteit). The results, both qualitative and quantitative, will be published in a forthcoming paper.

Generally the fluorescence colours of zircon are yellow, orange and brown; other colours such as red and green are exceptional (Gleason, 1960). According to Stoke's law the emitted light is of a longer wave-

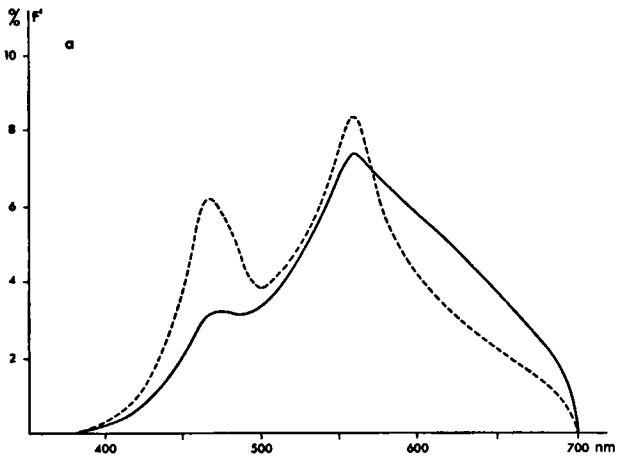

Fig. II-6. a. Relative fluorescence spectra (Leitz MPV-system) of zircons. Full curve: orange fluorescent zircon from megacrystal-bearing granodiorite (St. 141804); dashed curve: yellow fluorescent zircon from a granodiorite inclusion (St. 141795).

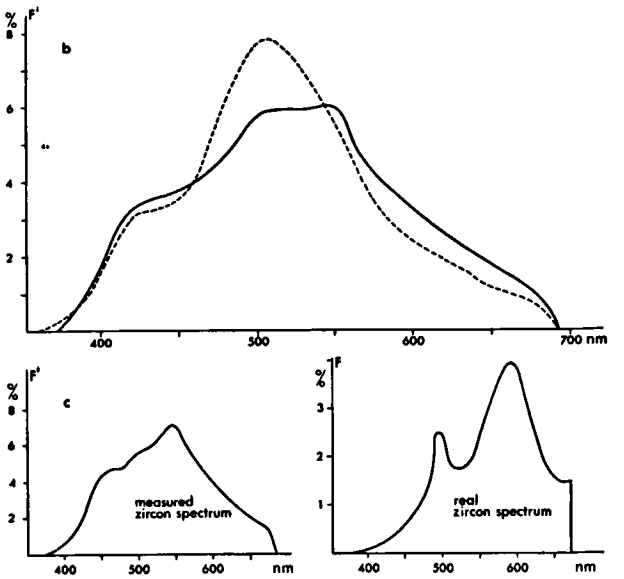

b. Relative fluorescence spectrum of a zoned zircon. Full line: orange-brown rim; dashed line: green core.
c. A zircon spectrum before and after correction for E.P. and all properties of the instrument (van Gijzel, 1970).

length than the excitation energy. The presence of certain trace elements (activators) may be responsible for the fluorescence ability of minerals (Haberlandt & Köhler, 1949). It has been suggested that yellow is activated by hafnium, while iron tends to inhibit the emission (Foster, 1948). Recently Nicholas (1967) came to the experimental conclusion that in zircon at least two centres are responsible for the yellow luminescence, i.e. tri-valent europium and centres caused by the radioactive decay of U and Th.

Many of the separated zircon crops have been investigated; the distribution of the fluorescence colours has been quantified for ten samples (Table II-5). The main colours are orange, yellow and brown in several variations and occasionally a zonal variation in orange and yellow. The brown "fluorescent" crystals nearly always correspond with the brown and "dirty" grains in transmitted normal (tungsten) light.

Generally the fluorescence colours of zircons from the intrusive rocks of the area are more uniform than those from the metasediments, with the exception of the metaquartzites. The palingenic granites, instead, demonstrate more variation in fluorescence than usual.

Remarkable is the presence of (emerald) green fluorescent zircons in some Hercynian granitic rocks, such as the muscovite granite (of the megacrystal-bearing granodiorite series), some two-mica granites (e.g. Ruña granite), the post-kinematic granites (Arbos, Pando and Caldas granites) and a granite porphyry; they are either zoned yellow-green crystals (Pando granite) or completely green. The element dysprosium may be responsible for the activation of a green fluorescence of zircon (Foster, 1948).

The emitted fluorescence spectra for many zircons from different rock-types as well as some monazites*, xenotimes and apatites were measured by means of the Leitz MPV-system. The measured fluorescence spectra of the zircons are indicated as frequency curves, where the intensities of the emission at various wavelengths (F') are expressed as a function of the total intensity of the emitted light.

The curves of yellow and orange fluorescent zircons are generally bimodal with a marked maximum at about 555 nm and a weaker maximum at about 465 nm (Fig. II-6a). In Fig. II-6b the spectrum of a zonal fluorescent zircon with a green core and a brown rim is shown and in Fig. II-6c, a real zircon spectrum is indicated after correction of the measured spectrum for E.P. (the amount of light of the microscopical picture) and all optical and photo-electrical properties of the instrument. These corrections are necessary when the microscopical fluorescence spectra are compared with spectra obtained by other measuring methods.

* As has been mentioned previously, both monazite and xenotime occur in most of the rocks of the area. Monazite generally has a dull bluish to greenish fluorescence colour and xenotime is yellowish in colour. The apatites (megacrystal-bearing granodiorite, St. 141802) vary widely from orange-yellow and greenish white to pink and violet. An important aspect of the fluorescence of apatite is its marked fading effect, contrary to the stability of zircon. Apatite shows a distinct shift in fluorescence spectrum and decrease in intensity under an 1 hour-exposure to UV light under the microscope (Van Gijzel, 1970).

CONCLUSIONS

1. Two groups of zircon morphologies can be distinguished. A combination of the forms p{101} and m {100} with subordinate u{301}, v{201} and x{211} typifies the zircons of the blastomylonitic orthogneisses, the post-kinematic Arbos, Pando and Caldas de Reyes granites and granite porphyries. The late magmatic members of the megacrystal-bearing granodiorite series, i.e. the muscovite granites and aplites, also belong to this group.

The zircons from the megacrystal-bearing granodiorite (main differentiation product) and the other granites and gneisses in the area have zircons characterized by the presence of the forms x{211} with a{110} and/or m{100} and/or p{101}; e{112} may sometimes occur. The faces of the form p{101} are generally very small, while the faces of x{211} may develop as the largest faces of the crystals. The zircons of the cognate inclusions include both types of morphologies.

Aberrant crystal shapes, due to a strong growth in one or two directions, are ubiquitous but they are more numerous in the crops of some granodioritic cognate inclusions, and the post-kinematic Pando and Caldas granites and granite porphyries.

Evidence of a hindered or incompletely developed growth of zircons is widespread in the cognate inclusions, the Caldas granite and the granite porphyries. The zircons of the same rock-types also often contain large phase inclusions (liquid or liquid and gas).

2. A relationship probably exists between zircon morphology, certain mineralogical aspects of the crystals and the rocks in which they occur. The zircons of the second group, characterized by the presence of x{211} as an important form, occur in the pre-Hercynian coarse-grained augengneisses and in the Hercynian syn-kinematic granodiorites and palingenic granites. The syn-kinematic rocks were emplaced under mesozonal conditions involving a relatively slow crystallization with all kinds of physico-chemical fluctuations. Evidence of such a crystallization may be found in the coarsely zoned zircons and the zircons with resorbed cores and zoned rims (Hoppe, 1963; Frasl, 1963).

That the zircons with x{211} as an important form possibly grew under these conditions has been suggested by Hartman & Perdok (1955), who stated that "the occurrence of S-forms (x{211} is an S-form, Fig. II-2) on minerals is due to alternating periods of growth and dissolution in an impure environment."

A similar relationship between zircons with the characteristic x{211} form and the rocks in which they occur has been suggested by Pupin et al. (1969) for

statistical parameter → / samples ↓	mode l	$\bar{l}$	S_l	mode b	$\bar{b}$	S_b	mode e	$\bar{e}$	S_e	$a = \frac{S_b}{S_l}$	α	r	n
12. amphibole-biotite granite (Caldas)	120	145.96	50.48	48	63.69	20.60	2.2	2.38	0.63	0.4082	22° 12′	0.6371	100
11. biotite granite (Pando)	108	136.68	47.40	40	55.67	21.75	2.25	2.54	0.62	0.4589	24° 39′	0.8050	100
10. megacryst.-bearing two-mica gran. (Arbos)	96	110.22	40.12	24	33.90	13.55	2.8	3.55	1.33	0.3378	18° 40′	0.3594	100
9. eastern two-mica granite	84	114.12	47.09	24	28.78	11.78	3.75	4.30	1.93	0.2502	14° 3′	0.3839	100
8. western two-mica granite (Barbanza)	88	110.89	36.81	40	43.27	16.04	2.25	2.65	0.64	0.4358	23° 33′	0.7206	100
7. muscovite granite	84	100.60	33.61	56	62.62	19.32	1.25	1.68	0.63	0.5747	29° 53′	0.4833	50
6. megacr.-bearing granodiorite	80	115.34	53.24	36	42.36	21.51	2.0	3.21	2.62	0.4041	22°	0.5246	100
5. cognate granodiorite inclusion	128	143.77	51.51	40	48.84	14.77	2.5	3.14	1.29	0.2868	16°	0.2043	100
4. biotite-ferrohastingsite orthogneiss	84	143.13	72.60	40	80.81	42.90	1.75	1.82	0.42	0.5909	30° 35′	0.9039	100
3. biotite orthogneiss	84	111.95	32.16	40	50.73	14.89	2.1	2.26	0.55	0.4630	24° 51′	0.6828	100
2. coarse-grained augengneiss	96	118.95	49.51	40	51.11	18.57	2.1	2.39	0.74	0.3751	20° 34′	0.7096	100
1. paragneiss (St. 141696)	80	85.23	23.20	40	49.95	12.91	1.75	1.75	0.44	0.5566	29° 6′	0.5146	100

Table II-6. Statistical dimensional parameters of zircon populations from 12 selected samples (see Table II-2). Calculations are based on 50 or 100 unbroken crystals per sample.
$\bar{l}$: mean length S_l : standard deviation of the length

analyses → / rock-types ↓	anal. pts	Zr in % mean	Zr in % range	anal. pts	Hf in % mean	Hf in % range	anal. pts	Zr/Hf ratio mean	Fe in ppm mean	Fe in ppm range	Y	U	Th	Ce	Al
											in ppm				
granite porphyry	3	47.8	47.6—48.3	5	1.14	1.01—1.31	3	41.9	630	460—960	Less than 1000	~ 500	~ 500	Less than 500	Less than 300
amphibole-biotite granite (Caldas)	5	50.0	49.5—50.3	5	1.13	0.93—1.82	5	43.8	710	180—1130		< 500		Less than 100	
megacrystal-bearing granodiorite	3	49.4	48.8—49.7	5	1.24	0.94—1.64	3	40.1	363	80—670		~ 500			
biotite-ferrohastingsite orthogneiss	3	48.6	48.1—49.0	5	0.80	0.63—0.91	3	60.7	160	150—170		Less than 500			
coarse-grained augengneiss	3	48.5	48.0—49.3	5	1.22	1.02—1.37	3	39.7	230	80—390					
metaquartzite	4	48.3	47.7—48.5	5	1.10	0.94—1.44	3	44.0	490	140—810					

Table II-7. Results of electron microprobe analyses (Geoscan) of six zircon samples.

zircons in anatectic rocks in SE France. The zircons from the Aston-Hospitalet gneisses in southern France (Kalsbeek & Zwart, 1967) and those in the older granites in northern Portugal (de Boorder, 1965) seem to indicate a similar relationship.

The zircon habits of the first group, on the other hand, are characteristic for granitic rocks with an indisputed magmatic origin: the Arbos, Pando and Caldas granites, the granite porphyries as well as the late-magmatic muscovite granites and aplogranites belonging to the megacrystal-bearing granodiorite series and the pre-Hercynian granites of the central

zone. The younger granites of northern Portugal (de Boorder, 1965), the Valle de Aran granite in southern France (Kalsbeek & Zwart, 1967) and the granite of l'Argentera (Pupin et al., 1969) also support this view.

It is possible that the physico-chemical conditions were such that a relatively short progressive crystallization of these granitic rocks (most of them under epizonal conditions) only yielded zircons with the simplest crystal forms (F-forms: Hartman, 1956), with low attachment energies.

3. The zircons belonging to the magmatic differentiation members of the megacrystal-bearing granodiorite series show an evolution trend in crystal forms. The populations of the cognate inclusions and the main granodiorite contain many similar forms, and seem to indicate that the two magmatic phases followed each other closely. The habit of the zircons of the late-magmatic muscovite granites and aplogranites is quite different; the crystals are equidimensional and have very simple forms.

4. The zircons of the metasediments are generally well-rounded and have pitted surfaces. Many grains are broken and rounded off again (during sedimentary transport); a minority is idiomorphic with sharp edges.

5. The greatest number of zircons occur in the peralkaline orthogneisses and the biotite-ferrohastingsite orthogneisses; the granodioritic cognate inclusions, the metaquartzites, the granite porphyries and the post-kinematic biotite granites are richly populated. The palingenic two-mica granites enclose variable amounts of zircon; the post-kinematic Arbos granite is poorly populated. The same holds for the metapelites and metagreywackes.

6. In addition to crystal morphology, the zircon crops of the granitic and granodioritic rocks may differ in the presence and character of zoning, magmatic resorption, inclusion and colour.

7. The zircons of the migmatites are characterized by an initial stage of corrosion; with increasing rates of mobilization the grains display outgrowths and overgrowths, while the ultimate products of mobilization, e.g. the granitoids, may contain many (as high as 68%) regenerated zircons. The parautochthonous to allochthonous granites contain fewer regenerated zircons. These crystals have also been encountered in the post-kinematic Arbos granite. The observations stress the fact that conditions for the anatexis in the present area were favourable for the regeneration of the zircons (Marshall, 1969).

8. Completely metamict zircons have not been encountered. Many coarsely zoned crystals, especially those enclosing large resorbed cores, have partly metamict rims (various syn-kinematic two-mica granites and the Pando granite). Many grains are radially fractured and/or show microcracks on the crystal surfaces.

9. Yellow, orange and brown are the most frequent fluorescence colours of the zircon crops studied; green fluorescent crystals occur in some of the syn-kinematic granites and all the post-kinematic intrusives. Some crystals demonstrate a zonal distribution of the fluorescence colour (Pando granite zircons have green fluorescent cores and yellow rims).

SUMARIO

La región descrita en esta tésis, forma parte de la zona axial del macizo Hespérico. Las rocas, de origen metamórfico e intrusivo, se presentan en tres unidades estructurales: una zona central (que de hecho forma parte de la denominada "fosa blastomilonítica"), un complejo migmático y las rocas en el sur y en el suroeste. Durante la orogénesis Hercínica estas unidades fueron colocadas en yuxtaposición. Con respecto a su edad y composición, las rocas pueden ser subdivididas en 1. metasedimentos, rocas metabásicas y ortogneises pre-Hercínicos; y 2. migmatitas, granitos palingénicos y granodioritas intrusivas, granitos, pegmatitas, aplitas, filones de cuarzo, pórfiros graniticos, lamprófiros y doleritas de olivino, todos de edad Hercínica.

Tomando como base la evidencia petrológica, la historia geológica puede ser reconstruida de la siguiente manera:

Los metasedimentos pre-Hercínicos, que muestran una deformación y metamorfismo Precámbricos (estaurolitas y granates reabsorbidos incluídos dentro de minerales metamórficos Hercínicos), fueron penetrados a lo largo de fallas fundamentales de rumbo N-S en el Ordoviciense Superior (hace 460–430 $\times$ 10^6 años) por granitos megacristalinos de dos micas, granitos de biotita y granitos per-alcalinos. La intrusión de un sistema de diques básicos tuvo lugar entre el emplazamiento de los dos últimos tipos de series de granito.

Durante la orogénesis Hercínica, las rocas pre-Hercínicas fueron en un principio deformadas intensivamente; los metasedimentos fueron replegados y los granitos fueron filonitizados a gneises glandulares de grano grueso o milonitizados a milonitas de granito (zona central). Esta fase principal de deformación Hercínica fue seguida por un período de plutonometamorfismo de tipo Abukuma. Durante este período de recristalización metablástica extensa de rocas no

migmáticas de la zona central es característica. Los minerales metamórficos en las rocas no migmáticas de la zona central indican una facies cordierita-anfibolita y los de los metasedimentos en el suroeste indican condiciones de facies de esquisto verde, mientras que las inclusiones en el granito palingénico de dos micas sufrieron unas condiciones de facies corneana de hornblenda superpuestas. En niveles mas profundos el metamorfismo Hercínico culminó en una anatexis. Durante un período corto de tensión y de fracturación normal, las rocas no migmáticas de la zona central fueron colocadas en yuxtaposición con las migmatitas. Mas o menos sincrónicamente las fallas fundamentales activas, que separan la zona central de las migmatitas occidentales, facilitaron la subida de gran cantidad de magma granodiorítico. Inmediatamente después, los productos finales de la anatexis, siempre y cuando hayan sido capaces de intrusión, penetraron en el complejo migmático y en las granodioritas bajo la forma de fases sucesivas de granitos de dos micas.

Este período de actividad plutónica fue interrumpido por la segunda y tercera deformación Hercínica que tenían solamente localmente un caracter penetrativa. La mayoría de los granitos y granodioritas Hercínicos fueron débilmente foliados durante la segunda deformación mientras que la tercera deformación filonitizó y milonitizó localmente las rocas en el norte, suroeste y oeste.

El ciclo orogénico Hercínico se concluyó con la intrusión de un granito de dos micas post-cinegético, dos granitos de biotita (hace 280 $\pm$ 11 $\times$ 10^6 años), algunos pórfiros graniticos y lamprófiros. Unos pocos diques de dolerita de olivino son probablemente mas jóvenes.

Se ha estudiado el hábito cristalino, fenomenos de crecimiento, inclusiones, reabsorción y fluorescencia de circones accesorios que ocurren en los metasedimentos, ortogneises, migmatitas y granitos.

Los distintos tipos de roca contienen circones con un hábito cristalino mas bien característico: asi los circones de los ortogneises blastomilonítticos, los granitos post-cinegéticos y los pórfiros graniticos estan constituidos por una combinación de las formas {101}, {100} y {110} y algunas veces {301} y {201}, mientras que en los gneises glandulares pre-Hercínicos de grano grueso, las granodioritas de megacristales Hercínicas y los granitos de dos micas, los circones estan formados por una combinación de {101}, {211}, {100} y/o {110}. Los circones de las rocas pertenecientes a la serie de granodioritas de megacristales muestran claramente diferencias en evolución. Los circones en las rocas migmáticas indican que las condiciones para la anatexis favorecieron la regeneración de los circones.

Los colores de fluorescencia de los cristales de circón son anaranjado, amarillo y marrón; conteniendo algunes muestras también un color de fluorescencia verde esmeralda. También se ha observado en los colores de fluorescencia alguna variación zonal.

SAMENVATTING

De resultaten van een tweetal onderzoeken zijn verwerkt in dit proefschrift. In het eerste hoofdstuk wordt de petrologie en strukturele geologie behandeld van een gebied in de omgeving van Noya in de provincie La Coruña (NW Spanje). Voor dit onderzoek werd veldwerk verricht in de zomers van 1964, 1965 en 1966; de gegevens werden daarna in Leiden uitgewerkt. Een geologische kaart van het gebied is bij dit proefschrift aanwezig, alsmede een chronologische tabel, waarin de geologische geschiedenis schematisch is samengevat.

In het tweede hoofdstuk zijn de resultaten vermeld van een detail onderzoek van het mineraal zirkoon, dat in accessorische hoeveelheden in de meeste gesteenten van het gebied aanwezig is en informatie verschaft over het ontstaan en de geschiedenis van deze gesteenten.

Het gebied in de omgeving van Noya maakt deel uit van de axiale zone van het Hesperische massief, een Hercynisch orogeen. Metamorfe en intrusive gesteenten komen hier voor in drie strukturele eenheden: de centrale zone, het migmatisch complex en de gesteenten in het S, SW en W. Tijdens de Hercynische orogenese zijn deze eenheden, oorspronkelijk op verschillende niveaux van het gebergte ontstaan, naast elkaar gekomen.

Gebaseerd op de petrologie is de geologische geschiedenis van het gebied als volgt te reconstrueren:

De oudste gesteenten zijn de metamorfe sedimenten van de centrale zone, het zijn hoofdzakelijk metagrauwacken, metapelieten en metakwartsieten. Sporen van een pre-Hercynische, vermoedelijk Precambrische deformatie en metamorfose lijken aanwezig te zijn. Relicten van een pre-Hercynische metamorfose zijn o.a. de geresorbeerde stauroliet en granaatkernen in metamorfe mineralen van Hercynische ouderdom.

In het Boven-Ordovicium (460–430 miljoen jaar geleden) zijn langs de N-S gerichte fundamentele breuken grofkorrelige porfierische twee-glimmer granieten, biotiet granieten en per-alkalische granieten (granieten die alkali amphibool en/of -pyroxeen bevatten) geïntrudeerd. Na de intrusie van de biotiet granieten, maar vóór die van de per-alkalische granieten, volgde de intrusie van vele basische gangen.

Tijdens de eerste belangrijke Hercynische deformatie (F_1) zijn alle metasedimenten geplooid door een zeer sterke (E)NE-(W)SW gerichte compressie. De biotiet granieten en per-alkalische granieten werden mylonitisch en de porfierische granieten kregen een phyllonitische struktuur (grove ogengneizen).

Hierop volgde een periode van regionale metamorfose van het Abukuma-type (relatief lage druk en

hoge temperatuur). Aanvankelijk leidde dit tot een metablastische rekristallisatie van de metasedimenten en graniet mylonieten (blastomylonitische orthogneizen) en uiteindelijk op diepere niveaux trad op grote schaal anatexis (opsmelting) op. De metamorfe mineraal associaties in de niet door anatexis beïnvloede gesteenten (centrale zone) zijn kenmerkend voor de cordiëriet-amphiboliet faciës en die van de metamorfe sedimenten in het S en SW voor de groenschistfaciës; de schist xenolieten in de palingene twee-glimmer granieten in het SW vertonen kenmerken die overeenkomen met hoornblende-hoornrots faciës condities.

Een korte periode van rekspanning veroorzaakte een daling langs een fundamentele NS breuk van een deel van het gebied (centrale zone), waardoor de niet-migmatische gesteenten op gelijk niveau met de migmatieten kwamen te liggen. Min of meer gelijktijdig intrudeerde langs dezelfde breuken een grote hoeveelheid granodioritisch materiaal. Vrijwel onmiddellijk hierop volgden de intrusies van de palingene twee-glimmer granieten; deze granieten zijn de producten van volledige opsmelting en bleken op vele plaatsen in staat te zijn in het migmatisch complex en de megakristen granodiorieten door te dringen (298 $\pm$ 10 miljoen jaar geleden).

Deze periode van de Hercynische magmatische activiteiten werd onderbroken door de tweede en derde plooiingsfasen; F_2 en F_3 zijn over het algemeen slechts lokaal penetratief geweest. F_2 heeft de megakristen granodioriet het sterkst beïnvloed, de megakristen zijn duidelijk gericht. De derde deformatie heeft langs bepaalde zones vooral de granitische gesteenten in het N, SW en W sterk gephyllonitiseerd en zelfs gemylonitiseerd.

Na F_3 volgde de intrusie van een post-kinematische porfierische twee-glimmer graniet, twee biotiet granieten (280 $\pm$ 11 miljoen jaar geleden), enige granietporfieren, lamprofieren en nog later enige olivijn dolerieten.

De accessorische zirkonen die volgens een bepaalde, ten dele nieuwe, methode uit gemalen gesteente monsters zijn geconcentreerd, zijn onderzocht op kristalhabitus, groeiverschijnselen, insluitsels, resorptie, fluorescentie en andere eigenschappen.

Opvallend is dat de verschillende gesteente typen zirkonen bevatten met een karakteristieke habitus, die verband houdt met de kristallisatie omstandigheden van het moedergesteente. Een combinatie van de vormen {101}, {100} en/of {110} en soms {301} en {201} werd aangetroffen aan de zirkonen afkomstig uit de pre-Hercynische blastomylonitische orthogneizen, de Hercynische post-kinematische granieten en granietporfieren; een combinatie van {101}, {211} en {100} en/of {110} is karakteristiek voor de pre-Hercynische grove ogengneis, de Hercynische granodiorieten en de twee-glimmer granieten.

De zirkonen, die afkomstig zijn uit de verschillende magmatische producten van de megakristen granodioriet serie (de cognate (grano) dioriet insluitsels, de megakristen granodioriet zelf en de muscoviet granieten) laten een duidelijke ontwikkeling zien.

De omstandigheden die hebben geleid tot anatexis bleken ook geschikt te zijn voor een regeneratie van zirkoon. De verschillende stadia van regeneratie zijn het duidelijkst te zien in de zirkonen van migmatieten van sedimentaire oorsprong.

De fluorescentie kleuren van zirkoon zijn geel, oranje en bruin. Smaragdgroene zirkonen zijn aangetroffen in de laat-Hercynische granieten en graniet porfieren. Een zonaire afwisseling van fluorescentie kleuren wordt sporadisch aangetroffen.

REFERENCES

Alling, H. L., 1938. Plutonic perthites. Jour. Geol., 46, pp. 142–165.

Arps, C. E. S., 1965. Petrografie, mineralogie en structurele geologie van het gebied rondom Noya (NW Spanje). M.Sc.thesis, Leiden Univ., unpublished.

—, 1965. Geomorphologie en sedimentpetrografie van het gebied tussen de mondingen van de Río Tambre en de Río Ulla (Prov. Coruña, NW Spanje). M.Sc.thesis, Leiden Univ., unpublished.

—, 1970. Zircon in granites, gneisses and metasediments from western Galicia (NW Spain): Preliminary report on investigations of crystal habit and other optical characteristics. Bol. Geol. Min., 81, pp. 30–42.

Arps, C. E. S. & Kluyver, H. M., 1969. Sedimentology of the northwestern shores of the Ría de Arosa (NW Spain). Leidse Geol. Med., 37, pp. 135–145.

Avé Lallemant, H. G., 1964. Petrografie, mineralogie en structurele geologie van het Outes-Muros gebied (NW Spanje). M.Sc.thesis, Leiden Univ., unpublished.

—, 1965. Petrology, petrofabrics and structural geology of the Sierra de Outes-Muros region (La Coruña, Spain). Leidse Geol. Med., 33, pp. 147–175.

Billings, M. P., 1945. Mechanics of igneous intrusion in New Hampshire. Am. Jour. Sci., 243-A, Daly volume, pp. 40–68.

Boorder, H. de, 1965. Petrological investigations on the Aguiar de Beira granite area, northern Portugal. Ph. D. thesis, Univ. of Amsterdam, 126 pp.

Bosch, J. B. M. ten, 1964. Geologie, petrologie en mineralogie van het gebied aan de NO-kant van de Ría de Arosa (NW Spanje). M.Sc.thesis, Leiden Univ., unpublished.

Brongersma, L. D. & Pannekoek, A. J., 1966. Investigations in and around the Ría de Arosa, North-West Spain, 1962–1964. Leidse Geol. Med., 37, pp. 1–5.

Buddington, A. F., 1959. Granite emplacement with special reference to North America. Geol. Soc. Am., Bull., 70, pp. 671–747.

Capdevila, R., 1965. Sur la géologie du Précambrien et du

paléozoique dans la région de Lugo et la question des plissements assyntiques et sardes en Espagne. Notas Comun. Inst. Geol. Min. Esp., 80, pp. 157–174.

Capdevila, R. & Floor, P., 1970. Les différents types de granites hercyniens et leur distribution dans le nord de l'Espagne. Bol. Geol. Min., 81, pp. 215–225.

Carlé, W., 1945. Ergebnisse geologischer Untersuchungen im Grundgebirge von Galicien. Geotekt. Forsch., 6, pp. 13–36.

Floor, P., 1966. Petrology of an aegirine-riebeckite gneiss-bearing part of the Hesperian massif: the Galiñeiro and surrounding areas, Vigo, Spain. Leidse Geol. Med., 36, pp. 1–203.

—, 1968. Basement rocks of western Galicia as sources for the minerals in the Ría de Arosa. Leidse Geol. Med., 37, pp. 69–76.

Floor, P., Kisch, H. J. & Oen Ing Soen, 1970. Essai de corrélation de quelques granites hercyniens de la Galice et du nord du Portugal. Bol. Geol. Min., 81, pp. 242–244.

Forbes, W. C., 1969. Zircons of the White Mountain magma series: Belknap Mountain Complex. Am. Min., 54, pp. 787–795.

Foster, W. R., 1948. Useful aspects of the fluorescence of accessory-mineral-zircon. Am. Min., 33, pp. 724–735.

Frasl, G., 1954. Anzeichen schmelzflüssigen und hochtemperierten Wachstums an den grossen Kalifeldspaten einiger Porphyrgranite, Porphyrgranitgneise und Augengneise Österreichs. Jb. Geol. Bund. Anst., 47, pp. 71–134.

—, 1963. Die mikroskopische Untersuchung der akzessorischen Zirkone als eine Routinearbeit des Kristallingeologen. Jb. Geol. Bund. Anst., 106, pp. 405–428.

Frietsch, R., 1957. Determination of the composition of garnets without chemical analysis. Geol. Fören. Förh., 79, pp. 43–51.

Gastil, R. G., DeLisle, M. & Morgan, J. R., 1967. Some effects of progressive metamorphism on zircons. Geol. Soc. Am., Bull., 78, pp. 879–906.

Gijzel, P. van, 1970. Die Anwendung der Fluoreszenz-Mikroskopie und Fluoreszenz-Mikrophotometrie in der Geologie und Palynologie. Leitz Mitt. f. Wiss. Tech., V (in press).

Gleason, S., 1960. Ultraviolet guide to minerals. D. Van Nostrand Comp., Inc. Princeton, New Jersey, 244 pp.

Goldschmidt, V., 1923. Atlas der Kristallformen. Heidelberg, Winter.

Gottfried, D., Jaffe, H. W. & Senftle, F. E., 1959. Evaluation of the lead-alpha (Larsen) method for determining ages of igneous rocks. U.S. Geol. Surv., Bull., 1097 A, 63 pp.

Graaff, W. P. F. H. de, 1962. Petrografische scriptie.M.Sc. thesis, Leiden Univ., unpublished.

Haberlandt, H. & Köhler, A., 1949. Die Bedeutung der Fluoreszenz in der Mineralogie und Petrographie. In: F. Bräutigam & A. Grabner: Beiträge zur Fluoreszenz-Mikroskopie, Verl. G. Fromme, Wien, pp. 102–118.

Harker, A., 1962. Petrology for students. 8th ed. Cambridge Univ. Press, 283 pp.

—, 1964. Metamorphism. 3rd ed. Methuen & Co. Ltd., London, 362 pp.

Harris, Jr., R. L., 1965. A watertower apparatus to improve zircon separation technique. Geol. Soc. Am., Bull., 76, pp. 971–974.

Harten, D. van, 1965. On the estimation of relative grain frequencies in heavy mineral slides. Geol. Mijnb., 44, pp. 357–363.

Hartman, P., 1956. The morphology of zircon and potassium dihydrogen phosphate in relation to the crystal structure. Acta Cryst., 9, pp. 721–727.

—, 1969. The dependence of crystal morphology on crystal structure. In: Growth of crystals, 7, pp. 3–18. Ed. N. N. Sheftal' (translated from Russian). Cons. Bur., New York-London.

Hartman, P. & Perdok, W. G., 1955. On the relations between structure and morphology of crystals. III. Acta Cryst., 8, pp. 525–529.

Hensen, B. J., 1965. Petrologie en structurele geologie van het westelijk gedeelte van het schiereiland Morrazo, Prov. Pontevedra, NW Spanje. M.Sc.thesis, Leiden Univ., unpublished.

Hietanen, A., 1967. On facies series in various types of metamorphism. Jour. Geol., 75, pp. 187–214.

Hilgen, J. D., 1971. The Lalín-unit, a new structural element in the Hercynian orogeny of Galicia, NW Spain. Leidse Geol. Med. (in press).

Hoppe, G., 1962. Petrogenetisch auswertbare morphologische Erscheinungen an akzessorischen Zirkonen. N. Jb. Min., Abh., 98, pp. 35–50.

—, 1963. Die Verwendbarkeit morphologischer Erscheinungen an akzessorischen Zirkonen für petrogenetische Auswertungen. Abh. Deutsch. Akad. Wiss., Kl. Bergb. Hüttenw. Montangeol., 1, 130 pp., Berlin.

Kalsbeek, F., 1962. Petrology and structural geology of the Berlanche-Valloire area (Belledonne Massif, France). Ph.D.thesis, Leiden Univ., 136 pp.

Kalsbeek, F. & Zwart, H. J., 1967. Zircons from some gneisses and granites in the central and eastern Pyrenees. Geol. Mijnb., 46, pp. 457–466.

Koldijk, W. S., 1968. Bottom sediments of the Ría de Arosa (Galicia, NW Spain). Leidse Geol. Med., 37, pp. 77–134.

Koster van Groos, A. F., 1962. Verslag van de petrografische kartering. M.Sc.thesis, Leiden Univ., unpublished.

Krasilnikova, A. V., 1966. Crystal typomorphology of accessory zircon and its use in granitoid correlation of the Kokchetav Block. Min. Sbornik, SSSR, 20, pp. 541–546.

Larsen, L. H. & Poldervaart, A., 1957. Measurement and distribution of zircons in some granitic rocks of magmatic origin. Min. Mag., 31, pp. 544–564.

Liakhovitch, V. V. & Balanova, T. G., 1966. Some peculiarities of accessory zircon. Min. Sbornik, SSSR, 20, pp. 559–565.

Lotze, F., 1945. Zur Gliederung der Varisziden der Iberischen Meseta. Geotekt. Forsch., 6, pp. 78–92.

Luth, W. C., Jahns, R. H. & Tuttle, O. F., 1964. The granite system at pressures of 4 to 10 kilobars. Jour. Geophys. Res., 69, pp. 759–773.

Marshall, B., 1967. The present status of zircon. Sedimentology, 9, pp. 119–136.

—, 1969, Zircon behaviour during extreme metamorphism. Geol. Soc. Australia, Spec. Publ., 2, pp. 349–351.

Mason, B. & Berry, L. G., 1968. Elements of mineralogy. W. H. Freeman & Comp., San Francisco, London, 550 pp.

Mehnert, K. R., 1957. Petrographie und Abfolge der Granitisation im Schwarzwald, II. N. Jb. Min., Abh., 90, pp. 39–90.

—, 1963. Petrographie und Abfolge der Granitisation im Schwarzwald. IV. N. Jb. Min., Abh., 99, pp. 161–199.

—, 1968. Migmatites and the origin of granitic rocks. Elsevier Publ. Comp., Amsterdam, 393 pp.

Metzsch, E. H. von, 1964. Een petrografische studie van het gebied ten S van Mazaricos (Galicië, NW Spanje). M.Sc. thesis, Leiden Univ., unpublished.

Monster, C., 1967. Petrografie van het gebied in de omgeving van Bayo (Coruña, Spanje). M.Sc.thesis, Leiden Univ., unpublished.

Nicholas, J. V., 1967. Origin of the luminescence in natural zircon. Nature, 215, p. 1476.

Oen Ing Soen, 1958. The geology, petrology and ore deposits of the Viseu region, northern Portugal. Com. Serv. Geol. Port., 41, pp. 5–199.

—, 1960. The intrusion mechanism of the late-Hercynian post-tectonic granite plutons of northern Portugal. Geol. Mijnb., Nw. Serie, 22, pp. 257–296.

—, 1970. Granite intrusion, folding and metamorphism in central northern Portugal. Bol. Geol. Min., 81, pp. 271–298.

Parga-Pondal, I., 1956. Nota explicativa del mapa geológico de la parte NO de la Provincia de La Coruña. Leidse Geol. Med., 21, pp. 467–484.

—, 1966. La investigacíon geológica en Galicia. Leidse Geol. Med., 36, pp. 207–210.

Pannekoek, A. J., 1966. The geomorphology of the surroundings of the Ría de Arosa (Galicia, NW Spain). Leidse Geol. Med., 37, pp. 7–32.

Phillips, F. C., 1960. An introduction to crystallography. 2nd ed. Longmans, Green and Co. Ltd., London, 324 pp.

Platen, H. von, 1965. Kristallisation granitischer Schmelzen. Beiträge Min. Petr., 11, pp. 334–381.

Poldervaart, A., 1950. Statistical studies of zircon as a criterion of granitization. Nature, 165, pp. 574–575.

—, 1956. Zircon in rocks: 2: Igneous rocks. Am. Jour. Sci., 254, pp. 521–554.

Poldervaart, A. & Eckelmann, F. D., 1955. Growth phenomena in zircon of autochtonous granites. Geol. Soc. Am., Bull., 66, p. 947.

Priem, H. N. A., 1962. Geological, petrological and mineralogical investigations in the Sierra de Marão region, northern Portugal. Ph.D.thesis, Univ. of Amsterdam, 160 pp.

Priem, H. N. A., Boelrijk, N. A. I. M., Verschure, R. H., Hebeda, E. H. & Verdurmen, E. A. Th., 1970. Dating events of acid plutonism through the Paleozoic of the western Iberian Peninsula. Eclogae Geol. Helv., 63, pp. 255–274.

Pupin, J. P., Boucarut, M. & Turco, G., 1969. Les zircons des granites et migmatites du massif de l'Argentera-Mercantour et leur signification pétrogénétique. Bull. Soc. Fr. Min. Cryst., 92, pp. 472–483.

Rankama, K., 1954. Isotope geology. Pergamon Press, London, 477 pp.

Raumer, J. von, 1963. Zur Tektonik und Genese des nordwest-spanischen Kernkristallins bei Noya (La Coruña). Geotekt. Forsch., 17, pp. 1–63.

Rijks, E. J. H., 1968. Petrografie en mineralogie van het gebied rondom Buño, Galicië, NW Spanje. M.Sc. thesis, Leiden, Univ., unpublished.

Rosenblum, S., 1958. Magnetic susceptibilities of minerals in the Frantz isodynamic magnetic separator. Am. Min., 43, pp. 170–175.

Rubbens, I. B. H. M., 1963. Resultaten van kartering en petrografisch onderzoek in het 'Complejo Antiguo', Galicië, Spanje. M.Sc.thesis, Leiden Univ., unpublished.

Sastri, G. G. K., 1958. Determination of the end-member composition of garnets from their physical properties. Records Geol. Surv. India, 87, pp. 757–780.

Schermerhorn, L. J. G., 1956a. Igneous, metamorphic and ore geology of the Castro Daire – São Pedro do Sul – Sátão region (northern Portugal). Com. Serv. Geol. Port., 37, pp. 5–617.

—, 1956b. The granites of Trancoso (Portugal): a study of microclinization. Am. Jour. Sci., 254, pp. 329–348.

Shelley, D., 1968. A note on the relationship of sillimanite to biotite. Geol. Mag., 105, pp. 543–545.

Shidô, F., 1958. Plutonic and metamorphic rocks of the Nakoso and Iritôno districts in the central Abukuma Plateau. Jour. Fac. Sci., Univ. Tokyo, sect. II, 11, pp. 131–217.

Smithson, F., 1939. Statistical methods in sedimentary petrology. Part II. Geol. Mag., 76, pp. 348–360.

Spotts, J. H., 1962. Zircon and other accessory minerals, Coast Range batholith, California. Geol. Soc. Am., Bull., 73, pp. 1221–1240.

Spry, A., 1969. Metamorphic textures. 1st ed., Pergamon Press, Ltd., New York, 350 pp.

Tex, E. den, 1965. Metamorphic lineages of orogenic plutonism. Geol. Mijnb., 44, pp. 105–132.

—, 1966. Aperçu pétrologique et structural de la Galice crystalline. Leidse Geol. Med., 36, pp. 211–222.

Tex, E. den & Floor, P., 1967. A blastomylonitic and polymetamorphic 'graben' in western Galicia (NW Spain). In: Etages tectonique, Ed. La Baconnière, Neuchâtel, pp. 169–178.

Tongeren, G. van, 1970. Petrografie van het gebied om Agualada (La Coruña, NW Spanje). M.Sc.thesis, Leiden Univ., unpublished.

Tröger, W. E., 1959. Optische Bestimmung der gesteinsbildenden Minerale. Teil 1. Bestimmungstabellen. Stuttgart, Schweizerbart'sche Verlagsbuchh., 147 pp.

Tuttle, O. F. & Bowen, N. L., 1958. Origin of granite in the light of experimental studies in the system $NaAlSi_3O_8$–$KAlSi_3O_8$–SiO_2–H_2O. Geol. Soc. Am., Mem. 74, 153 pp.

Vance, J. A., 1961. Polysynthetic twinning in plagioclase. Am. Min., 46, pp. 1097–1119.

Veniale, F., Pigorini, B. & Soggetti, F., 1968. Petrological significance of accessory zircon in the granites of Baveno, M. Orfano and Alzo (N Italy). XXIIIth Int. Geol. Congress, Proc. Sect. 13, pp. 243–268.

Vogel, D. E., 1967. Petrology of an eclogite- and pyrigarnite-bearing polymetamorphic rock complex at Cabo Ortegal, NW Spain. Leidse Geol. Med., 40, pp. 121–213.

Vogel, W., 1967. Petrografie van het gebied rond Sangenjo (Prov. Pontevedra, Spanje). M.Sc.thesis, Leiden Univ., unpublished.

Warnaars, F. W., 1967. Petrography of a peridotite-, amphibolite- and gabbro-bearing polyorogenic terrain NW of Santiago de Compostela (Spain). Ph. D. thesis, Leiden Univ., 208 pp.

Winkler, H. G. F., 1967. Die Genese der metamorphen Gesteine. Berlin, Springer-Verl., 2nd ed., 237 pp.

Woensdregt, C. F., 1966. Informe preliminar sobre los estudios de la petrografia del extremo occidental de Galicia. Leidse Geol. Med., 36, pp. 261–278.

Yushkin, N. P., Fishman, M. V., Goldin, B. A., Kalinin, E. P. & Davidov, V. P., 1966. Typomorphism and correlation significance of accessory zircon from igneous and metamorphic rocks in the cispolar Urals and Thiman. Min. Sbornik, SSSR, 20, pp. 547–553.

Zavjalova, I. V., 1966. Habitus types of accessory zircon in granitoids of eastern Transbaikal. Min. Sbornik, SSSR, 20, pp. 524–531.

Zuuren, A. van, 1965. Mineragrafie, genese en economische geologie van de tin- en wolfraam-mineralisaties te San Finx (Prov. La Coruña). M. Sc. thesis, Leiden Univ., unpublished.

—, 1969. Structural petrology of an area near Santiago de Compostela (NW Spain). Leidse Geol. Med., 45, pp. 1–71.